GAMMA/DELTA T-CELLS IN PATIENTS WITH EPITHELIAL OVARIAN CANCER

A DISSERTATION
Submitted to
The Temple University Graduate Board

In Partial Fulfillment
Of the Requirements for the Degree
DOCTOR OF PHILOSOPHY

By
Fatima B. Whitfield
August 2008

ABSTRACT

Title: Gamma-delta T-cells in Epithelial Ovarian Carcinoma

Candidate's Name: Fatima B. Whitfield

Degree: Doctor of Philosophy

Temple University, 2008

Doctoral Advisory Committee Chair: C.D. Platsoucas, Ph.D.

Ovarian cancer is the fifth most common cancer among women and cause more deaths in the western world than any other gynecological cancers. The epithelial ovarian carcinomas (EOC) represent approximately 90% of all human ovarian malignant neoplasm. The five-year survival rate for patients with EOC is attributed to late diagnosis and poor response to therapy.

T-cells play an important role in tumor immunity of EOC, evidence includes infiltrating CD3+ T-cells in EOC lesions and a specific antigen driven immune response. Human $\gamma\delta$ TCR + T-cells are a minor subset of T-cells (1-10%) in the peripheral blood. The majority of the T cells in the peripheral blood are $\alpha\beta$ TCR + T-cells. Like the $\alpha\beta$ T-cells, $\gamma\delta$ TCR + T-cells bear a T-cell receptor that functions in antigen recognition. Most importantly most $\gamma\delta$ TCR+ T cells recognize mainly whole proteins. In contrast, $\alpha\beta$ TCR+ T cells primarily recognize peptide in association with MHC. Upon specific antigen recognition, these T cells undergo clonal expansion, generating multiple identical T cell clones. Previously in our lab clonal expansion of $\alpha\beta$ TCR+ T cells was observed in patients with EOC. Also preliminary data indicate that clonal expansion of $\gamma\delta$ TCR+ T cells in patients with EOC.

The hypothesis to be tested in this study is whether $\gamma\delta$ TCR+ T-cells are clonally expanded in tumors from patients with EOC and whether they recognize tumor cells. Data from recent studies show that tumor infiltrating $\gamma\delta$ TCR+ T cells recognize and have antitumor activity towards epithelial derived cancer cells. Following V-specific amplification of the various $\gamma\delta$ T-cell receptors (TCR) chains we observed the presence of statistically significant populations of oligoclonal γ-chain and δ-chain TCR+ transcripts in the EOC samples studied.

To further characterize the $\gamma\delta$ TCR+ T-cells in EOC lesions, full-length transcripts of clonally and non-clonally expanded γI-, γII-,δ1 and δ2-chain TCR transcripts from EOC tumors were constructed. These full-length transcripts were transduced into a mutant TCR-negative Jurkat T cell line. The transduced cells were analyzed by flow cytometry (FACS) for expression of $\gamma\delta$ TCR on the cell surface. $\gamma\delta$ TCR+ CD3+ transduced T cells were then incubated with the ovarian cancer cell lines, SKOV3, CAOV3 or OV2774. Following co-incubation experiments of these cancer cells with $\gamma\delta$ TCR+ CD3+ transduced T cells we observed killing of the target cell (SKOV3, CAOV3 and OV2774) by various $\gamma\delta$ TCR + T cell transduced cell lines. This killing was not observed by control T cell lines transduced either with vector only or single chain of TCR. Furthermore, the production of cysteine proteases such as caspase 3/7, procaspase 8 and 9 involved in target cell death were also observed following co-incubation experiments. These data suggest that our $\gamma\delta$ TCR+ transduced T cells induce SKOV3, CAOV3 and OV2774 cancer cell death measured by cytotoxicity and activation of cell death proteases.

ACKNOWLEDGEMENTS

I would like to thank and acknowledge the individuals who have been involved in the completion of my Ph.D. degree; First, I would like to thank my Lord and Saviour Jesus Christ for His guidance and continued blessings. I would like to thank my advisor, Dr. Chris D. Platsoucas for his mentorship and support leading to the completion of my Ph.D. degree. My deepest appreciation is extended to Dr. E. Oleszak for her input. I would like to thank my other committee members; Dr. B. Ashby, Dr. L-G. Parkson-Chong, Dr. A. Tsygankov, Dr. T. Skorski and Dr. D. Monos (external examiner) for their support and expertise that assisted me in accomplishing my Ph.D. requirements. All the support from previous and current lab members is most appreciated Ify Nwaneshiudu M.D./Ph.D., Adaobi Nwaneshiudu, Dr. Weon-Ju Jung, Dr. Song-Lu, Dr. Rayevskaya, Dr. L. Herrera, Dr. C. Herrera, Kyle Evans and Nickolaos Zacharakis. I would like to thank the departmental office for all their help. Finally my greatest admiration and appreciation is to my two beautiful daughters Nyla and Chyna, without you girls I would have given up too soon. I would like to thank my mother, sister and grandmother for being the best cheerleaders in the world. To my best friend Kevin thank you for that final encouragement that was so desperately needed your love is immeasurable. To my late Uncle Rick may you fly high with the angels, thanks for being an example of a "GREAT" man and your love will always be cherished.

TABLE OF CONTENTS

LIST OF TABLES

Table

Page

LIST OF FIGURES

CHAPTER 1
BACKGROUND INFORMATION

Ovarian carcinoma is one of the most deadly gynecological cancers with the highest mortality rate in the Western countries. Most often patients are diagnosed at an advanced stage of the disease. EOC involves uncontrolled cell proliferation and metastasis resulting in organ failure. Currently, first line agents have a 70-80% response rate; most patients eventually die of recurrent chemotherapy-resistant disease, leaving the overall 5-year survival rate around 30%. Therefore, if diagnosed early ovarian cancer is a chemo-sensitive tumor, however an initial platinum-sensitive based chemotherapy can eventually produce chemo-resistant tumor cells. Researchers are continuing to develop novel therapy to combat EOC.

Definition of Epithelial Ovarian Cancer (EOC)

Tumors cells arise from normal cells by a process that involves many genomic changes. In normal epithelial cells genomic sequences are subject to corruption by various mechanisms that alter their sequences often leading to structure or regulatory modifications. The resulting mutations/modifications may result in cells acquiring novel, often highly abnormal phenotypes. Furthermore, sustained cell proliferation in an environment rich in inflammatory cells, growth factors, activated stroma, and DNA-damage-promoting agents have the potential to promote and enhance neoplastic risk (Coussens et. al., 2002). Genomic changes resulting in cellular phenotypic changes frequently cause abnormal signal processing and may result in deregulation of proliferating programs. Cells

1

with alterations in their growth properties and morphology are undergoing malignant transformation, a process that occurs over many years.

There are three main cell types that ovarian tumors are derived from: germ cells, stromal cells, and epithelial cells. The majority of human ovarian cancer tumors arise from epithelial tissues. These tumors are responsible for more than 80% of the cancer-related deaths in the Western world. The epithelial and stromal cells of the ovary work together in forming and maintaining the epithelial sheets. Epithelial tumors start from the cells that cover the outer surface of the ovary. The two major functions of epithelia are 1) to seal the cavity or channel that they line and to protect the underlying cell populations and 2) to provide specialized cells that secrete substances into the ducts or cavities that they line. Tumors that arise from the epithelial cells of the former are termed squamous cell carcinomas. Tumors that arise from epithelia of the latter are termed adenocarcinomas (Weinberg, 2007).

Common stages of EOC

EOC prognosis is based on type (I or II), grade (high or low), stage (I-VI), and is determined by the amount and aggressiveness of cancer cells during diagnosis or following surgery. EOC can be grouped into two categories: type I low grade neoplasm that arise in a stepwise manner from borderline tumors and type II which are high grade neoplasm in which morphology initiation has not yet been determined (Ueda et. al., 2006). The grade is on a scale of 1, 2, or 3. Grade 1 epithelial ovarian carcinomas look similar to normal tissue and tend to have a better prognosis. Grade 3 epithelial ovarian carcinomas look less like

2

normal tissue and usually have a poor prognosis. EOC tumor stage (I-IV)

describes how far the tumor has spread from where it started in the ovary.

Classification of EOC

Many epithelial ovarian tumors are benign, do not spread, and generally

do not lead to serious illness. These types of tumors include serous adenomas,

mucinous adenomas, and Brenner tumors. However, some ovarian epithelial

tumors may be termed as borderline epithelial ovarian carcinomas in that they do

not grow into the supporting tissue of the ovary (i.e. the ovarian stroma). EOC

cells have several appearances identified microscopically. These features are

used to classify EOC into serous, mucinous, endometreioid, and clear cell types.

Serous is the most common type of EOC.

Based on the five main histological subtypes of ovarian cancer (serous,

mucinous, clear cell, endometreioid and transitional cell/Brenner tumors) as well

as undifferentiated adenocarcinomas many ovarian cancer cell lines have been

derived. Each subtype is thought to differ in its etiology and genetic aberrations

making these differences useful to the progression of ovarian cancer research.

The following ovarian cell lines have been established and provide powerful

research tools to study the various subtypes of ovarian cancer: OV-MZ 1-6 are

recognized as serous cystadenocarcinoma, A2780 and H134 form

undifferentiated tumors, OVCAR3 form poorly differentiated serous

adenocarcinomas, SKOV3 tumors were derived from clear cell carcinomas,

OVCA 429 form papillary adenocarcinomas with clear cell characteristics and

OV2008 form tumors of endometrioid differentiation.

Clinical signs and symptoms of EOC

Most patients with EOC are asymptomatic. When symptoms are present they include bloating, pelvic or abdominal pain, difficulty eating or feeling full quickly, urinary symptoms, indigestion, and a change in bowel habits. Women with these symptoms daily for more than two weeks should consult a gynecologist. Many women complaining of these symptoms are treated and diagnosed for the wrong disease. In addition to the above symptoms ovarian cancer patients often complain of fatigue, back pain, pain with intercourse and menstrual irregularities at the outset of the disease. The onset of EOC signs and symptoms require medical attention due to the aggressiveness generally associated with the late onset of symptoms. Furthermore EOC spreads rapidly and throughout the organs of the body.

Diagnosis of EOC

When women are diagnosed in stage I of the disease there is a 90% survival rate. However, poor diagnosis of EOC in patients with solid tumors is due to late detection and stage progression. Therefore, once diagnosed with advanced ovarian cancer 30-40% of patients have a five-year survival rate and respond poorly to therapy. Initially patients under go non-laboratory testing which include an ultrasound (pelvic and/or transvaginal), CT scan, and an X-ray of the GI tract. Next, patients undergo laboratory testing such as the OvaCheck, which involves a method of low-molecular-weight serum protein pattern recognition. This test is based on certain patterns "signature" that are distinct for EOC. In some cases patients may receive antigen testing for epithelial tumor,

germ cell tumor, or stromal tumor associated antigens. Examples of which may include, CA-125, BRCA-1/BRCA-2, Alpha feto protein (AFP), and inhibin. Once patients are diagnosed a combination of positron emission tomography (PET) scans and CT scans are used to track and detect recurrences. Scientist are searching for the origins of the disease that may assist in the development of a reliable screening test.

Treatment of EOC

1. Surgery

Once diagnosed treatment is of most concern. Growth inhibition before the cancer travels throughout the body is ideal. Surgery is the first step in treatment and allows the type and stage of cancer to be determined. A vertical cut in the abdomen exposes the pelvic region where samples are taken and all visible tumors are removed. Most likely at least one ovary will be removed. However, if advanced stage is obvious both ovaries and fallopian tubes are removed.

2. Chemotherapy

Chemotherapy combinations that include an alkylating agent and a platinum coordination complex have high response rates in women with advanced ovarian cancer. After initial surgery patients with advanced ovarian cancer receive chemotherapy. Cisplatin-based combination therapy has been shown to be more effective compared to alkylating agents alone (Thigpen et. al., 1989). The survival was 24 to 38 months in advanced ovarian cancer patients treated when combinations containing platinum were used (McGuire et. al., 1996

and Skarlos et. al., 1997). On the other hand, advanced ovarian cancer patients

treated with combinations not containing platinum the median survival was 12 to

15 months (Thigpen et. al., 1989). Therefore following adequate surgical therapy

a combined drug therapy containing platinum based chemotherapy is standard in

the United States. Still, many patients with EOC have developed tumors that

have become resistant to these chemotherapeutic agents as a result of repeated

courses of these agents. Patients with recurrent EOC are generally treated with

estrogen-blocking tamoxifen, which blocks blood vessel growth. Researchers

are continuously discovering and developing alternative treatments to combat

recurrent and advanced EOC.

3. Adoptive Cellular Immunotherapy

Adoptive cellular immunotherapy (ACT) is a process in which a large

number of autologous T cells are expanded in vitro and infused into patients for

the treatment of disease. The first evidence of efficacy using adoptive T cell

transfer in cancer patients was identified in the early 1990s. This type of therapy

enhances the immune response initiated and prorogated by the host. Tumor

infiltrating lymphocytes (TILs) expanded in vitro in rIL-2 were used for the

treatment of ovarian carcinoma by adoptive immunotherapy (Freedman et. al.,

1994).

Although ACT has been shown in ovarian cancer to transfer antigen-

specific T cell populations with the ability to restore immunity and eradicate

tumors the limitations are quickly noted (Dudley et. al., 2002). Cancer regression

and autoimmunity was observed in patients following ACT with antitumor

lymphocytes. Patients respond well to ACT following lymphodepleting chemotherapy as demonstrated in patients with metastic melanoma (Dudley et. al., 2005). Furthermore, the acquisition of CTLs specific for tumor antigens is time-consuming and laborious failing on many occasions. Due to the lack of antigen specific CTLs and other limitations scientist have identified an alternate cellular therapy involving the use of genetically engineered lymphocytes for cellular immunotherapy.

4. ACT using engineered T-cells

Most recently $\alpha\beta$ TCR + T cells have been genetically engineered with the ability to recognize and kill tumor cells. Recent evidence has shown the ability of primary human lymphocytes transduced with cDNAs encoding TCR $\alpha\beta$ specific for HLA-A2 restricted cancer testis Ag NY-ESO-1 to efficiently recognize NY-ESO-1 positive nonmelanoma tumor cell lines (Zhao et. al., 2005). Furthermore, studies showed that an anti-p53 TCR transduced into PBL recognized fresh human tumors. Cancer regression was observed in patients following transfer of genetically engineered lymphocytes. Using retroviral vectors with antigen specific TCR gene patients produced in vivo populations of antigen-specific lymphocytes. TCR gene expression was stable and modified lymphocytes developed into memory helper T lymphocytes. This modified T cell provides an attractive strategy to develop antigen-specific immunotherapy with autologous lymphocytes as a genetic treatment option (Morgan et. al., 2006).

5. Vaccines

The availability of molecularly cloned tumor antigens permitted the development of peptide based or recombinant tumor vaccines. The use of oregovomab a murine derived monoclonal antibody directed against CA125 conjugated to CA125 antigen as an immune complex was shown to elicit a humoral T cell immune response (Gordon et. al., 2004). CD8+ and CD4+ lymphocytes underwent TCR genes transfer providing an opportunity to use the same TCR specificity to produce antigen-specific killer and cell mediated immune response in patients with recurrent ovarian cancer. The results indicate tolerance to oregovomab and induced multiple antigen-specific immune responses and a significant survival benefit. Anti-idiotypic (ID) vaccines such as murine anti-Id ACA125 mAb mimic an epitope of CA125 have been shown in both animals (Schlebusch et. al., 1995) and humans (Wagner et. al., 2001 and Reinartz et. al., 1999) to effectively induce a specific anti-anti-Id antibody (Ab3) response against CA125+ tumor patients. Peptide-based vaccines have been shown to induce immunity in patients with breast and ovarian cancer (Disis et. al., 1999 and Knutson et. al., 2002).

Prevalence and incidence of EOC

Ovarian carcinoma (Oca) continues to be the leading cause of death due to gynecologic malignancies. Over 23,300 will be diagnosed and 13,900 patients will die each year from OCa. The incidence of OCa varies widely in frequency among different geographic regions and ethnic groups, with high incidences observed in Scandinavia, Western Europe and North America and low incidences found in Asian countries. Epithelial ovarian cancer (EOC) generally

8

occurs in women fifty years of age or older. Approximately 1 in 57 women in the U.S. and 1 in 108 in Australia are diagnosed with EOC. EOC results in a 5-year survival rate for 25-30% of patients with stage III and IV disease, contrasting with the 90% survival rates of patients with stage I disease.

EOC risk factors

The etiology of ovarian cancer is poorly understood however; certain factors have been implicated in ovarian cancer, such as, environmental agents, racial, geographical, hormonal, infertility, social, and family history (Wong and Auersperg, 2003). Most often, family history accounts for 5-10 % of all cases.

Caffeine, alcohol and smoking have all been speculated in the risk of developing EOC. Recent studies have shown a link between cigarette smoking and ovarian cancer. Evidence indicates that smoking may only increase the risk for mucinous ovarian tumors. Furthermore, the risk associated with EOC and caffeine was prevalent in women not previously taking oral contraceptives (Tworoger et. al., 2008). However, these preliminary studies warrant the need for future research to further understand the link between environmental and social factors associated with EOC.

EOC Pathogenesis

1. Putative genes involved in EOC pathogenesis

Cancer associated genes include the following: growth factor, growth factor receptors, signal transducers, and transcription factors. Normally expression of growth factors and growth factor receptors are carefully regulated. However, overexpression of growth factor receptors such as HER2/neu are

9

observed in 20% of ovarian cancer specimens and results in uncontrolled proliferation (Skirnisdottir et. al., 2001). Furthermore, genomic alteration of both the HER2-neu and EGFR genes is frequent (25%) in ovarian cancer. High polysomy of the EGFR gene was observed in 13% of the invasive epithelial cancers and amplification of the HER2-neu gene was found in 10% and correlated with a high expression level. EGFR/HER2-neu targeted therapies may potentially be a benefit for patients with invasive EOC (Vermeij et. al., 2008).

Cancer associated genes termed tumor suppressor genes, or anti-oncogenes encode proteins that inhibit cellular proliferation. The normal activity of genes within this group is cell cycle regulation. The suppressor of retinoblastoma, *Rb*, is a prototype of this group. Loss of heterozygosity at the *Rb* gene locus occurs in 30% of ovarian cancers compared to *Rb* pathway abnormalities which occur in 80% of ovarian cancer patients. Likewise, in advance ovarian cancers 50-70% of patients had gene alterations or expression in a nuclear phosphoprotein, p53. p53 is a transcription factor that regulates the cell cycle and thus functions as a tumor suppressor (Hashiguch et. al., 2001). Loss of heterozygosity at 17p13 was identified in a high proportion of advanced stage serous adenocarcinomas (Eccles et. al., 1992).

Genes that regulate programmed cell death and encode proteins that either block or induce apoptosis are believed to be involved in EOC. The prognostic importance of the biologic factors p53, bcl-2, and bax, which are key regulators of apoptosis, was identified in patients with early stage EOC (Skirnisdóttir et. al., 2002). Furthermore, mutations in tumor suppressor genes

such as BRCA1/BRCA2 (Pal et. al., 2005) are also found in EOC patients. In

addition such genes have been used as biomarkers for treatment of patients with

EOC using chemotherapy (Yurkovetsky et. al., 2006). Investigations show that

inhibition of endogenous BRCA1 expression in ovarian cancer cell lines results in

increased sensitivity to platinum therapy and decreased sensitivity to

antimicrotubule agents. In addition, it is shown that patients with low/intermediate

levels of BRCA1 mRNA have a significantly improved overall survival following

treatment with platinum-based chemotherapy in comparison with patients with

high levels of BRCA1 mRNA (Quinn et. al., 2007).

Conversion of proto-oncogenes to oncogenes has been associated with

cellular transformation and/or disease progression. The resulting altered gene

products and enhanced expression of gene products may initiate and/or

propagate events leading to transformation.

Frequent ovulation may increase the risk of EOC as a result of repeated

rupture and repair of ovarian surface epithelium. Recent studies indicate that

inflammation may also play a role in developing cancer. Inflammation is

characteristic of the peritoneum of EOC and understanding the linkage between

the coagulation cascade and the cytokines/chemokines involved in inflammation

may lead to a new approach to cancer therapeutics. In addition, recent evidence

supports the role of the coagulation pathway and inflammation in promoting

tumor cell progression and the formation of ascites. Studies have shown that a

number of genes involved in the coagulation cascade and genes encoding

proteins associated with inflammatory responses demonstrated altered

expression in the pelvic peritoneum and stroma, as well as the vicinity of EOC implants. Coagulation pathway proteins involved in tumorigenesis consist of thrombin, protease activated receptor, tissue factor, fibrinogen and fibrin. Several other coagulation regulatory proteins including heparin cofactor-II and epithelial protein C receptor (EPCR) were also upregulated in the peritoneum of EOC (Wang et. al., 2005).

2. Changes in pathology leading to EOC

Pathological changes in ovarian surface epithelium (OSE) have been indicated in EOC. Researchers believe that these changes in OSE may result in development and/or progression of epithelial ovarian carcinomas. OSE is a monolayered squamous-to cuboidal epithelium. OSE is characterized by keratin types 7, 8, 18, and 19, which represent the keratin complement typical for simple epithelia. OSE is distinguished from extraovarian mesothelium, apical microvilli, and a basal lamina due to the expression of mucin antigen MUC1, 17B-hydroxysteroid dehydrogenase, and cilia. Normal OSE contact and epithelial integrity is maintained by incomplete tight junctions, integrins, and cadherins.

A dense collagenous connective tissue layer, tunica albuginea, provides an inherent barrier against bioactive agents between the ovarian stroma and OSE. With age the human ovary assumes irregular contours and forms OSE-lined surface invaginations and epithelial inclusion cyst in the ovarian cortex. Within these clefts and cyst ovarian cells assume columnar shapes. Over time, the OSE within these surface invaginations are susceptible to metaplastic changes. OSE secrete IL-6 and IL-1 both of which result in proliferation of

ovarian cells and/or the release of autocrine growth regulators resulting in

changes in gene expression which promotes neoplasia. IL-1 induces TNFα

which is a mitogen for OSE leading to immortalization of cells and selective

growth advantages. Furthermore, autocrine mechanisms via OSE derived

cytokines and hormones within inclusion cyst allow accumulation of blood borne

bioactive agents that would otherwise diffuse on the ovarian surface. (Auersperg

et. al., 2001).

3. Tumor Antigens

The significance of identifying tumor antigens and the immune response to

these antigens may help increase the effectiveness of cancer therapy. Prior to

the development of cancer vaccines researchers have identified and

characterized of tumor antigens. During the past decade many tumor antigens

have been identified (Ghazizadeh et. al., 1997, Wang et. al., 1996, Odunsi et. al.,

2003, Yakirevich et. al., 2003). Tumor antigens may be categorized into two

main groups: tumor-specific antigens (TSA) and tumor-associated antigens

(TAA). Tumor specific antigens are expressed only on tumor cells and not on

normal cells. TSA can be presented with class I HLA molecules and induce a

cell-mediated response by tumor-specific CTLs. TAAs are expressed on tumor

and normal cells as well as embryonal or fetal cells (Kawakami et. al., 1994,

Bakker et. al., 1994 and Wang et. al., 1996).

Cancer testis (CT) antigens are promising targets for the development of

human cancer vaccines. Important characteristics of CT antigens are high

expression levels in adult male germ cells, absence of expression in other normal

adult tissues, and aberrant expression in a variable proportion of a wide range of different cancer types. They are also expressed in fetal ovarian cells (Pal et. al., 2005 and Nelson et. al., 2007). The CT antigens reported to be expressed frequently in EOC include: NY-ESO-1, MAGE-A1, and MAGE-A4 (Odunsi et. al., 2003, van den Eynde et. al., 1995, and Yakirevich et. al., 2003). In addition to CT antigens sialyl-Tn and CA125 are antigens currently used as ovarian cancer markers. Sialyl-Tn is a carbohydrate associated with MUC1 mucin, which is expressed by up to 90% of ovarian tumors, and has been a popular choice of antigen for several past clinical trials (Ghazizadeh et. al., 1997). Cancer Antigen 125 (CA125), also known as MUC16, is most often used to determine tumor growth in vivo. Doubling or halving of the CA125 serum values correlated with tumor progression or regression, respectively (Yurkovetsky et. al., 2006). Many ovarian antigens have been identified as well as the ability of TIL to recognize peptides from these antigens in association with HLA. However, there are currently no studies that have identified definitive ovarian cancer antigens recognized by $\gamma\delta$ TCR+ T-cells.

Tumor Immunity

1. Immune cells involved in EOC

Tumor antigens have been shown to induce both humoral and cell mediated immune responses to tumor antigens and both *in vivo* and *in vitro* experiments have shown tumor cell death due to immunological effector mechanisms. Tumor-infiltrating monoculear cells derived from the inflammatory infiltrate in human solid tumors and/or ascites. These cells consist of T

14

lymphocytes, natural killer cells (CD56+), B-lymphocytes, and macrophages (CD68+). T lymphocytes can be grouped into two major lymphocyte populations CD3+ CD4+CD8-, CD3+CD4-CD8+. CD4+ helper T cells and CD8+ cytotoxic T cells play a role in anti-tumor responses.

a. Innate immunity cells

Natural killer (NK) cells and macrophage/monocytes have been implicated in antitumor effector response. In epithelial ovarian cancer the ovarian tumor marker MUC16 (CA125) inhibits the cytotoxic responses of human natural killer (NK) cells and down-regulates CD16 (Belisle et. al., 2007). NK cells belong to the family of cytotoxicity cells. NK cells have been shown to recognize tumor cells and induce killing of these cells. Furthermore following ligand binding activation of the NKG2D receptor on the surface of NK cells may lead to NK-cell-mediated tumor cell effector functions. Ligands for NKG2D have been found on several tumor cells. Stimulated macrophages have been shown expression of NKG2D on the cell surface as well. Activation through NKG2D leads to the production of NO and TNF-α in macrophages. In the case of EOC tumoricidal activity was reduced by inhibition of nitric oxide synthesis in vivo using the human epithelial ovarian cancer cell line, NIH:OVCAR3 for intraperitoneal transplantation (Farias-Eisner et. al., 1994). Monocytes and macrophages are involved in antibody-mediated mechanisms of tumor cell killing, such as antibody-dependent cell-mediated cytotoxicity (ADCC) and phagocytosis. These activated mononuclear leukocytes are important to the innate immune system and more importantly can be directly cytotoxic to tumor cells. Defective antitumor functions

involving monocyte-derived macrophages were shown in patients with EOC. This population of monocyte-derived macrophages were involved in suppression of T-cell proliferation through the production of interleukin (IL)-10 and transforming growth factor-α (Loercher et. al., 1999).

b. B-cells

Hybridomas have been prepared from the B cells of tumor patients that produce monoclonal antibodies. Furthermore, monoclonal antibodies have been developed against ovarian cancer cell surface antigens. Bevacizumab, anti-VEGF antibody has been shown to neutralize vascular endothelial growth factor (VEGF) (Burger et. al., 2007). These antibodies are not specific for antigens expressed exclusively on tumor cells. Bevacizumab has also been used in patients with colorectal carcinoma as well as other solid malignancies (Shih and Lindley, 2006). Antibody mediated destruction of tumor cells is attributed to complement activation, or antibody-dependent cell-mediated cytotoxicity in which Fc receptor-bearing macrophages or NK cells mediate the killing. Patients with EOC have shown production of anti-tumor antibodies following vaccination with tumor-associated antigens such as CA-125.

c. T-cells

CD8+ tumor associated lymphocytes isolated from patients with ovarian carcinoma demonstrate cytolytic activity towards autologous tumor cells in a TCR dependent manner (Ioannides et. al., 1991). Cytotoxic T lymphocytes derived from breast and ovarian cancer patients have been shown to recognize peptides from HER2/neu (Peoples et. al., 1995). Following analysis of different cytokine

profiles released by CD4+ and CD8+ T cells data suggest IFN-γ, GM-CSF, and IL-2 contribute to tumor regression (Aruga et. al., 1997). CD4+ helper T cells are not generally cytotoxic to tumors, however they may secrete cytokines as well as tumor necrosis factor (TNFα) or interferon-γ (IFN-γ). IFN-γ has been shown to induce apoptosis in ovarian cancer cells in vivo and in vitro (Wall et. al., 2003). To identify whether tumor infiltrating lymphocytes in patients with ovarian cancer are clonally expanded, V-specific PCR analysis were carried out using primers for the β-chain of $\alpha\beta$ TCR + T cell infiltrates. Experimental evidence indicates a substantial proportion of β-chain transcripts are present at the tumor site showing oligoclonal/monoclonal expansion in patients with ovarian cancer (Pappas et. al., 2005). The presence of clonally expanded $\alpha\beta$ TCR + T cells in patients with ovarian cancer is evidence that an antigen driven immune response has taken place in situ at the tumor site. A component of tumor infiltrating mononuclear cells in ovarian carcinoma is CD8+ and CD68+ cells. However, the frequency of these cells is suggested to relate with tumor type rather than the degree of tumor differentiation (Helal et. al., 2004). Patients with higher frequencies of intraepithelial CD8+ T cells demonstrated improved. In addition, favorable prognosis did not correlate to the amount of NY-ESO-1 or MAGE, CT antigen expression (Sato et. al., 2005).

Suppression of the host immune function plays an important role in the progression of cancer. In fact patients with advanced ovarian malignancies exhibit progressively impaired immune responses. More specifically epithelial cancers are frequently coated by a layer of carbohydrate-rich mucins (ie CA-125

and Sialyn Tn) that play a role in immune escape by blocking T cells interaction, shedding attacking antibodies from the cell surface and hindering access for CTL.

Suppressed T-cell activation is one characteristic of advanced ovarian cancer (Berek et. al., 2003). Regulatory T cells T(reg)s mediate homeostatic peripheral tolerance by suppressing autoreactive T cells. Disregulation or failure of host antitumor immunity may be caused by suppression of tumor-associated antigen-reactive lymphocytes mediated by T(reg) cells; however, definitive evidence that T(reg) cells have an immunopathological role in human cancer is lacking. Evidence indicates CD4(+)CD25(+)FOXP3(+) T(reg) cells in 104 individuals affected with ovarian carcinoma, show suppressed tumor-specific T cell immunity and these T(reg) cells contribute to growth of human tumors in vivo. Researchers show that tumor T(reg) cells are associated with reduced survival. Human T(reg) cells preferentially move to and accumulate in tumors and ascites, but rarely enter draining lymph nodes in later cancer stages. Tumor cells and microenvironmental macrophages produce the chemokine CCL22, which mediates trafficking of T(reg) cells to the tumor. This specific recruitment of T(reg) cells represents a mechanism by which tumors may foster immune privilege. Therefore, researchers believe, blocking T(reg) cell migration or function may help to defeat human cancer and lead to effective alternative immunotherapy (Curiel et. al., 2004).

Heat shock protein-10 (HSP-10) was detected in both sera and ascites of patiens with ovarian cancer. HSP-10 appeared to be produced and released

form ovarian tumor cells. This circulating HSP-10 suppressed T-cell expression of CD3-zeta, a key activation component in T cells. Researchers conclude that release of HSP-10 may be an important factor allowing the tumor to escape immune surveillance by suppression of T cell activation (Akoyl et. al., 2006). To design effective immune-based antitumor therapies depletion of Tregs may help achieve increased antitumor effects with immunotherapy. Other important factors involved in tumor escape include TGF-B1 and IL-10. Host problems also involve development of tolerance to self-antigen(s) and impaired immune function from previous chemoradiotherapy.

Although the precise evaluation of the immune response at the primary tumor site is currently being studied progress in the field will help to develop therapies for EOC and other related cancers.

2. Soluble factors involved in EOC

TGF-β has been shown be an important cytokine involved in inflammation in ovarian cancer. to stimulate tumor cell attachement and invasion by upregulation plasminogen activator inhibitor type I. TGF-β also deregulates expression of the MHC complex and deregulates costimulatory antigen expression by dendritic cells. Suppression of Th1-Th2 cells and the conversion of pro-cytotoxic T lymphocytes to cytotoxic T lymphocytes is also contributed to the presence of TGF-β. Other cytokines such as IL-6 upregulates tumor cell attachment and suppress Th1-Th2 transformation. IL-10 has been shown to suppress Th1-Th2 transformation and cytotoxic T lymphocytes activation, as well as inhibit T cell and IFN production (Curiel et. al., 2004).

Cytokines have been used for the treatment of tumors. IFN-γ directly inhibits human tumor cell growth and induces apoptosis. IFN-γ has been used in the treatment of patients with advanced ovarian cancer. 108 patients with residual disease following first-line cisplatin-based chemotherapy upon second look laparotomy were treated with i.p. IFN-γ twice a week for 3-4 months. Out of 98 patients assessed 23 were completely responsive and 8 patients were partially responsive to IFN-γ. In ovarian cancer IFN-γ had antiproliferative activity in 8 of 8 ovarian cancer cell lines and 11 0f 14 primary cultures. In two of six patients, there was a 90% reduction in tumor cells in ascites after IFN-γ treatment, and this was related to clinical benefit as assessed by intervals between paracentesis (Wall et. al., 2003).

Alpha-interferon (IFN-α) is a type I interferon, produced largely by leukocytes and also have antiproliferative effects on cells *in vitro*. IFN-α has been shown to increase class I MHC expression on various cell types. In EOC down regulation of HLA-1 has been shown as one of many mechanisms of tumor cell escape.

High doses of IL-2 administered in conjugation with adoptive cellular immunotherapy are associated with increased blood lymphocytes, NK and LAK cell activity. IL-2 may work by stimulating anti-tumor activity of NK cells and/or CTLs. However, the treatment of patients with high levels of IL-2 alone can be extremely toxic causing fever, pulmonary edema, and often shock. This is due to the production of other cytokines by T cells as a result of IL-2 activating CD25 ligand receptor. TNF has potent anti-tumor effects but like IL-2 having highly

toxic effects at doses necessary for tumor cell killing. In addition ovarian cancer cells have develop resistance to TNF receptor mediated induction of apoptosis as shown in ovarian cancer cell lines such as SKOV3.

<p align="center">γδ TCR+ T-cells</p>

While αβ TCR + T cells may prove to be effective in antitumor immunity one mechanism by which ovarian cancer cells evade the immune system is via down regulated HLA expression (Kooi et. al., 1996). Therefore, γδ TCR + T cells may provide an alternate mechanism for antitumor immunity indicating a need for studies similar to the aforementioned to identify EOC antigens and EOC antigen-specific γδ TCR + T cells.   In humans γδ T cells make up only a small percentage (1-5%) of spleen and lymph node T cells. The γδ TCR+ T cells account for nearly 1%-10% of T lymphocytes and thymocytes in the peripheral blood of humans.

1. Subsets of γδ TCR + T cells

Two groups of γδ TCR + T cells exist VγII(9)Vδ2 and Vδ1.   VγII(9)Vδ2 T cells as the major population can be found within the peripheral blood and play a role in intracellular pathogens and hematological malignancies. This group of γδ TCR + T cells has been shown to kill myeloma and lymphoma cells in vitro. Vδ1 are primarily line the epithelial layers of various organs, such as the small intestine, liver and reproductive tract (Bukowski et. al., 1995 and Kobayashi et. al., 2001).

2. Genetic organization of the T-cell receptor chain loci

Each chain of the TCR is composed of multiple regions; the V (variable region), the J (junctional region), the D (diversity region, found only in the β- and

δ-chain), and the constant (C) region. Each region is typically coded for by multiple gene segments within the locus of the chain. The γ-chain gene locus is located on chromosome 7, and consists of approximately 12 variable region (Vγ) gene segments (and only 8 out of the 12 gene segments are functional), 5 junctional region (Jγ) gene segments and 2 constant region (Cγ) gene segments. The Vγ consists of four groups; VγI includes Vγ2, Vγ3, Vγ4, Vγ5 and Vγ8, VγII consists of only Vγ9, VγIII consist of only Vγ10 and VγIV consist of only Vγ11. The VγI and VγII subgroups consist of about 95% of the γ-chain TCR+ T-cell transcripts. The Cγ consists of two groups. The Cγ1 group contains a cysteine residue in the second exon of the gene that may function in disulfide linkages with the corresponding Cδ chain. The second Cγ (Cγ2) contains no cysteine residues in exon 2 but has an exon 2 polymorphism; one subtype has two copies of exon 2 and the other subtype has three copies of exon 2. The TCR δ-chain gene locus is located within the TCR α-chain gene locus on chromosome 14 between the variable region and the junctional region. The δ-chain locus has three variable region (Vδ) gene segments, 3 joining region (Jδ) gene segments, 3 diversity region (Dδ) gene segments and one constant region (Cδ) segment. Because the δ-chain gene locus is within the α-chain gene locus, successful rearrangement of a δ-chain TCR transcript preferentially forms a heterodimer with a successfully rearranged γ-chain TCR transcript to form γδ TCR heterodimer (Butrum et al, 1996) and is expressed on the T-cell in which it was rearranged. This expression excludes the expression of an α-chain TCR

transcript, which preferentially forms a heterodimer with a successfully rearranged β-chain TCR transcript to form αβ TCR heterodimer, and vice versa. Hence, the expression of αβ TCR and the γδ TCR on same T-cell is mutually exclusive. The γδ TCR heterodimers can either be disulfide-linked, if the γ-chain rearrangement involves Cγ1 that contain cysteine residue in its exon 2 or can be non-disulfide linked γδ TCR heterodimer, if the γ-chain rearrangement involves Cγ2, which lacks the cysteine residue found in Cγ1 (Seki et. al., 1989). Frequency analysis suggests that the Jδ1 segment is the most frequently used Jδ segment, followed by Jδ3, and then in turn by Jδ2 (Davodeau et. al., 1994). Although the germ line genes of γδ TCR contains fewer variable (V) and junctional (J) region gene segments than that of αβ TCR+ T-cells, the potential for diversity in the γδ TCR+ T-cells is potentially higher due to various factors including, a) combinational joining of V-J, V-D-J gene segment joining, b) the presence of two or more tandemly rearranged segments in the diversity (D) regions of the δ-chain transcript, c) the junctional flexibility at the V-D and D-J junctions, and d) N-nucleotide insertions catalyzed by N-terminal de-oxynucleotidyl transferase enzyme (tdt). Rearrangement of the different V-D-J gene segments during maturation of lymphocytes, junctional flexibility and N-nucleotide addition creates a larger degree of diversity in the complement determining region 3 (CDR3) loops, i.e. the hypervariable region that contacts the antigen. The CDR3 loops of γδ TCR+ T-cells are more similar to that of the immunoglobulin of B-cells than to that of αβ TCR+ T-cells in their ligand binding domains. This is believed to be the fundamental difference in antigen recognition

23

between $\gamma\delta$ TCR+ T-cells and $\alpha\beta$ TCR+ T-cells, leading to speculations that $\gamma\delta$ TCR+ T-cells recognize antigens in a similar fashion to immunoglobulin receptors, i.e. whole proteins and not like the $\alpha\beta$ TCR+ T-cells that recognize peptides in association with MHC molecules.

Figure 1 – TCR genetic locus

Human TCR β chain locus (chromosome 7)

Human TCR α, δ chain locus (chromosome 14)

Human TCR γ chain locus (chromosome 7)

$$V\alpha\text{-}N\text{-}J\alpha\text{-}C\alpha$$
$$V\gamma\text{-}N\text{-}J\gamma\text{-}C\gamma$$
$$V\delta\text{-}N\text{-}D\delta1\text{-}N\text{-}D\delta2\text{-}N\text{-}J\delta\text{-}C\delta$$
$$V\beta\text{-}N\text{-}D\beta\text{-}N\text{-}J\beta\text{-}C\beta$$
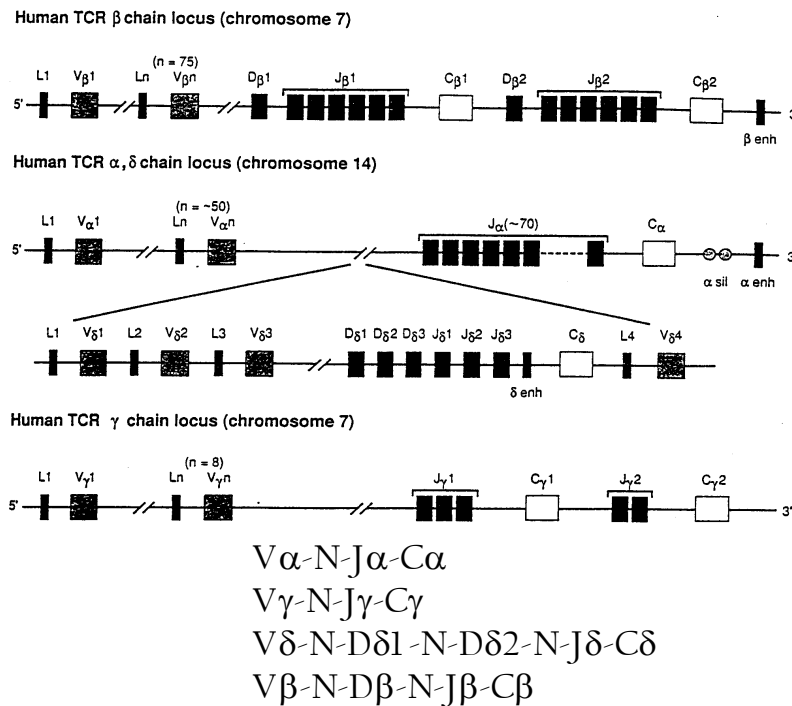
3. Antigen recognition of $\gamma\delta$ TCR+ T-cells

Majority of $\alpha\beta$ TCR + T- recognize processed antigen(s) as peptides restricted to MHC. In contrast, the recognition of antigen(s) by majority of $\gamma\delta$ TCR+ T-cells is still being elucidated and may not be MHC-restricted. $\gamma\delta$ TCR+ T-cells may recognize whole proteins expressed at a site distal from the MHC peptide-binding groove on the surface of antigen presenting cells (APCs). The proteins recognized by $\gamma\delta$ TCR+ T-cells do not require antigen processing.

24

Examples of ligands recognized by $\gamma\delta$ TCR+ T-cells include MHC class Ia, Ib and II, and serpins. $\gamma\delta$ TCR+ T-cells can also recognize antigens presented by CD1 molecules as well as natural or synthetic non-peptide antigen(s) including, superantigen(s), viral proteins, lipids, phosphates, N-formylated peptides and possibly carbohydrates (Tanaka et. al., 1995). Majority of $\gamma\delta$ TCR+ T-cells in humans are typically CD3+ CD4- CD8-, although some can express the CD4 or CD8 co-receptor. Functional analysis suggest that $\gamma\delta$ TCR+ T-cells have cytolytic activity against specific stimulating target cells and is inhibited by specific monoclonal antibody to HLA class I determinants suggesting that these CD3+ CD4- CD8- TCR+ T-cell clones recognize class I MHC determinants on target cells (Rivas et. al., 1989). This finding is significant because all cells in the body express class I MHC, suggesting that $\gamma\delta$ TCR+ T-cells may play a role in surveillance of tumor and "stressed" cells leading to their destruction. Other studies suggest that $\gamma\delta$ TCR+ T-cells may also function in wound repair and maintaining the integrity of epithelial cells that are exposed to the environment, and in immuno-regulation (Girardi et. al., 2006).

4. $\gamma\delta$ TCR + T cells in tumor immunity

Several findings suggest that $\gamma\delta$ TCR + T cells recognize certain tumor related antigens, in a TCR dependent manner, and play a role in tumor surveillance. Most recent data has identified nine peptides and two proteins for $\gamma\delta$ TCR + T cells, including human mutS homolog 2 (hMSH2) and heat shock protein HSP60. All nine tested epitope peptides not only bind to $\gamma\delta$ TCR + T cells, but also functionally activate $\gamma\delta$ TCR + T cells in vitro. Identification of HSP60

confirms the use of this method for the identification of $\gamma\delta$ TCR + T cells ligands as HSP60 is an identified ligand for TCR gamma delta. Also, hMSH2 is expressed on the surface of SKOV3 tumor cells and cytotoxicity of Vdelta2 $\gamma\delta$ TCR + T cells to SKOV3 cells was blocked by anti-hMSH2 antibody, suggesting that hMSH2 may be a new ligand for $\gamma\delta$ TCR + T cells. These findings support evidence that indicate the role of $\gamma\delta$ TCR + T cells in epithelial ovarian cancer (Chen et. al., 2008). Early studies utilized TCR negative Jurkat cells transfected with cDNA for $V\gamma II(9)V\delta 2$ TCR to demonstrate using more definitive methods the role of $\gamma\delta$ TCR-dependent recognition of Daudi Burkitt lymphoma and myeloma cells (Bukowski et. al., 1995). To determine the numbers of $\gamma\delta$ TCR + T cells in peripheral blood and tumor infiltrates in patients with renal carcinoma CD3+ T cells were analyzed for the presence of $\gamma\delta$ TCR + T cells compared to healthy individuals. Results showed that the $\gamma\delta$ TCR+ T cells expressing $V\gamma II(9)$ and $V\delta 2$ TCR were elevated in the peripheral blood of 10/41 patients (greater than 10% of T lymphocytes) and in 3 patients greater than 30% of T lymphocytes. The proportion of patients with elevated numbers increased with cancer stage and decreased after surgery. Following evaluation of the junctional diversity region the peripheral blood $\gamma\delta$ T cells showed oligoclonal rather than polyclonal expansion (Kobayashi et. al., 2001). During analysis of CD8+ T cells from ascites of colon cancer patients a $V\gamma II(9)V\delta 2$ T cell clone was isolated showing tumor cell recognition which was HLA-class I-independent but IPP and ICAM-1 dependent (Corvaisier et. al., 2005).

Vδ1 $\gamma\delta$ TCR + T cells are believed to be important in infections and malignancies. A study using human intestinal Vδ1+ T lymphocytes showed that Vδ1 $\gamma\delta$ TCR+ T cells are able to recognize tumor cells of epithelial origins. This recognition was evident by the production of IFNγ and cytolytic activity of Vδ1 $\gamma\delta$ TCR+ T cells towards autologous and allogeneic colorectal cancer cells, renal cancer cells, and pancreatic cancer cells (Maeurer et. al., 1996).

The above evidence indicates the significance of studying $\gamma\delta$ TCR + T cells as they relate to tumor immunity. Identifying the mechanisms by which $\gamma\delta$ TCR + T cells recognized tumor antigens and their role in reducing and/or eliminating tumor growth, development, and progression will increase our understanding of T cell mediated tumor immunity. $\gamma\delta$ TCR + T cells may provide an additional approach for adoptive immunotherapy which is not subject to the expression of HLA-class I by tumor cells.

Thus far experimental evidence obtained has shown oligoclonal expansion of $\gamma\delta$ TCR+ T cells in patients with EOC. We have constructed full-length TCR transcripts of the most clonally expanded transcripts. Most recently we have generated retroviral vector containing γ-chain and δ-chain transcripts from one patient. Transduction experiments are currently underway and subsequent characterization studies will follow. Examination of T cell receptor γ-chain and δ-chain sequences showing oligoclonal expansion indicates an antigen-specific response. Identification of functional and antitumor activities will improve our understanding of the immune response during EOC disease progression and the role of $\gamma\delta$ TCR+ T cells in patients with EOC.

5. Homing signals for $\gamma\delta$ TCR+ T cells

Epithelial tumors consist of tumor infiltrating lymphocytes such as $\alpha\beta$ and $\gamma\delta$ T lymphocytes. $\gamma\delta$ TCR + T cells make up a small portion of this population. Some of these $\gamma\delta$ TCR + T cells are resisdent and recognize over expressed tumor antigens at the site. Furthermore, circulating $\gamma\delta$ T cells respond to IL-12 and also recognize tumor antigens. Natural killer receptor proteins 1A play a role in homing of circulating $\gamma\delta$ T cells to the site of tumor formation and also MIP1α, MIP1β, and RANTES. Chemotactic gradients target $\gamma\delta$ T cells to damaged tissue. The antigens are nonpeptide antigens such as phosphorylate thymidine related products involved in salvage pathway in nucleic acid synthesis and repair. This phosphorylate thymidine is over expressed by damaged or stressed cells. Other antigens may include protein antigens such as MHCI/MHCII and HSV glycoprotein or proteins with post translational modifications such as N-linked glycosylation. Malignant transformation and infections alter glycosylation patterns due to stress signals. Stress induced signals may induce expression and overproduction of antigens such as MICA/MICB both of which are molecules on neoplastic and normal epithelial and are MHC I related molecules, CD1.

6. Cytotoxic T lymphocytes

Cytotoxic T lymphocytes express either $\alpha\beta$ TCR or $\gamma\delta$ TCR+ CD3+ T-cells exhibit cytotoxicity following antigen driven TCR receptor stimulation/activation. These effector functions may be the result of intracellular infected cells, transformed cells, and rejection of transplants. The mechanisms involved in cell-mediated cytotoxicity include specific-antigen recognition and cell-to-cell contact.

During cell-to-cell contact adhesion molecules help to form stable conjugates.

Once the conjugate is formed two pathways are triggered which results in death

of the specific target cell. One pathway is a secretory pathway involving

receptor-triggered exocytosis of preformed secretory granules, while the other

uses receptor-induced surface membrane expre ssion of Fas ligand (FasL),

which cross-links Fas on target cells. CTL use both of these pathways to kill

target cells. However, during mutagenesis cancer cells have undergone genetic

alterations allowing the avoidance of tumor cell apoptosis.

Apoptotic signaling and execution induced by cytotoxic T lymphocytes

including $\gamma\delta$ TCR+ T cells may involve the activation of caspase proteinase which

cleave proteins on the basis of primary structure. The procaspases can be

divided into two classes: caspase-2, -8, -9 and –10 which contain long amino-

terminal prodomains and act as initiators. The second class includes caspase-3,

-6 and –7. Caspase 3 is the most common activated caspase and is involved in

DNA fragmentation. Procaspase-8 or –9 may activate Caspase 3.

CHAPTER 2
HYPOTHESIS AND SPECIFIC AIMS

The hypothesis to be tested in this study is whether $\gamma\delta$ TCR+ T-cells are clonally expanded in tumors from patients with EOC and whether they recognize/lyse EOC tumor cells.

The specific aims for this project are:

1. To determine whether T cells infiltrating solid EOC tumors contain oligoclonal populations of $\gamma\delta$ TCR+ T-cells. Specifically,

   a. Fresh (not expanded in culture) $\gamma\delta$ TCR+ T-cells infiltrating the EOC specimen, contain substantial proportions of identical γ-chain TCR+ T cells.

   b. Fresh (not expanded in culture) $\gamma\delta$ TCR+ T-cells infiltrating the EOC specimen, contain substantial proportions of identical δ-chain TCR+ T cells.

2. To construct full-length transcripts of the most clonally expanded and non-clonally expanded TCR + T-cell γI-chain and γII(9)-chain transcripts that are present in the EOC specimen examined, for use in expression using MSCV retroviral expression system.

3. To construct full-length transcripts of the most clonally expanded TCR + T-cell δ1-chain and δ2-chain transcripts that are present in the EOC specimen examined, for use in expression using MSCV retroviral expression system.

4. To determine whether T cells transduced with γ-chain and δ-chain TCR transcripts recognize ovarian tumor cells. Specifically,

   a. Caspase 9, 8, and 3 activity on ovarian carcinoma cell line (SKOV3, CAOV3 and/or OV2774) by γδ TCR+ transduced cell lines.

   b. Cytotoxicity of γδ TCR+ transduced cell lines to ovarian carcinoma cell line (SKOV3, CAOV3 and/or OV2774)

CHAPTER 3
MATERIALS AND METHODS

A) Tissue specimen collection and processing

Solid tumor and malignant ascites specimens form previously untreated patients with EOC were used in this study. Solid tumor specimens from patients with EOC were collected during therapeutic surgery and were immediately placed on ice upon removal. Fatty tissue, normal, and necrotic tissue were removed from the tumor specimens. In most specimens a small part of the tumor specimen was embedded onto optimum cutting technology (OCT) formulation, snap frozen in liquid nitrogen, and kept at $-70°C$ to be used for Immunohistochemistry. The rest of the tumor specimen was kept in liquid nitrogen and used for RNA preparation. In other tumor specimens the entire specimen was kept in liquid nitrogen and used for RNA preparation. Ascites specimens from patients with EOC were collected under sterile conditions with heparin added to 1U/ml of ascites. The IRB of Temple University Hospital approved these studies.

B) RNA preparation

Total RNA was isolated from solid tumor specimens, single cell suspensions derived from malignant ascites of patients with EOC, and PBMC from normal by the guanidinium thiocyanate phenol-chloroform extraction method using the TRIzol® RNA isolation solution (Invitrogen) according to the manufacturer's instructions. The quality of the RNA was determined by examining the 28S and 18S bands of the rRNA after agarose gel electrophoresis.

C) cDNA synthesis

CDNA was synthesized from oligo (dT) Not I
(TGCGGCCGCTTTTTTTTTTTTTT) – primed total RNA by using the Superscript II
(Invitrogen) cDNA synthesis kit following manufacturer's instructions. The first
strand of the cDNA of the isolated RNA was synthesized in a reaction using first-
strand buffer, dNTPs (25mM), Superscript II reverse transcriptase (Invitrogen)
and the primer (Genosys custom oligo, 500ug/mL) at 42^oC for one hour in a 20ul
reaction. The resulting cDNA/RNA hybrid underwent the second strand cDNA
synthesis in a 150 ul reaction of the second-strand buffer, 25mM dNTPs, E. coli
DNA polymerase, E. coli DNA ligase and RNAse H (Invitrogen) to remove the
RNA from the hybrid, at 16^oC for 2hrs. T4 DNA polymerase was added for
45mins at 16^oC followed by a phenol:chloroform extraction and ethanol
precipitation of the synthesized cDNA, washing with 600ul of 100% ethanol and
resuspended in nuclease free water.

D) V-specific PCR

PCR was performed using V-specific primers (γI-, γII(9)-, δ1-, and δ2-
chain) to amplify the gene of interest, which was the CDR3 region of the $\gamma\delta$ TCR
gene. The VγI subgroup (Vγ2-5) specific primer 5'-
TGCGGTGGGCCCTACTGGTGCTT-3' and 5'-
GCCTTCTGGAGCTTTGTTTCAG-3' Cγ primer. The VγII subgroup transcripts
VγII(9) specific primer 5'-TGCTGTCACTGCTCCACACATC-3' primer and 5'-
GCCTTCTGGAGCTTTGTTTCAG-3' Cγ primer. The Vδ2 specific primer used

was 5'-GTGTGGCCCAGAAGGTTACT – 3', Vδ2 – 5' –

CATTGAGTTGGTGCCTGAA – 3', Cδ 5'– CTTGGATGACACGAGATTTATT – 3'.

Each amplification reaction was conducted in a reaction containing optimized volumes of the template, 10mM dNTPs, 25mM MgCl$_2$, 10xPCR buffer, and 100U Platinum Taq polymerase (Invitrogen). The reaction conditions for the V-specific PCR amplification were denaturation (94ºC, 1min) annealing (57ºC 2min) for Vγ and (55ºC 2min) for Vδ, and elongation (72ºC, 3min), for 30 cycles; and a final extension at 72ºC for 20min.

E) Cloning and sequencing

VγI-, Vδ1-, VγII(9)-, Vδ2-chain V-specific primers were each used to amplify the CDR3 region from the cDNA of each sample. The PCR product was gel purified, cloned into the TA vector and sequenced. Specifically, the PCR products of each transcript were separated in a 1% agarose gel in 1x TAE and purified using sodium iodide (Geneclean kit), following the supplier's instructions. This was followed by ligation into the pCR2.1 vector with overhanging single 3' deoxythymidine residues (Invitrogen). The ligation products were added to "one-shot" chemically-competent *E. coli* cells (Invitrogen) on ice followed by a 42ºC heat shock treatment for 30 seconds before being placed back on ice. The cells were then incubated in 250ul SOC medium (GibcoBRL) in a horizontal shaker at 200rpm, 37ºC for an hour and plated onto agar plates containing X-gal (100ug/ml) and ampicillin (100ug/ml) to facilitate blue-white screening. After 18 hours of incubation, white colonies were cultured in LB/Amp media and the plasmids were isolated, using the Perfect Prep plasmid purification mini kit

(Eppendorf) following supplier's instructions. The transcripts underwent the

sequencing PCR amplification using the Big dye terminator sequencing kit v3.1

(Applied Biosystems) per manufacturer's instructions, and the PCR products

were purified using Amersham Biosciences Auto Seq^{TM} columns, denatured and

analyzed using an automated 3130 DNA sequencer (Applied Biosystems).

Computer analyses of the sequences and identification of the $\gamma\delta$ CDR3 region of

the gene was carried out by alignment comparisons to those in the

GenBank/EMBL databases using the BLAST sequence alignment program.

The maximum theoretical number of unique $\gamma\delta$ TCR+ T-cells in humans is

approximately 10^{19}. Therefore, the probability of finding by chance, two identical

copies of (γI-, δ1-, γII- or δ2-chain TCR+ T-cell) transcripts in a given independent

sample of T-cells is negligible. In rare cases during the transformation and

growth of the chemically competent *E. coli* cells, there is a possibility that the

transformed cell can undergo a cell division cycle resulting in the presence of 2

identical clones after sequencing. This occurs because during the log phase

growth of *E. coli* (ideal growth conditions), a cell undergoes a division in about

20-30 minutes, which could result in two doublings within 60 minutes (Hanahan

et. al., 1983), the amount of time the transformed cells are grown in SOC media

prior to plating. However, because of the heat shock, *E. coli* cells are found to

have a longer lag phase than usual and therefore, decrease the chance of

doubling within the hour incubation but in some rare cases, this may still occur.

Therefore, a doublet after sequence analysis, i.e. two identical TCR+ T-cell

transcripts might be due to a single transformed *E. coli*, which doubled during

transformation and growth as described above or might be evidence of a true clonal expansion.

F) Statistical analysis of sequencing data

Binomial distribution was employed to calculate the probability, p, that the number of observed multiple identical transcripts were statistically significant as previously described (Lin et. al., 2005, Xu et. al., 2003, and Snedecor and Cohran, 1989). Briefly, the results obtained was tested against the probability of observing; one unique copy of each transcript analyzed, two identical copies and all other transcripts expressed once and three identical copies and all other transcripts expressed only once.

G) Full-length TCR transcript construction

VγI/Vδ1-chain and VγII (9)-/Vδ2-chain TCR+ T-cell transcripts from patients with EOC were extracted and the full-length transcripts were constructed for each chain. The full-length constructs were designed using primers to amplify each third of the full-length transcript followed by a PCR-mediated ligation of the transcripts. Each segment was verified qualitatively by size on the gel and quantitatively by cloning and sequencing, as was the final full-length product. The first third i.e. segment 1, began from the initiating methionine (ATG) of the V-region to about 5 amino acids before the end of the V-region, to accommodate for junctional flexibility. The second third, (segment 2), extended from the last 10 amino acids of the V-region, included the N-(D in the case of δ-chain)-J region, to the first 6 amino acids of the C-(constant) region. The third segment, (segment 3) includes the beginning of the C-region to the stop codon (TAA). The three

segments of the full-length transcript overlapped sufficiently with each other to

facilitate a subsequent PCR-mediated ligation. After obtaining each segment,

the PCR product was verified by gel purification, cloning and sequencing. Then,

the subsequent ligation PCR steps were performed to construct a final full-length

transcript containing the most clonally expanded CDR3 region. The sketch of the

VγI/VγII(9) and Vδ1/Vδ2 full-length constructs is shown below in figure 2 and

figure 3, respectively.

Figure 2 - VγI/VγII (9) Full length construction diagram
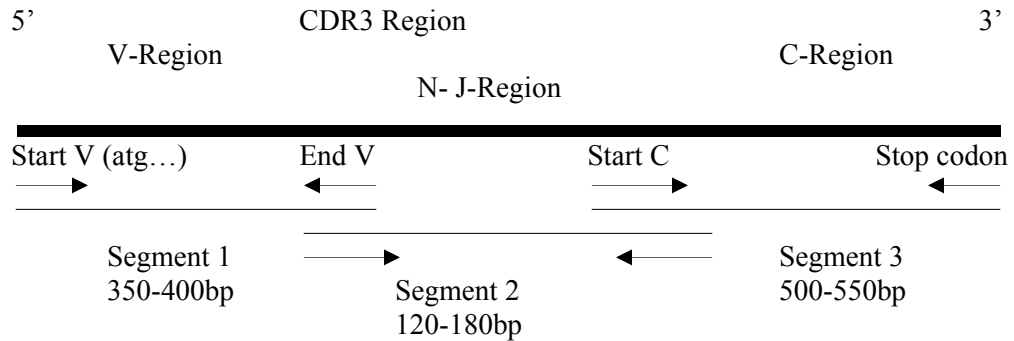
The primers for the construction VγI were as follows; Segment 1 forward,

5'ATGCGGTGGGCCCTACTGG3', Segment 1 reverse,

5'CCGTGTCATTATCTGGGGTCTTAG3'. Segment 2 forward,

5'CTCGGAGGGTGTTCCGTGTCATCAT3', Segment 2 reverse

5;ATAATGATCACGGTGGACC3', Segment 3 forward

5'GATAAACAACTTGACGCAGATGTTTCCC3', Segment 3 reverse

5'TTATGATTTCTCTCCATTGCAGCAG3'.

The primers for the construction of VγII(9) were as follows; Segment 1

forward, 5'ATGCTGTCACTGCTCCACACATC3', Segment 1 reverse,

5'CCGTGTCATCATCCATCGATACAG3', Segment 2 forward

5'TACTACTGTGCCTTGTGGGAGGTG3', Segment 2 reverse

5;ATAATGATCACGGTGGACC3', Segment 3 forward

5'GATAAACAACTTGACGCAGATGTTTCCC3', Segment 3 reverse

5'TTATGATTTCTCTCCATTGCAGCAG3'.

.

Figure 3 - Vδ1/Vδ2-chain full-length construction diagram
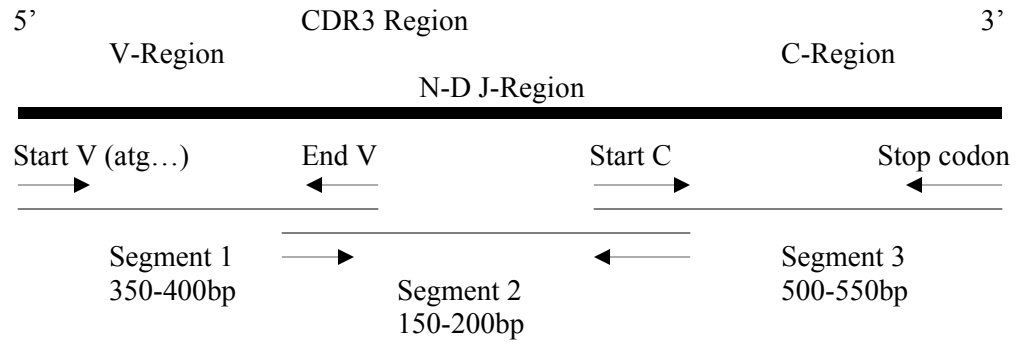
The primers for the construction of Vδ1 were as follows; Segment 1

forward, 5' ATGCTGTTCTCCAG 3', Segment 1 reverse,

5'GTTTCATACAGGCAGTTCAGGGTGC 3' Segment 2 forward,

5'CCATGAAGGAGAAGCGATCGGTAACTAC3' , Segment 2 reverse,

5'GGTATGAGGCTGACTTCTTGGTTCCAC3', Segment 3 forward,

GTGGAACCAAGAAGTCAGCCTCAT, Segment 3 reverse,

TTACAAGAAAAATAACTTGGCAGTCAAGAG .

The primers for the construction of Vδ2 were as follows; Segment 1

forward, ATGCAGAGGATCTCCTCCCTCATC , Segment 1 reverse,

GTAGTTACCGATCGCTTCTCCTTTCATGG , Segment 2 forward,

GCACCCTGAACTGCCTGTATGAAAC , Segment 2 reverse,

5'GGTATGAGGCTGACTTCTTGGTTCCAC3', Segment 3 forward,

GTGGAACCAAGAAGTCAGCCTCAT, Segment 3 reverse,

TTACAAGAAAAATAACTTGGCAGTCAAGAG .

Figure 4 – pMSCV expression vector (Clontech)
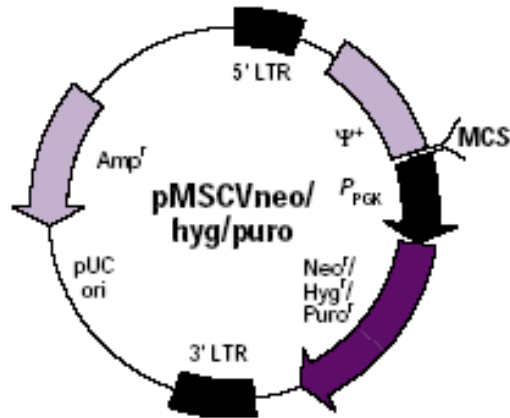
Figure 5 – γ-chain/δ-chain TCR retroviral vector multiple cloning site (MCS)
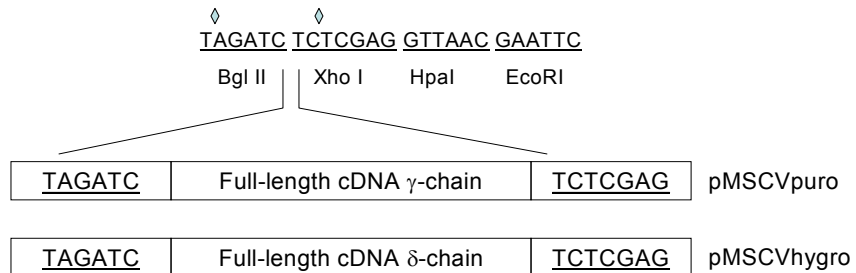
H) MSCV expression

The retroviral vector backbone used in this study, pMSCV, is a murine

stem cell virus vector, which uses an MSCV long terminal repeat (LTR) with

mutations allowing expression in a large host range (Figure 4). The NIH 3T3 fibroblast packaging cell line PT67 contains the gag-env-pol. Retroviral vectors with the packaging gene as well as containing specific γ- and δ-chain TCR transcripts were constructed (Figure 5). First, we obtained a pMSCV puromycin resistant plasmid (pMSCVpuro) and inserted our γ-chain cDNA of interest. We then constructed a similar neomycin resistant plasmid (pMSCVneo) containing our δ-chain cDNA of interest. Once our expression plasmid was constructed we transfected the NIH 3T3 fibroblast packaging cell line using the ProFection Mammalian Transfection System (Promega). Briefly, using a calcium-phosphate mediated co-precipitation with 10-20ug of plasmid vector, 2M $CaCl_2$, and water for a total volume of 500ul. This DNA solution was slowly added to 500ul of 2x HEPES solution until a opaque precipitate formed. Following a 30min incubation this precipitate was added to freshly cultured packaging cell line and placed in 37°C 5% CO_2 humidified incubator. Retroviral supernants were collected following 10-14 days of appropriated antibiotic selection according to the vector construct used. PT67 cells transfected with the pMSCVhygro were selected for 4-6 days with 300ug/ml of hygromycin, PT67 cells transfected with the pMSCVpuro were selected for 8-10days with 3ug/ml of puromycin and PT67 cells transfected with pMSCVneo were selected for 5-7days with 1mg/mL of G418. The retroviral supernants from each transfectant cell line was collected and used for subsequent fibronectin transduction experiments.

I) Transduction of Mutant Jurkat Cells

The JRT5.3 mutant jurkat cell line (ATCC) were washed in DPBS, then resuspended at a concentration of 1 x 10^6/ml in RPMI supplemented with sodium bicarbonate, 2x HEPES, glucose, 10%FBS, L-glutamine, penicillin and streptomycin. These TCR- mutant jurkat T cells were plated at 1 x 10^6/ml and cultured in vitro for 48-72 h before transduction. Next, the cells were transduced with retroviral vectors by transfer to culture dishes precoated with retroviral vectors. To coat culture plates with retroviral vectors the supernant was added to non-tissue culture-treated, six-well fibronectin coated plates (RetroNectin; Takara) and allowed to incubate at 4°C overnight. To these plates was added cells at a concentration of one half confluency in culture medium (3-4ml). Cells were then incubated overnight at 37°C, and the procedure was repeated the following day, after which the cells were expanded at 37°C in a 5% CO2 incubator and split as necessary to maintain cell density between 0.5 and 1 x 10^6 cells/ml. These single chain cells were selected in 6 well non-treated tissue culture plates. Those transduced with retroviral particles with the hygromycin resistant gene were selected for 6 days in media containing 500ug/ml hygromycin, puromycin resistant gene were selected for 6 days in media containing .25ug to .35ug/ml of puromycin and neomycin resistant gene were selected for 8-10 days in media containing 3mg-5mg/ml G418.

J) FACS analysis

Cell surface expression of $\gamma\delta$ TCR and CD3 molecules on TCR+ transduced T cells was measured by immunofluorescence using PE and FITC

conjugated Abs, as directed by the supplier of anti-TCR $\gamma\delta$ (Gibco). For analysis,

the relative log fluorescence of live cells was measured using a FACScan flow

cytometer (The Wistar Institute).

K) Cytotoxicity Assay

The in vitro cytotoxic activity of the expanded $\gamma\delta$ TCR+ transduced T cell

lines were evaluated by the Cytotox 96® a non-radioactive cytotoxicity assay.

The target cells used were tumor cell lines SKOV3, CAOV3 and OV2774. The

effector cells used were the, $\gamma\delta$ TCR+ transduced T cell lines. Using round

bottom 96-well non-treated tissue culture plates, the following experiments were

set up: constant number of target cells (1 x 10^4) and varying number of effector

cells (100:1, 50:1, 40:1, 10:1, and 1:1) to experimental wells, effector cells at

each effector cell concentration for effector cell spontaneous LDH release

control, target cells with no effector cells for target cell spontaneous LDH release

control, target cells and lysis solution (10x) for target maximum release control,

culture medium and lysis solution for volume correction control, and culture

medium for culture medium background control. The cells were then centrifuged

at 250 x g for 4 minutes followed by incubation at 37°C for 4.5 hours. Forty-five

minutes prior to supernatant harvest, lysis solution (10x) was added to target cell

maximum and culture medium volume correction control wells. 50ul of the

supernatant from each well of the assay plate was harvest and added to a flat-

bottom enzymatic assay plate. 50ul of the substrate/buffer mix was added to

each well of the plate containing supernatant. The plate was covered and

incubated at room temperature and protected from light for 30 minutes. 50ul of

stop solution was added to the plate and sample absorbance was recorded

(490nm). And the percentage of cytotoxicity was calculated as:

% Cytotoxicity = Experimental-Effector Spontaneous-Target Spontaneous/Target

Maximum-Target Spontaneous x 100

L) Measurement of Caspase Activity

The Caspase-Glo® Assay (Promega) luciferase based assay was used to

observe caspase 3/7, 8, and 9 activity in SKOV3, CAOV and OV2774 following

co-incubation of these targets with $\gamma\delta$ TCR+ transduced T cell lines. Briefly,

following caspase cleavage, the substrate luciferase (amino-luciferin) is released,

resulting in the luciferase reaction and production of light measured by

luminometer. Using round bottom 96-well non-treated tissue culture plates target

cells were seeded at 1 x 10^4 cells/well and incubated for 4 hours prior to

addition of the effector cells. The effector cells were added to these wells at a

10:1 and 1:1 effector to target ratio, effector cells were added to wells containing

no target cells and target cells were added to wells containing no effector cells to

account for background caspase production. For caspase 9 and 8 the samples

(effector plus target) were added to an equal volume of reagent following a 45min

co-incubation period. However, to measure caspase 3 activity the samples

(effector plus target) were added to an equal volume of reagent following 5 hours

of incubation.

CHAPTER 4
RESULTS

A) Sequencing results of the VγI-chain TCR Transcripts

Previous studies done in our laboratory indicate the following results: (a) The presence of $\alpha\beta$ TCR + T-cell infiltrating solid tumor of patients with EOC (data not shown) by immunohistochemical staining using specific monoclonal antibodies to CD3+, CD4+, and CD8+ molecules, (b) The presence of statistically significant oligoclonal β-chain TCR transcripts in the solid tumor of patients with EOC (Pappas et. al., 2005) by the amplification, cloning and sequencing, (c) The presence of $\gamma\delta$ TCR+ and CD3+ T-cells infiltrating the solid tumor of patients with EOC.

To establish whether fresh (not expanded in culture) mononuclear cells infiltrating the solid tumor of patients with EOC contain oligoclonal T-cell populations, γI-chain TCR transcripts from seven patients were amplified, cloned and sequenced. Of the results obtained, less than 2.4% of the deduced VγI-N-Jγ transcripts were nonproductively rearranged and these were not included in the analysis. The productively rearranged transcripts were analyzed using the GENBANK database. Results revealed the presence of statistically significant substantial proportions of identical VγI-chain TCR+ T-cell transcripts in five out of seven solid tumor specimens obtained from patients with EOC, suggesting the presence of oligoclonal populations of T-cells infiltrating the solid tumor from patients with EOC.

Table 1. Vγl-chain TCR+ T-cell Transcripts (CDR3 Region) Expressed in the Solid Tumor from patient OV38T

Transcript No.	Vγ	N	Jγ	Transcript Frequency	p-value 1/39	2/39	3/39
1	Y Y C A T W D G P		Y Y K K	Vγ2Jγ1.3/2.3			
	TATTACTGTGCCACCTGGGATGGGCCA		TATTATAAGAAA	15/39 38%	<0.0001	<0.0001	<0.0001
11	Y Y C A T W D		Y Y K K	Vγ2Jγ1.3/2.3			
	TATTACTGTGCCACCTGGGAC		TATTATAAGAAA	11/39 33%	<0.0001	<0.0001	<0.0001
22	Y Y C A T W G G I R N S L A V E Y Y K K			Vγ2Jγ1.3/2.3			
	TATTACTGTGCCACCTGGGGCGGTATAAGAAACTCTTTGGCAGTGGAATATTATAAGAAA			8/39 20%	NS	NS	NS
15	Y Y C A T W D G Y E S D		Y Y K K	Vγ2Jγ1.3/2.3			
	TATTACTGTGCCACCTGGGACGGCTACGAGTCGGAT		TATTATAAGAAA	1/39 3%	NS	NS	NS
4	Y Y C A T W D G P R E L G		Y Y K K	Vγ2Jγ1.3/2.3			
	TATTACTGTGCCACCTGGGACGGGCCCCGTGAGTTGGGCAAAAAA		TATTATAAGAAA	1/39 3%	NS	NS	NS
9	Y Y C A T W D E D		Y Y K K	Vγ2Jγ1.3/2.3			
	TATTACTGTGCCACCTGGGAC GAAGAT		TATTATAAGAAA	1/39 3%	NS	NS	NS
7	Y Y C A T W D		Y Y K K	Vγ2Jγ1.3/2.3			
	TATTACTGTGCCACCTGGGAC		TATTATAAGAAA	1/39 3%	NS	NS	NS
2	Y Y C A T W D G W G		Y Y K K	Vγ2Jγ1.3/2.3			
	TATTACTGTGCCACCTGGGACGGGCTGGGG		TATTATAAGAAA	1/39 3%	NS	NS	NS

Table 2. Vγl-chain TCR+ T-cell Transcripts (CDR3 Region) Expressed in the Solid Tumor from patient OV26T

Transcript No.	Vγ	N	Jγ	Transcript Frequency	p-value 1/35	2/35	3/35
1	Y Y C A T W D	R L P R P	Y Y K K L	Vγ2Jγ1.3/2.3			
	TATTACTGTGCCACCTGGGAC	AGGCTGCCGCGGCCT	TATTATAAGAAACTC	35/35 100%	<0.0001	<0.0001	<0.0001

Table 3. Vγl-chain TCR+ T-cell Transcripts (CDR3 Region) Expressed in the Solid Tumor from patient OV42T

Transcript No.	Vγ	N	Jγ	Transcript Frequency	p-value 1/17	2/17
22	Y Y C A T W D G	P L F	K K L F G S	Vγ2Jγ1.3/2.3		
	TATTACTGTGCCACCTGGGACGGG	CCCTTGTTT	AAGAAACTCTTTGGCAGT	10/17 59%	<0.0001	<0.0001
3	Y Y C A T W D G	P E K P	F G S G T T	Vγ2Jγ1.3/2.3		
	TATTACTGTGCCACCTGGGACGGG	CCGGAGAAACCC	TTTGGCAGTGGAACAACA	2/17 12%	NS	NS
21	Y Y C A T W D G	P G	N Y K K L F	Vγ2Jγ1.3/2.3		
	TATTACTGTGCCACCTGGGACGGT	CCAGGG	AATTATAAGAAACTCTTT	2/17 12%	NS	NS
14	Y Y C A T W D G	H	Y K K L F G S	Vγ2Jγ1.3/2.3		
	TATTACTGTGCCACCTGGGATGGG	CAC	TATAAGAAACTCTTTGGCAGT	2/17 12%	NS	NS
18	Y Y C A T W D G	P E	K L F G S	Vγ2Jγ1.3/2.3		
	TATTACTGTGCCACCTGGGACGGG	CCGGAG	AAACTCTTTGGCAGT	1/17 6%	NS	NS

Table 4. Vγl-chain TCR+ T-cell Transcripts (CDR3 Region) Expressed in the Solid Tumor from patient OV31T

Transcript No.	Vγ	N	Jγ	Transcript Frequency	p-value 1/44	2/44
3	Y Y C A T W D G	H F	Y K K L F G	Vγ2Jγ1.3/2.3		
	TATTACTGTGCCACCTGGGACGGG	CATTTT	TATAAGAAACTCTTTGGC	44/44 100%	<0.0001	<0.0001

Table 5. Vγl-chain TCR+ T-cell Transcripts (CDR3 Region) Expressed in the Solid Tumor from patient OV805T

Transcript No.	Vγ	N	Jγ	Transcript Frequency	p-value 1/19	2/19
9	Y Y C A T W D G TATTACTGTGCCACCTGGGACGGG	R E CGAGAG	D W I K T F A GATTGGATCAAGACGTTTGCA	Vγ3Jγ1.3/2.3 3/19 16%		
					NS	NS
23	Y Y C A T W D G TATTACTGTGCCACCTGGGACGGG	P CCC	K K L F G AAGAAACTCTTTGGC	Vγ3Jγ1.3/2.3 3/19 16%	NS	NS
22	Y Y C A T W D G TATTACTGTGCCACCTGGGACGGC	H R P CATCGACCC	K K L F G S AAGAAACTCTTTGGCAGT	Vγ2Jγ1.3/2.3 2/19 11%	NS	NS
20	Y Y C A T W D G TATTACTGTGCCACCTGGGACGGG	L L N CTCCTTAAT	K K L F G S AAGAAACTCTTTGGCAGT	Vγ5Jγ1.3/2.3 2/19 11%	NS	NS
14	Y Y C A T W D TATTACTGTGCCACCTGGGAC	A S N GCTTCCAAT	Y K K L F G S TATAAGAAACTCTTTGGCAGT	Vγ5Jγ1.3/2.3 2/19 11%	NS	NS
17	Y Y C A T W D G TATTACTGTGCCACCTGGGACGGG	P L F CCCTTGTTT	K K L F G S AAGAAACTCTTTGGCAGT	Vγ4Jγ1.3/2.3 1/19 5%	NS	NS
18	Y Y C A T W D G TATTACTGTGCCACCTGGGACGGG	G K Q N GGGAAGCAAAAT	Y Y K K L F G S TATTATAAGAAACTCTTTGGCAGT	Vγ3Jγ1.3/2.3 1/19 5%	NS	NS
11	Y Y C A T W D G TATTACTGTGCCACCTGGGACGGG	P R CCTCGT	Y Y K K L F G S TATTATAAGAAACTCTTTGGCAGT	Vγ2Jγ1.3/2.3 1/19 5%	NS	NS
4	Y Y C A T W D G TATTACTGTGCCACCTGGGACGGG	P N CCAAAT	Y Y K K L F G S TATTATAAGAAACTCTTTGGCAGT	Vγ2Jγ1.3/2.3 1/19 5%	NS	NS
5	Y Y C A T W D G TATTACTGTGCCACCTGGGACGGG	P G CCGGGG	K L F G S G AAACTCTTTGGCAGTGGA	Vγ2Jγ1.3/2.3 1/19 5%	NS	NS
21	Y Y C A T W TATTACTGTGCCACCTGG	M S V I D ATGTCGGTTATTGAT	Y K K L F G S TATAAGAAACTCTTTGGCAGT	Vγ2Jγ1.3/2.3 1/19 5%	NS	NS
7	Y Y C A T W D G TATTACTGTGCCACCTGGGACGGG		Y Y K K L F G TATTATAAGAAACTCTTTGGC	Vγ2Jγ1.3/2.3 1/19 5%	NS	NS

Table 6. Vγl-chain TCR+ T-cell Transcripts (CDR3 Region) Expressed in the Solid Tumor from patient OV1T

Transcript No.	Vγ	N	Jγ	Transcript Frequency	p-value 1/17 2/17
11	Y Y C A T W D G TATTACTGTGCCACCTGGGATGGG		Y Y K K L F TATTATAAGAAACTCTTT	Vγ2Jγ1.3/2.3 3/17 18%	NS NS
13	Y Y C A T W D G TATTACTGTGCCACCTGGGACGGG	F TTT	Y Y K K L F TATTATAAGAAACTCTTT	Vγ2Jγ1.3/2.3 2/17 12%	NS NS
19	Y Y C A T W TATTACTGTGCCACCTGG	V N GTGAAT	Y Y K K L F TATTATAAGAAACTCTTT	Vγ2Jγ1.3/2.3 1/17 6%	NS NS
20	Y Y C A T W D TATTACTGTGCCACCTGGGAT	L T CTCACT	G W F K I F GGTTGGTTCAAGATATTT	Vγ2Jγ1.1 1/17 6%	NS NS
17	Y Y C A T W TATTACTGTGCCACCTGG	V R L G S Y Y K K L F GTCCGGCTGGGGTCTTATTATAAGAAACTCTTT		Vγ2Jγ1.3/2.3 1/17 6%	NS NS
22	Y Y C A T W D TATTACTGTGCCACCTGGGAT	V GTA	G W F K I F GGTTGGTTCAAGATATTT	Vγ2Jγ1.1 1/17 6%	NS NS
14	Y Y C A T W D TATTACTGTGCCACCTGGGAT	P K CCCAAG	N Y Y K K L F AATTATTATAAGAAACTCTTT	Vγ2Jγ1.3/2.3 1/17 6%	NS NS
12	Y Y C A T W D G TATTACTGTGCCACCTGGGATGGG	T TAC	N Y Y K K L F AATTATTATAAGAAACTCTTT	Vγ2Jγ1.3/2.3 1/17 6%	NS NS
10	Y Y C A T W TATTACTGTGCCACCTGG	P L V T CCCCTGGTTACG	N Y Y K K L F AATTATTATAAGAAACTCTTT	Vγ2Jγ1.3/2.3 1/17 6%	NS NS
5	Y Y C A T W D TATTACTGTGCCACCTGGGAC	K P G K AAGCCTGGGAAG	Y Y K K L F TATTATAAGAAACTCTTT	Vγ2Jγ1.3/2.3 1/17 6%	NS NS
8	Y Y C A T W D TATTACTGTGCCACCTGGGAT	N P S AATCCGTCT	Y Y K K L F TATTATAAGAAACTCTTT	Vγ2Jγ1.3/2.3 1/17 6%	NS NS
11	Y Y C A T W D TATTACTGTGCCACCTGGGAT	A R D GCCAGGGAT	K K L F AAGAAACTCTTT	Vγ2Jγ1.3/2.3 1/17 6%	NS NS
6	Y Y C A T W D TATTACTGTGCCACCTGGGAT	P S Q G CCTTCCCAGGGG	Y K K L F TATAAGAAACTCTTT	Vγ2Jγ1.3/2.3 1/17 6%	NS NS
1	Y Y C A T W D G TATTACTGTGCCACCTGGGATGGG	R AGG	Y Y K K L F TATTATAAGAAACTCTTT	Vγ2Jγ1.3/2.3 1/17 6%	NS NS

Table 7. Vγl-chain TCR+ T-cell Transcripts (CDR3 Region) Expressed in the Solid Tumor from patient OV22T

Transcript No.	Vγ	N	Jγ	Transcript Frequency	p-value 1/26	2/26
26	Y Y C A T W D P V	Y Y K K	Vγ2Jγ1.3/2.3			
	TATTACTGTGCCACCTGGGAC CCGGTG	TATTATAAGAAA	11/26 42%	<0.0001	<0.00001
2	Y Y C A T W D V	Y Y K K	Vγ2Jγ1.3/2.3			
	TATTACTGTGCCACCTGGGAC GTT	TATTATAAGAAA	8/26 31%	<0.018	<0.028
24	Y Y C A T W D L P	Y Y K K	Vγ2Jγ1.3/2.3			
	TATTACTGTGCCACCTGGGAC ACCCCG	TATTATAAGAAA	3/26 8%	NS	NS
25	Y Y C A T W D P R	Y Y K K	Vγ2Jγ1.3/2.3			
	TATTACTGTGCCACCTGGGAC CCGAGA	TATTATAAGAAA	2/26 8%	NS	NS
22	Y Y C A T W D P	Y Y K K	Vγ2Jγ1.3/2.3			
	TATTACTGTGCCACCTGGGAC CCG	TATTATAAGAAA	2/26 8%	NS	NS

Table 8. Summary of clonal expansion of Vγl-chain TCR+ T -cell transcripts in the solid tumor of patients with EOC

OV38T: 15/39:#1: 38%:CDR3:YYCATWDGPYYKK
OV38T: 11/39:#11:33%:CDR3:YYCATDYYKK
OV26T: 35/35:#1:100%:CDR3:YYCATWDRLPRPYYKK
OV42T: 10/17:#22:59%:CDR3:YYCATWDGPLFKKLFGS
OV31T: 44/44:#3:100%:CDR3:YYCATWDGHFYKKLFGS
OV22T: 11/26:#26:42%:CDR3:YYCATWDPVYYKK

Table 9. Percent clonal expansion of Vγl-chain TCR+ T-cell transcripts in the solid tumor of patients with EOC

EOC Patient Sample	% Clonal Expansion
OV38T #1	38%
#11	33%
OV26T	100%
OV42T #22	59%
OV31T	100%
OV22T #26	42%

In patient OV38T, analysis of the Vγl-chain TCR+ T-cell transcripts

revealed that 15 out of 39 (38.4%) transcripts sequenced each had a CDR3

region identical to that of OV38T transcript number 1 with its CDR3 region as:

Vγ2Jγ1.3/2.3: YYCATWDGPYYKKLFGSGTTLVVT: $p < 0.05$ (a statistically

significant oligoclonal expansion) (see table 1). 12 out of 39 (30.7%) transcripts

each had a CDR3 region identical to that of OV38T transcript number 11 with its

CDR3 region as: Vγ2Jγ1.3/2.3 YYCATWDYYKKLFGSGTTLVVT: $p < 0.001$ (a

statistically significant oligoclonal expansion. 8 out of 39 (20.5%) transcripts

each had a CDR3 region identical to that of OV38T transcript number 22 with its

CDR3 region as: Vγ2Jγ1.3/2.3 YYCATWGYYKKLFGSGTTLVVT: $p > 0.05$ (a

statistically insignificant oligoclonal expansion. There were four unique non-

clonally expanded TCR+ T-cell transcripts, OV38T numbers 15, 4, 9, and 2, each

with a unique CDR3 region as (see Table 1): Vγ2Jγ1.3/2.3

YYYCATWDG<u>YESD</u>YYKKLFSGTLVVT: 2.6% p>0.05, Vγ2Jγ1.3/2.3

YYYCATWDG<u>PRELG</u>YYKKLFSGTLVVT: 2.6% p>0.05, Vγ2Jγ1.3/2.3

YYYCATWDG<u>ED</u>YYKKLFSGTLVVT: 2.6% p>0.05, Vγ2Jγ1.3/2.3

YYYCATWDGWGYYKKLFSGTLVVT: 2.6% p>0.05, respectively.

In patient OV26T, sequence analysis of VγI-chain TCR+ T-cell transcripts

revealed that 35 out of 35 (100%) TCR+ transcripts sequenced each had a

CDR3 region identical to that of OV26T number 1, each with a CDR3 region (see

Table 2) Vγ2Jγ1.3/2.3 YYYCATWD<u>RLPRP</u>YYKKLFSGTLVVT: p<0.05.

In patient OV42T, sequence analysis of VγI-chain TCR+ T-cell transcripts

revealed that 10 out of 17 (58.8%) TCR+ transcripts sequenced each had a

CDR3 region identical to that of OV42T number 22 with its CDR3 region as:

Vγ2Jγ1.3/2.3 YYYCATWDG<u>PLF</u>KKLFSGTLVVT: p<0.05 (a statistically significant

oligoclonal expansion) (see Table 3). 2 out of 17 (11.7%) unique transcripts with

CDR3 region identical to that of OV42T number 3 with its CDR3 region as:

Vγ2Jγ1.3/2.3 YYYCATWD<u>PEKP</u>FSGTLVVT: p>0.05 (a statistically insignificant

oligoclonal expansion). 2 out of 17 (11.7%) unique transcripts with CDR3 region

identical to that of OV42T number 21 with its CDR3 region as: Vγ2Jγ1.3/2.3

YYYCATWD<u>PGN</u>YKKLFSGTLVVT: p>0.05 (a statistically insignificant oligoclonal

expansion). 2 out of 17 (11.7%) unique transcripts with CDR3 region identical to

that of OV42T number 14 with its CDR3 region as: Vγ2Jγ1.3/2.3

YYYCATWD<u>H</u>YKKLFSGTLVVT: p>0.05 (a statistically insignificant oligoclonal

expansion). 2 out of 17 (11.7%) unique transcripts with CDR3 region identical to that of OV42T number 18 with its CDR3 region as: Vγ2Jγ1.3/2.3 YYYCATWD<u>PE</u>KLFSGTLVVT: p>0.05 (a statistically insignificant oligoclonal expansion).

In patient OV31T, sequence analysis of VγI-chain TCR+ T-cell transcripts revealed that 44 out of 44 (100%) TCR+ T-cell transcripts sequenced each had a CDR3 region identical to that of OV31T number 3 with its CDR3 region as: Vγ2Jγ1.3/2.3 YYYCATWDG<u>HF</u>YKKLFSGTLVVT: p<0.05 (see Table 4).

In patient OV805T, sequence analysis of VγI-chain TCR+ T-cell transcripts revealed that 3 out of 19 (15.9%) TCR+ T-cell transcripts sequenced each had a CDR3 region identical to that of OV805T number 9 with its CDR3 region as: Vγ3Jγ2.1 YYYCATWD<u>RED</u>WIKTFA: p>0.05 (see Table 5). 3 out of 19 (15.9%) TCR+ T-cell transcripts each had a CDR3 region identical to that of OV805T number 23 with its CDR3 region as: Vγ2Jγ1.3/2.3 YYYCATWD<u>P</u>KKLFSGTLVVT: p>0.05. 2 out of 19 (10.5%) TCR+ T-cell transcripts sequenced each had a CDR3 region identical to that of OV805T number 22 with its CDR3 region as: Vγ2Jγ1.3/2.3 YYYCATWD<u>HRP</u>KKLFSGTLVVT: p>0.05. 2 out of 19 (10.5%) TCR+ T-cell transcripts sequenced each had a CDR3 region identical to that of OV805T number 20 with its CDR3 region as: Vγ5Jγ1.3/2.3 YYYCATWGLLNKKLFSGTLVVT: p>0.05. 2 out of 19 (10.5%) TCR+ T-cell transcripts sequenced each had a CDR3 region identical to that of OV805T number 14 with its CDR3 region as: Vγ5Jγ1.3/2.3 YYYCATW<u>ASN</u>YYKKLFSGTLVVT: (10.5%) p>0.05. There were seven

transcripts, each with a unique CDR3 region: OV805T number 17 Vγ4Jγ1.3/2.3 YYYCATWG<u>PLF</u>KKLFSGTLVVT: (5.3%) p>0.05, OV805T number 18 Vγ3Jγ1.3/2.3 YYYCATWG<u>GKQN</u>YYKKLFSGTLVVT: (5.3%) p>0.05, OV805T number 11 Vγ2Jγ1.3/2.3 YYYCATWG<u>PR</u>YYKKLFSGTLVVT: (5.3%) p>0.05, OV805T number 4 Vγ2Jγ1.3/2.3 YYYCATWG<u>PN</u>YYKKLFSGTLVVT: (5.3%) p>0.05, OV805T number 5 Vγ2Jγ1.3/2.3 YYYCATWG<u>PG</u>KLFSGTLVVT: (5.3%) p>0.05, OV805T number 21 Vγ2Jγ1.3/2.3 YYYCATWG<u>MSVID</u>KKLFSGTLVVT: (5.3%) p>0.05, OV805T number 7 Vγ2Jγ1.3/2.3 YYYCATWG(no N region)KKLFSGTLVVT: (5.3%) p>0.05.

In patient OV22T, sequence analysis of VγI-chain TCR+ T-cell transcripts revealed that 11 out of 26 (42.3%) TCR+ T-cell transcripts sequenced each had a CDR3 region identical to that of OV22T number 26 with its CDR3 region as: Vγ2Jγ1.3/2.3 YYYCATWD<u>PV</u>YYKKLFSGTLVVT: p<0.05. 8 out of 26 (30.8%) TCR+ T-cell transcripts sequenced each had a CDR3 region identical to that of OV22T number 2 with its CDR3 region as: Vγ2Jγ1.3/2.3 YYYCATWD<u>V</u>YYKKLFSGTLVVT: p<0.05. 3 out of 26 TCR+ T-cell transcripts sequenced each had a CDR3 region identical to that of OV22T number 24 with its CDR3 region as: Vγ2Jγ1.3/2.3 YYYCATWD<u>LP</u>YYKKLFSGTLVVT: (11.5%) p>0.05. 2 out of 26 (7.8%) non-clonally expanded TCR+ T-cell transcripts sequenced had a CDR3 region as: Vγ2Jγ1.3/2.3 YYYCATWD<u>PR</u>YYKKLFSGTLVVT: p>0.05. 2 out of 26 (7.8%) non-clonally expanded TCR+ T-cell transcripts sequenced had a CDR3 region as: Vγ2Jγ1.3/2.3 YYYCATWD<u>P</u>YYKKLFSGTLVVT: p>0.05.

In patient OV1T, sequence analysis of Vγl-chain TCR+ T-cell transcripts revealed that 3 out of 17 (17.6%) transcripts sequenced each had a CDR3 region identical to that of OV1T number 11 with its CDR3 region as: Vγ2Jγ1.3/2.3 YYYCATWDG(no N region)YYKKLFSGTLVVT: p>0.05 (an statistically insignificant clonal expansion). 2 out of 17 (11.8%) transcripts sequenced each had a identical CDR3 regions as: Vγ2Jγ1.3/2.3 YYYCATWDG<u>F</u>YYKKLFSGTLVVT: p>0.05. There were twelve unique non-clonally expanded TCR+ T-cell transcripts with CDR3 regions as: Vγ2Jγ1.3/2.3 YYYCATW<u>V</u>NYYKKLFSGTLVVT: (5.9%) p>0.05, Vγ2Jγ1.1

YYYCATWDLTGWFKIF: (5.9%) p>0.05, Vγ2Jγ1.3/2.3

YYYCATW<u>VRLGS</u>YYKKLFSGTLVVT: (5.9%) p>0.05, Vγ2Jγ1.1

YYYCATWVGWFKIF: (5.9%) p>0.05, Vγ4Jγ1.3/2.3

YYYCATWD<u>PK</u>NYYKKLFSGTLVVT: (5.9%) p>0.05, Vγ2Jγ1.3/2.3

YYYCATWDG<u>T</u>NYYKKLFSGTLVVT: (5.9%) p>0.05, Vγ2Jγ1.3/2.3

YYYCATW<u>PLVT</u>NYYKKLFSGTLVVT: (5.9%) p>0.05, Vγ2Jγ1.3/2.3

YYYCATWD<u>KPGK</u>YYKKLFSGTLVVT: (5.9%) p>0.05, Vγ2Jγ1.3/2.3

YYYCATWD<u>NPS</u>YYKKLFSGTLVVT: (5.9%) p>0.05, Vγ2Jγ1.3/2.3

YYYCATWD<u>ARD</u>KLFSGTLVVT: (5.9%) p>0.05, Vγ2Jγ1.3/2.3

YYYCATWD<u>PSQG</u>YKKLFSGTLVVT: (5.9%) p>0.05, Vγ2Jγ1.3/2.3

YYYCATWDG<u>R</u>YYKKLFSGTLVVT: (5.9%) p>0.05, which were the CDR3 regions of TCR+ T-cell transcripts OV1T number 19, 20, 17, 22, 14, 12, 10, 5, 8, 11, 6 and 1, respectively (Table 6).

B) Sequencing results of the VγII (9)-chain TCR Transcripts

Similar procedures to the VγI sequence analysis described above were employed for the VγII, also know as Vγ9, sequence analysis. The productively rearranged transcripts were analyzed using the GENBANK database. Results revealed the presence of statistically significant substantial proportions of identical VγII-chain TCR+ T-cell transcripts in five out of five solid tumor specimens obtained from patients with EOC, suggesting the presence of oligoclonal populations of T-cells infiltrating the solid tumor from patients with EOC.

Table 10. VγII (9)-chain TCR+ T-cell Transcripts (CDR3 Region) Expressed in the Solid Tumor from patient OV27T

Transcript No.	Transcript Frequency	p-value Vγ 1/18	2/18	3/18	N	Jγ
13	Y Y C A L W E V G E Vγ9Jγ1.2 TACTACTGTGCCTTGTGGGAGGTGGGGGAG 15/18 84% <0.0001<0.0001<0.0001				L G K K I TTGGGCAAAAAAATC	
3	Y Y C A L W E V G Vγ9Jγ1.2 TACTACTGTGCCTTGTGGGAGGTGGGG 3/18 26% NS NS NS				L G K K I TTGGGCAAAAAAATC	

Table 11. VγII (9)-chain TCR+ T-cell Transcripts (CDR3 Region) Expressed in the Solid Tumor from patient OV42T

Transcript No.	Transcript Vγ Frequency	p-value 1/16	2/16	3/16	N						Jγ						
7	Y Y C A L W E V				P C						Y Y K K L F G						
	Vγ9Jγ1.3/2.3																
	TACTACTGTGCCTTGTGGGAGGTGCCGTGT										TATTATAAGAAACTCTTTGGC						
	7/16 44%	<0.0001	<0.0001	<0.0001													
15	Y Y C A L W E V				H						Y Y K K L F G						
	Vγ9Jγ1.3/2.3																
	TACTACTGTGCCTTGTGGGAGGTG				CAT						TATTATAAGAAACTCTTTGGC						
		6/16 38%	<0.0001	<0.0001	<0.0001												
5	Y Y C A L W E V										Y Y K K L F G						
	Vγ9Jγ1.3/2.3																
	TACTACTGTGCCTTGTGGGAGGTG										TATTATAAGAAACTCTTTGGC						
	1/16 6%	NS	NS	NS													
10	Y Y C A L W E V				S E						Y Y K K L F G						
	Vγ9Jγ1.3/2.3																
	TACTACTGTGCCTTGTGGGAGGTG				AGTGAG						TATTATAAGAAACTCTTTGGC						
	1/16 6%	NS	NS	NS													
2	Y Y C A L W E V				R						Y Y K K L F G						
	Vγ9Jγ1.3/2.3																
	TACTACTGTGCCTTGTGGGAGGTG				AGG						TATTATAAGAAACTCTTTGGC						
	1/16 6%	NS	NS	NS													

Table 12. VγII (9)-chain TCR+ T-cell Transcripts (CDR3 Region) Expressed in the Solid Tumor from patient OV45T

Transcript

No.	Transcript Vγ Frequency	p-value 1/18	 2/18	 3/18	N	Jγ
9	Y Y C A L W E V I Vγ9Jγ1.3/2.3 TACTACTGTGCCTTGTGGGAGGTGATT 8/18 44%	<0.0001	<0.0001	<0.0001		Y Y K K L F G TATTATAAGAAACTCTTTGGC
3	Y Y C A L W Y P R Vγ9Jγ1.3/2.3 TACTACTGTGCCTTGTGG TACCCTAGG 7/18 39%	<0.0001	<0.0001	<0.0001		K L F G AAACTCTTTGGC
11	Y Y C A L W P R Vγ9Jγ1.3/2.3 TACTACTGTGCCTTGTGG CCTAGG 2/18 11%	NS	NS	NS		K L F G AAACTCTTTGGC
17	Y Y C A L W E V Vγ9Jγ1.3/2.3 TACTACTGTGCCTTGTGGGAGGTG 1/18 6%	NS	NS	NS		Y Y K K L F G TATTATAAGAAACTCTTTGGC

Table 13. VγII (9)-chain TCR+ T-cell Transcripts (CDR3 Region) Expressed in the Solid Tumor from patient OV38T

Transcript No.	Transcript Frequency	p-value Vγ			N	Jγ
		1/18	2/18	3/18		
12	Y Y C A L W E V Vγ9Jγ1.3/2.3 TACTACTGTGCCTTGTGGGAGGTG 11/20 55%	<0.0001	<0.0001	<0.0001	R CGA	Y Y K K L F G TATTATAAGAAACTCTTTGGC
17	Y Y C A L W E V Vγ9Jγ1.3/2.3 TACTACTGTGCCTTGTGGGAGGTG 3/20 15%	NS	NS	NS	R F V AGGTTTGTG	Y Y K K L F G TATTATAAGAAACTCTTTGGC
2	Y Y C A L W E V Vγ9Jγ1.3/2.3 TACTACTGTGCCTTGTGGGAGGTG 2/20 10%	NS	NS	NS	L CTG	Y Y K K L F G TATTATAAGAAACTCTTTGGC
16	Y Y C A L W E V Vγ9Jγ1.3/2.3 TACTACTGTGCCTTGTGGGAGGTG 1/20 6%	NS	NS	NS	E W E GAGTGGGAG	Y Y K K L F G TATTATAAGAAACTCTTTGGC
19	Y Y C A L W E V Vγ9Jγ1.3/2.3 TACTACTGTGCCTTGTGGGAGGTG 1/20 6%	NS	NS	NS	R F AGGTTT	Y Y K K L F G TATTATAAGAAACTCTTTGGC
14	Y Y C A L W E V Vγ9Jγ1.3/2.3 TACTACTGTGCCTTGTGGGAGGTG 1/20 6%	NS	NS	NS		Y Y K K L F G TATTATAAGAAACTCTTTGGC
1	Y Y C A L W Vγ9Jγ1.3/2.3 TACTACTGTGCCTTGTGG 1/20 6%	NS	NS	NS		K K L F G AAGAAACTCTTTGGC

Table 14. VγII (9)-chain TCR+ T-cell Transcripts (CDR3 Region) Expressed in the Solid Tumor from patient OV26T

Transcript No.	Transcript Vγ Frequency	p-value 1/27	2/27	3/27							N						Jγ

2 Y Y C A L W E V L P   Y Y K K L
Vγ9Jγ1.3/2.3
TACTACTGTGCCTTGTGGGAGGTGCTTCCT   TATTATAAGAAACTC
24/27 89%   <0.0001<0.0001<0.0001

1 Y Y C A L W E V G E L G K K
Vγ9Jγ1.3/2.3
TACTACTGTGCCTTGTGGGAGGTGGGTGAGTTGGGCAAAAAA
1/27 4%   NS   NS   NS

6 Y Y C A L W E V C   Y Y K K L F G
Vγ9Jγ1.3/2.3
TACTACTGTGCCTTGTGGGAGGTGTGT   TATTATAAGAAACTCTTTGGC
1/27 4%   NS   NS   NS

9 Y Y C A L W E V   K K L F G
Vγ9Jγ1.3/2.3
TACTACTGTGCCTTGTGGGAGGTG   AAGAAACTCTTTGGC
1/27 4%   NS   NS   NS

Table 15. Summary of clonal expansion of VγII (9)-chain TCR+ T -cell transcripts in the solid tumor of patients with EOC

OV27T:15/18:#13:84%:CDR3:YYCALWEVGELGKKI
OV42T:7/16:#7:44%:CDR3:YYCALWEVHYYKKLFG
OV42T:6/16:#15:38%:CDR3:YYCALWEVYYKKLFG
OV45T:8/18:#9:44%:CDR3:YYCALWEVIYYKKLFG
OV45T:7/18:#3:39%:CDR3:YYCALWYPRKLFG
OV38T:11/20:#12:55%:CDR3:YYCALWEVRYYKKLFG
OV26T:24/27:#2:89%:CDR3:YYCALWEVLPYYKKL

Table 16. Percent clonal expansion of VγII-chain TCR+ T-cell transcripts in the solid tumor of patients with EOC

EOC Patient Sample	% Clonal Expansion
OV27T #13	84%
OV42T #7	44%
OV42T #15	38%
OV45T #9	44%
OV45T #3	39%
OV38T #12	55%
OV26T #2	89%

In patient OV27T sequence analysis of VγII(9)-chain TCR+ T-cell transcripts revealed that 15 out of 18 (83.3%) TCR+ T-cell transcripts each had a CDR3 region identical to that of OV27T number 13 with its CDR3 region as: Vγ9Jγ1.2: YYCALWEV<u>GE</u>LGKKI: $p < 0.05$ (a statistical significant oligoclonal expansion) (Table 10). There was one non-clonally expanded TCR+ T-cell transcript OV27T number 3 with a CDR3 region as: YYCALWEVGLGKKI: $p > 0.05$.

In patient OV42T sequence analysis of VγII(9)-chain TCR+ T-cell transcripts revealed that 7 out of 16 (43.8%) TCR+ T-cell transcripts each had a CDR3 region identical to that of OV42T number 7 with its CDR3 region as: Vγ9Jγ1.3/2.3: YYCALWEV<u>PC</u>YYKKLFG: $p < 0.05$ (a statistical significant oligoclonal expansion) (Table 11). 6 out of 16 (37.5%) TCR+ T-cell transcripts each had a CDR3 region identical to that of OV42T number 15 with its CDR3 region as: Vγ9Jγ1.3/2.3: YYCALWEV<u>H</u>YYKKLFG: $p < 0.05$ (a statistically significant oligoclonal expansion). There were three non-clonally expanded TCR+ T-cell transcripts with a CDR3 region as: Vγ9Jγ1.3/2.3: YYCALWEV (no N region) YYKKLFG: (6.3%) $p > 0.05$, Vγ9Jγ1.3/2.3: YYCALWEV<u>SE</u>YYKKLFG: (6.3%) $p > 0.05$ and Vγ9Jγ1.3/2.3: YYCALWEV<u>R</u>YYKKLFG: (6.3%) $p > 0.05$ which were the CDR3 regions of the TCR+ T-cell transcripts numbers 5, 10 and 2, respectively (see Table 11).

In patient OV45T, sequence analysis of VγII (9)-chain TCR+ T-cell transcripts revealed that 8 out of 18 (44.4%) TCR+ T-cell transcripts each had a CDR3 region identical to that of OV45T number 9 with its CDR3 region as:

61

Vγ9Jγ1.3/2.3: YYCALWEV<u>I</u>YYKKLFG: p<0.05 (a statistically significant oligoclonal expansion): (Table 12). 7 out of 18 (38.9%) TCR+ T-cell transcripts each had a CDR3 region identical to that of OV45T number 3 with its CDR3 region as: Vγ9Jγ1.3/2.3: YYCALWEV<u>YPR</u>KLFG: p<0.0001. 2 out of 18 (11.1%) TCR+ T-cell transcripts each had a CDR3 region as: Vγ9Jγ1.3/2.3: YYCALWEV<u>PR</u>KLFG: p>0.05. One additional transcript which was non-clonally expanded had a CDR3 region as: Vγ9Jγ1.3/2.3: YYCALWEV (no N region) YYKKLFG: (5.6%) p>0.05.

In patient OV38T, sequence analysis of VγII (9)-chain TCR+ T-cell transcripts revealed that 11 out of 20 (55%) TCR+ T-cell transcripts sequenced each had a CDR3 region identical to OV38T number 12 with its CDR3 region as: Vγ9Jγ1.3/2.3: YYCALWEV<u>R</u>YYKKLFG: p<0.05 (a statistically significant oligoclonal expansion) (Table 13). 3 out of 20 (15%) TCR+ T-cell transcripts sequenced each had a CDR3 region identical to OV38T number 17 with it CDR3 region as: Vγ9Jγ1.3/2.3: YYCALWEV<u>RFV</u>YYKKLFG: p>0.05 (a statistically insignificant oligoclonal expansion). 2 out of 20 (10%) TCR+ T-cell transcripts sequenced each had a CDR3 region as: Vγ9Jγ1.3/2.3: YYCALWEV<u>LYYK</u>KLFG: p>0.05. There were four non-clonally expanded TCR+ T-cell transcripts each had a CDR3 region as: Vγ9Jγ1.3/2.3: YYCALWEV<u>EWE</u>YYKKLFG: (5%) p>0.05, Vγ9Jγ1.3/2.3: YYCALWEV<u>RF</u>YYKKLFG: (5%) p>0.05, Vγ9Jγ1.3/2.3: YYCALWEV(no N region)KLFG: (5%) p>0.05 and Vγ9Jγ1.3/2.3: YYCALW(no N region)KLFG: (5%) p>0.05 which were transcripts number 16, 19, 14 and 1, respectively.

In patient OV26T, sequence analysis of VγII(9)-chain TCR+ T-cell transcripts revealed that 24 out of 27 (89%) TCR+ T-cell transcripts sequenced each had a CDR3 region identical to OV26T number 2 with its CDR3 region as: Vγ9Jγ1.3/2.3: YYCALWEVLPYYKKL: p<0.05 (statistically significant oligoclonal expansion) (see Table 14). There were three non-clonally expanded TCR+ T-cell transcripts each had a CDR3 region as: Vγ9Jγ1.3/2.3: YYCALWEVGELGKK: (4%) p>0.05, Vγ9Jγ1.3/2.3: YYCALWEVCYYKKLFG: (4%) p>0.05, Vγ9Jγ1.3/2.3: YYCALWEV(no N region)KK: (4%) p>0.05 which were transcripts number 1, 6, and 9, respectively.

C) Sequencing results of the Vδ1-chain TCR Transcripts

Similar procedures to the VγI and VγII sequence analysis described above were employed for the Vδ1 sequence analysis. The productively rearranged transcripts were analyzed using the GENBANK database. Results revealed the presence of statistically significant substantial proportions of identical Vδ1-chain TCR+ T-cell transcripts in four out of six solid tumor specimens obtained from patients with EOC, suggesting the presence of oligoclonal populations of T-cells infiltrating the solid tumor from patients with EOC.

Table 17. Vδ1-chain TCR+ T-cell Transcripts (CDR3 Region) Expressed in the Solid Tumor from patient OV27T

Transcript No.	Vδ	N	Dδ2	N	Jδ	Transcript Frequency	p-value 1/45	p-value 2/45
3	C A L G D TGTGCTCTTGGGGAC		Y G S T F S W V TACGGAAGTACTTTTTCATGGGTC		I F Vδ1/Dδ2/Jδ1 ATCTTT	23/45 51%	<0.0001	<0.0001
9	C A L G D E A F L N L V P D S Y T TGTGCTCTTGGGGACGAGGCCTTCCTAAATCTAGTACCCGATTCGTACACC				D K Vδ1/Dδ2/Jδ1 GATAAA	21/45 47%	<0.0001	<0.0001
5	L G E L P P G Y W G I V S P V G N T CTTGGGGAACTTCCCCCTGGGTACTGGGGGATTGTCTCTCCTGTAGGTAACACC				D K Vδ1/Dδ2/Jδ1 GATAAA	1/45 2%	NS	NS NS
7	C A L G E S D Y E V G G V L V TGTGCTCTTGGGGAATCCGACTACGAAGTGGGGGGGGTCCTAGTC				D K Vδ1/Dδ2/Jδ1 GATAAA	1/45 2%	NS	NS NS

64

Table 18. Vδ1-chain TCR+ T-cell Transcripts (CDR3 Region) Expressed in the Solid Tumor from patient OV33T

Transcript No.	Vδ	N	Dδ2Dδ3	N	Jδ	Transcript Frequency	p-value 1/20	2/20
10	Y F C A L G TACTTTTGTGCTCTTGGG		D Y G S T F S W V GACTACGGAAGTACTTTTTCATGGGTC		D K GATAAA	Vδ1/Dδ2/Jδ1 7/20 35%	<0.0001	<0.0001
8	Y F C A L G D E A F L N L V P D S Y T TACTTTTGTGCTCTTGGGGACGAGGCCTTCCTAAATCTAGTACCCGATTCGTACACC				D K GATAAA	Vδ1/Dδ2/Jδ1 3/20 15%	NS	NS
6	Y F C A L G E L T G G W Y E V D T TACTTTTGTGCTCTTGGGGAACTTACTGGGGGGTGGTATGAGGTTGACACC				D K GATAAA	Vδ1/Dδ2/Jδ1 3/20 15%	NS	NS
1	Y F C A L G TACTTTTGTGCTCTTGGG		D L P V L G D S E GACCTACCCGTACTGGGGGATAGTGAG		D K GATAAA	Vδ1/Dδ2/Jδ1 2/20 10%	NS	NS

Transcript No.	Vδ	N	Dδ2	N	Jδ	Transcript Frequency 1/20	2/20	3/20
18	Y F C A L G TACTTTTGTGCTCTTGGG		D L P V L G D GACCTACCCGTACTGGGGGAT		D K GATAAA	Vδ1/Dδ2/Jδ1 1/20 5%	NS NS	NS
2	F C A L G D T R D E L Y W G I R Q C P T TTTTGTGCTCTTGGG GACACCAGGGACGAACTTTACTGGGGGATACGCCAATGCCCAACC				D K GATAAA	Vδ1/Dδ2/Jδ1 1/20 5% NS	NS	NS
3	Y F C A L G TACTTTTGTGCTCTTGGG		T P P G D T K I P Y P ACCCCGCCCGGGGATACGAAGATCCCTTACCCC		D K GATAAA	Vδ1/Dδ2/Jδ1 1/20 5%	NS	NS
14	Y F C A L G TACTTTTGTGCTCTTGGG		D R H P Y T T S L A GACCGACATCCCTACACTACCTCCCTGGCC		D K GATAAA	Vδ1/Dδ2/Jδ1 1/20 5%	NS	NS
22	Y F C A L G E K R L P T P L V P D H T TACTTTTGTGCTCTTGGGGAAAAACGACTTCCTACGCCCTTGGTCCCAGACCACACC				D K GATAAA	Vδ1/Dδ2/Jδ1 1/20 5%	NS	NS

Table 19. Vδ1-chain TCR+ T-cell Transcripts (CDR3 Region) Expressed in the Solid Tumor from patient OV39T

Transcript No.	Vδ	N	Dδ2	N	Jδ	Transcript Frequency	p-value 1/17	2/17	3/17
2	C F C A L G E GCTTTTGTGCTCTTGGGGAAT		S D Y E V G G V L V CCGACTACGAAGTGGGGGGGGGTCCTAGTC		D K Vδ1/Dδ2/Jδ1 GATAAA	12/17 70.6%	<0.0001	<0.0001	<0.0001
18	Y F C A L G E TACTTTTGTGCTCTTGGGGAA		L P F L L W G I T CTCCCCTTCCTACTCTGGGGGATCACC		D K Vδ1/Dδ2/Jδ1 GATAAA	3/17 17.6	NS	NS	NS
8	Y F C A L G E L W P P T K R I L G T TACTTTTGTGCTCTTGGGGAACTCTGGCCTCCTACTAAGCGGATATTAGGTACC				D K Vδ1/Dδ2/Jδ1 GATAAA	1/17 5.8%	NS	NS	NS
12	Y F C A L G E TACTTTTGTGCTCTTGGGGAA		P V G D W G Q D P F CCCGTGGGGGACTGGGGCCAAGACCCCTTC		D K Vδ1/Dδ2/Jδ1 GATAAA	1/17 5.8%	NS	NS	NS

Table 20. Vδ1-chain TCR+ T-cell Transcripts (CDR3 Region) Expressed in the Solid Tumor from patient OV1T

Transcript No.	Vδ	N	Dδ2	N	Jδ	Transcript Frequency	1/30	2/30	3/30
								p-value	
9	Y F C A L G		V P G G G P P A D T		D K Vδ1/Dδ2/Jδ1				
	TACTTTTGTGCTCTTGGG		GTCCCCGGGGGGGGGACCGCCTGCCGACACC		GATAAA	22/30 73.3%	<0.0001	<0.0001	<0.0001
16	Y F C A L G E P K I L P P N G D Y T				D K Vδ1/Dδ2/Jδ1				
	TACTTTTGTGCTCTTGGGGAACCCAAAATCCTTCCCCCCAACGGGGATTACACC				GATAAA	1/30 3.3%	NS	NS	NS
19	Y F C A L G E V Q G S R T T T G G H T				D K Vδ1/Dδ2/Jδ1				
	TACTTTTGTGCTCTTGGGGAAGTTCAGGGCTCCCGAACAACTACTGGGGGGCACACCGATAAA					1/30 3.3%	NS	NS	NS
17	Y F C A L G E G G I A R G P R				D K Vδ1/Dδ2/Jδ1				
	TACTTTTGTGCTCTTGGGGAAGGGGGAATCGCACGGGGACCCCGC				GATAAA	1/30 3.3%	NS	NS	NS
23	Y F C		P Q Q R V G V P R G Y T		D K Vδ1/Dδ2/Jδ1				
	TACTTTTGT		CCTCAACAGCGAGTGGGGGTTCCCCGCGGGTACACCGATAAA			1/30 3.3%	NS	NS	NS
14	Y F C A L G		Q P L G L P S T G G D T		D K Vδ1/Dδ2/Jδ1				
	TACTTTTGTGCTCTTGGA		CAACCCCTAGGCCTTCCCTCTACTGGGGGAGACACC		GATAAA	1/30 3.3%	NS	NS	NS
12	Y F C A L G D T R L G D T D T				D K Vδ1/Dδ2/Jδ1				
	TACTTTTGTGCTCTTGGGGATACGAGGCTGGGGGATACCGACACC				GATAAA	1/30 3.3%	NS	NS	NS
8	Y F C A L G E L A F P P Y W G S S Y T				D K Vδ1/Dδ2/Jδ1				
	TACTTTTGTGCTCTTGGGGAACTCGCCTTTCCTCCCTACTGGGGGTCTTCGTACACC				GATAAA	1/30 3.3%	NS	NS	NS
2	Y F C A L G E G G I A R G P R				D K Vδ1/Dδ2/Jδ1				
	TACTTTTGTGCTCTTGGGGAAGGGGGAATCGCACGGGGACCCCGC				GATAAA	1/30 3.3%	NS	NS	NS

Table 21. Vδ1-chain TCR+ T-cell Transcripts (CDR3 Region) Expressed in the Solid Tumor from patient OV1C

Transcript NO.	Vδ	N	Dδ2	N	Jδ	Transcript Frequency	p-value 1/26	2/26	3/26
22	Y F C A L G D E A	F L N	L V P D S Y T		D K Vδ1/Dδ2/Jδ1	2/26 7.8%	NS	NS	NS
	TACTTTTGTGCTCTTGGGGACGAGGCCTTCCTAAATCTAGTACCCGATTCGTACACC				GATAAA				
21	Y F C A L G E L		V A P G W D I R F		D K Vδ1/Dδ2/Jδ1	2/26 7.8%	NS	NS	NS
	TACTTTTGTGCTCTTGGGGAACTA		GTCGCTCCTGGGTGGGATATACGGTTT		GATAAA				
7	Y F C A L G E L		S T P D W G I L S		D K Vδ1/Dδ2/Jδ1	2/26 7.8%	NS	NS	NS
	TACTTTTGTGCTCTTGGGGAACTA		TCAACGCCCGACTGGGGGATACTCTCC		GATAAA				
2	Y F C A L G E L		G S S P K P N		D K Vδ1/Dδ2/Jδ1	1/26 3.8%	NS	NS	NS
	TACTTTTGTGCTCTTGGGGAACTA		GGATCTTCCTCCCCTAAACCAAAC		GATAAA				
4	Y F C A L G E L		P W S T G G Y A P		D K Vδ1/Dδ2/Jδ1	1/26 3.8%	NS	NS	NS
	TACTTTTGTGCTCTTGGGGAACTC		CCATGGAGTACTGGGGGATACGCACCC		GATAAA				
5	Y F C A L G E L P	L I Q L G D L R E T			D K Vδ1/Dδ2/Jδ1	1/26 3.8%	NS	NS	NS
	TACTTTTGTGCTCTTGGGGAACTGCCCCTCATTCAACTGGGGGACCTCCGAGAACACC				GATAAA				
6	Y F C A L G E R S H Y W G I Q W R S R S				D K Vδ1/Dδ2/Jδ1	1/26 3.8%	NS	NS	NS
	TACTTTTGTGCTCTTGGGGAGCGAAGCCATTACTGGGGGATACAATGGAGGAGCCGGAGC				GATAAA				
8	Y F C A L G E L		P G S T G G Y A R		D K Vδ1/Dδ2/Jδ1	1/26 3.8%	NS	NS	NS
	TACTTTTGTGCTCTTGGGGAACTC		CCAGGGAGTACTGGGGGATACGCACGC		GATAAA				
9	Y F C A L G E L		D Q T T T E G Y G D T		D K Vδ1/Dδ2/Jδ1	1/26 3.8%	NS	NS	NS
	TACTTTTGTGCTCTTGGGGAACTA		GACCAGACGACTACGGAGGGATACGGGGACACC		GATAAA				
11	Y F C A L G E		P R M D W G I L H T		D K Vδ1/Dδ2/Jδ1	1/26 3.8%	NS	NS	NS
	TACTTTTGTGCTCTTGGGGAA		CCTCGGATGGACTGGGGGATCCTACACACC		GATAAA				
12	Y F C A L G		F F L T G G Y R T		D K Vδ1/Dδ2/Jδ1	1/26 3.8%	NS		NS
	TACTTTTGTGCTCTTGGG		TTCTTCCTAACCGGGGGATATTGACACC		GATAAA				
14	Y F C A L G D Y G S T F S W V I F G K G T				D K Vδ1/Dδ2/Jδ1	1/26 3.8%	NS	NS	
	TACTTTTGTGCTCTTGGGGACTACGGAAGTACTTTTTCATGGGTCATCTTTGGAAAAGGAACCGATAAA								
18	Y F C A L G E L		S T G G Y A P		D K Vδ1/Dδ2/Jδ1	1/26 3.8%	NS	NS	NS
	TACTTTTGTGCTCTTGGGGAACTC		AGTACTGGGGGATACGCACCC		GATAAA				

Table 21. Continued

Transcript No.	Vδ	N	Dδ2	N	Jδ	Transcript Frequency	p-value 1/26	2/26	3/26

15
```
      Y  F  C  A  L  G  E  L        L  G  D                                                    D  K    Vδ1/Dδ2/Jδ1
      TACTTTTGTGCTCTTGGGGAACTG       CTGGGGGAC                                                  GATAAA  1/26 3.8% NS   NS   NS
```
16
```
      Y  F  C  A  L  G  E           W  G  I                                                    D  K    Vδ1/Dδ2/Jδ1
      TACTTTTGTGCTCTTGGGGAG          TGGGGGATA                                                 GATAAA  1/26 3.8% NS   NS   NS
```
17
```
      Y  F  C  A  L  G  E           P  D  W  G  I  L                                           D  K    Vδ1/Dδ2/Jδ1
      TACTTTTGTGCTCTTGGGGAA          CCCGACTGGGGGATACTC                                        GATAAA  1/26 3.8% NS   NS   NS
```
25
```
      Y  F  C  A  L  G  E  L        P  L  I  Q  L  G  D  E  T                                  D  K    Vδ1/Dδ2/Jδ1
      TACTTTTGTGCTCTTGGGGAACTG       CCCCTCATTCAACTGGGGGACGAAACC                               GATAAA  1/26 3.8% NS   NS   NS
```
27
```
      Y  F  C  A  L  G  E           R  S  H  Y  W  G  I  Q  W  R  S                            D  K    Vδ1/Dδ2/Jδ1
      TACTTTTGTGCTCTTGGGGAG          CGAAGCCATTACTGGGGGATACAATGGAGGAGC                         GATAAA  1/26 3.8% NS   NS   NS
```
8
```
      Y  F  C  A  L  G  E  L        P  G  S  T  G  G  Y  A  R                                  D  K    Vδ1/Dδ2/Jδ1
      TACTTTTGTGCTCTTGGGGAACTC       CCAGGGAGTACTGGGGGATACGCACGC                               GATAAA  1/26 3.8% NS   NS   NS
```
19
```
      Y  F  C  A  L  G  E  L        D  Q  T  T  T  E  G  Y  G  D  T                            D  K    Vδ1/Dδ2/Jδ1
      TACTTTTGTGCTCTTGGGGAACTA       GACCAGACGACTACGGAGGGATACGGGGACACC                         GATAAA  1/26 3.8% NS   NS   NS
```
3
```
      Y  F  C  A  L  G  E           P  R  M  D  W  G  I  L  H  T                               D  K    Vδ1/Dδ2/Jδ1
      TACTTTTGTGCTCTTGGGGAA          CCTCGGATGGACTGGGGGATCCTACACACC                            GATAAA  1/26 3.8% NS   NS   NS
```
13
```
      Y  F  C  A  L  G              L  T  G  G  G                                              D  K    Vδ1/Dδ2/Jδ1
      TACTTTTGTGCTCTTGGG             CTAACCGGGGGGGGGGGG                                        GATAAA  1/26 3.8% NS   NS   NS
```
20
```
      Y  F  C  A  L  G  D           Y  G  S  T  F  S  W  V                                     D  K    Vδ1/Dδ2/Jδ1
      TACTTTTGTGCTCTTGGGGAC          TACGGAAGTACTTTTTCATGGGTC                                  GATAAA  1/26 3.8% NS   NS   NS
```

Table 22. Summary of clonal expansion of Vδ1-chain TCR+ T -cell transcripts in the solid tumor of patients with EOC

OV27T: 23/45:#3:51%:CDR3:CALGDYGSTFSWVIF
OV27T: 21/45:#9:47%:CDR3:CALGDEAFLNLVPDSYTDK
OV33T: 7/20:#10:35%:CDR3:YFCALGDYGSTFSWVDK
OV39T: 12/17:#2:70.6%:CDR3:FCALGESDYEVGGVLVDK
OV1T: 22/30:#9:73.3%:CDR3:YFCALGVPGGGPPADTDK

Table 23. Percent clonal expansion of Vδ1-chain TCR+ T-cell transcripts in the solid tumor of patients with EOC

EOC Patient Sample	% Clonal Expansion
OV27T #3	51%
OV27T #9	47%
OV33T #10	35%
OV39T #2	70.6%
OV1T #9	73.3%

In patient OV27T, sequence analysis of Vδ1 -chain TCR+ T-cell transcripts revealed that 23 out of 45 (51%) TCR+ T-cell transcripts each had a CDR3 region identical to that of OV27T number 3 with its CDR3 region as: Vδ1Dδ2Jδ1 CALGDYGSTFSWVIF $p < 0.0001$ (a statistically significant oligoclonal expansion) (see Table 14). 21 out of 45 (47%) TCR+ T-cell transcripts sequenced each had a CDR3 region identical to OV27T number 9 with it CDR3 region as: Vδ1Dδ2Jδ1 CALGDEAFLNLVPDSYT $p < 0.0001$ (a statistically significant oligoclonal expansion) (see Table 14). There were 2 non-clonally expanded TCR+ T-cell transcripts each had a CDR3 region as Vδ1Dδ2Jδ1 CALGELPPGYWGIVSPVGNTDK: (2%) $p > 0.05$ and Vδ1Dδ2Jδ1

CALGESDYEVGGVLV: (2%) p>0.05 which were transcripts 5 and 7, respectively.

In patient OV33T, sequence analysis of Vδ1 -chain TCR+ T-cell transcripts revealed that 7 out of 20 (35%) TCR+ T-cell transcripts each had a CDR3 region identical to that of OV33T number 10 with its CDR3 region as: Vδ1Dδ2Jδ1 YFCALGDYGSTFSWVDK p<0.0001 (a statistically significant oligoclonal expansion) (see Table 18). 3 out of 20 (15%) TCR+ T-cell transcripts sequenced each had a CDR3 region identical to OV33T number 8 with its CDR3 region as: Vδ1Dδ2Jδ1 YFCALGDEAFLNLVPDSYTDK p>0.05 (a statistically insignificant oligoclonal expansion) (see Table 18). 3 out of 20 (15%) TCR+ T-cell transcripts sequenced each had a CDR3 region identical to OV33T number 6 with its CDR3 region as Vδ1Dδ2Jδ1 YFCALGELTGGWYEVDTDK p>0.05 (a statistically insignificant oligoclonal expansion). 2 out of 20 (10%) TCR+ T-cell transcripts sequenced each had a CDR3 region identical to OV33T number 1 with its CDR3 region as Vδ1Dδ2Jδ1 YFCALGDLPVLGDSEDK p>0.05 (a statistically insignificant oligoclonal expansion). There were five non-clonally expanded TCR+ T-cell transcripts each had a CDR3 region as Vδ1Dδ2Jδ1 YFCALGDLPVLGDDK: (5%) p>0.05, Vδ1Dδ2Jδ1 FCALGDTRDELYWGIRQCPTDK: (5%) p>0.05, Vδ1Dδ2Jδ1 YFCALGTPPGDTKIPYPDK (5%) p>0.05, Vδ1Dδ2Jδ1 YFCALGDRHPYTTSLADK (5%) p>0.05, Vδ1Dδ2Jδ1 YFCALGEKRLPTPLVPDHTDK (5%) p>0.05 which were transcripts 18, 2, 3, 14, and 22, respectively.

D) Sequencing results of the Vδ2-chain TCR Transcripts

Similar procedures to the VγI, VγII and Vδ1 sequence analysis described above were employed for the Vδ2 sequence analysis. The productively rearranged transcripts were analyzed using the GENBANK database. Results revealed the presence of statistically significant substantial proportions of identical Vδ2-chain TCR+ T-cell transcripts in four out of five solid tumor specimens obtained from patients with EOC, suggesting the presence of oligoclonal populations of T-cells infiltrating the solid tumor from patients with EOC.

Table 24. Vδ2-chain TCR+ T-cell Transcripts (CDR3 Region) Expressed in the Solid Tumor from patient OV1T

Transcript No.	Vδ	N	Dδ2	N	Jδ	Transcript Frequency	p-value 1/25	2/25
4	Y Y C A C D T		A G D T R		D K L I Vδ1/Dδ2/Dδ3/Jδ1			
	TACTACTGTGCCTGTGACACC		GCAGGGGATACACGC		GATAAACTCATC	10/25 40%	<0.0001	<0.0001
8	Y Y C A C D T		V L G D P R S T		D K L I Vδ1/Dδ2/Dδ3/Jδ1			
	TACTACTGTGCCTGTGACACC		GTCCTGGGGGACCCGAGGAGCACC		GATAAACTCAT	7/25 28%	<0.0001	<0.004
12	Y Y C A C D F		V L G D T G Y T		D K L I Vδ1/Dδ2/Dδ3/Jδ1			
	TACTACTGTGCCTGTGAC	TTC	GTACTGGGGGATACGGGGTACACC		GATAAACTCATC	1/25 4%	NS	NS
20	Y Y C A C D S	L G D T S			D K L I Vδ1/Dδ2/Dδ3/Jδ1			
	TACTACTGTGCCTGTGAC	TCT	CTGGGGGATACG	TCC	GATAAACTCATC	1/25 4%	NS	NS
22	Y Y C A C D K	L G V T			D K L I Vδ1/Dδ2/Dδ3/Jδ1			
	TACTACTGTGCCTGTGAC	AAG	CTGGGG	GTTACC	GATAAACTCATC	1/25 4%	NS	NS
17	Y Y C A C D		V L G D T P G T		D K L I Vδ1/Dδ2/Dδ3/Jδ1			
	TACTACTGTGCCTGTGAC		GTACTGGGGGATACCCCGGGCACC		GATAAACTCATC	1/25 4%	NS	NS
11	Y Y C A C D M	V G D T N A			D K L I Vδ1/Dδ2/Dδ3/Jδ1			
	TACTACTGTGCCTGTGAC	ATG	GTCGGGGATACT	AATGCC	GATAAACTCATC	1/25 4%	NS	NS
2	Y Y C A C D T V N G G P Y T				D K L I Vδ1/Dδ2/Dδ3/Jδ1			
	TACTACTGTGCCTGTGACACCGTGAATGGGGGTCCCTACACC				GATAAACTCATC	1/25 4%	NS	NS

Table 25. Vδ2-chain TCR+ T-cell Transcripts (CDR3 Region) Expressed in the Solid Tumor from patient OV42T

Transcript No.	Vδ	N	Dδ2	N	Jδ	Transcript Frequency	p-value 1/24	2/24
11	Y Y C A C D T V		G T G G G T		D K L I Vδ2Dδ2Jδ1			
	TACTACTGTGCCTGTGACACCGTG		GGAACTGGGGGGGGGCACC		GATAAACTCATC	18/24 75%	<0.0001	<0.0001
17	Y Y C A C D		I L G D T		D K L I Vδ2Dδ2Jδ1			
	TACTACTGTGCCTGTGAC		ATACTGGGGGATACG		GATAAACTCATC	3/24 13%	NS	NS
2	Y Y C A C D		V L G D N T		D K L I Vδ2Dδ2Jδ1			
	TACTACTGTGCCTGTGAC		GTACTGGGGGATAACACC		GATAAACTCATC	2/24 13%	NS	NS
24	Y Y C A C D		G V A S G D T S		D K L I Vδ2Dδ2Jδ1			
	TACTACTGTGCCTGTGAC		GGTGTGGCTTCGGGGGATACGTCC		GATAAACTCATC	1/24 13%	NS	NS

Table 26. Vδ2-chain TCR+ T-cell Transcripts (CDR3 Region) Expressed in the Solid Tumor from patient OV27T

Transcript No.	Vδ	N	Dδ2	N	Jδ	Transcript Frequency	p-value 1/30	2/30
13	Y Y C A C D T V TACTACTGTGCCTGTGACACCGTA		T L G I N T ACTCTGGGGATTAACACC		D K L I Vδ2Dδ2Jδ1 GATAAACTCATC	11/30 36%	<0.0001	<0.0001
22	Y Y C A C D T V TACTACTGTGCCTGTGACACCGTA		L G D R CTGGGGGATCGG		D K L I Vδ2Dδ2Jδ1 GATAAACTCATC	8/30 27%	<0.0001	<0.0005
3	Y Y C A C D T V TACTACTGTGCCTGTGACACCGTA		G E D T GGGGAAGACACC		D K L I Vδ2Dδ2Jδ1 GATAAACTCATC	1/30 3%	NS	NS
4	Y Y C A C D T V TACTACTGTGCCTGTGACACCGTT		G D H R H T GGGGATCACAGGCACACC		D K L I Vδ2Dδ2Jδ1 GATAAACTCATC	1/30 3%	NS	NS
1	Y Y C A C V W G I L P S P P I A TACTACTGTGCCTGT GTCTGGGGGATACTCCCGTCACCCCCCATCGCC				D K L I Vδ2Dδ3Jδ1 GATAAACTCATC	1/30 3%	NS	NS
6	Y Y C A C D TACTACTGTGCCTGTGAC	P CCC	L L G D P P N T TTACTGGGGGATCCCCCCAACACC		D K L I Vδ2Dδ2Jδ1 GATAAACTCATC	1/30 3%	NS	NS
7	Y Y C A C D T V G G G G S TACTACTGTGCCTGTGACACCGTTGGGGGGGGGAGGGTCC				D K L I Vδ2Dδ3Jδ1 GATAAACTCATC	1/30 3%	NS	NS
8	Y Y C A C D T I G T G D N L G P TACTACTGTGCCTGTGACACGATTGGTACTGGGGACAACCTGGGGCCT				D K L I Vδ2Dδ2Jδ1 GATAAACTCATC	1/30 3%	NS	NS
5	Y Y C A C D TACTACTGTGCCTGTGAC		V A G V T GTGGCCGGGGTCACC		D K L I Vδ2Dδ2Jδ1 GATAAACTCATC	1/30 3%	NS	NS
10	Y Y C A C D T L E V L G D N T TACTACTGTGCCTGTGACACCCTCGAAGTACTGGGGGATAACACC				D K L I Vδ2Dδ2Jδ1 GATAAACTCATC	1/30 3%	NS	NS
11	Y Y C A C D V L A V T TACTACTGTGCCTGTGACGTGCTCGCTGTGACC				D K L I Vδ2Dδ2Jδ1 GATAAACTCATC	1/30 3%	NS	NS

Table 27. Vδ2-chain TCR+ T-cell Transcripts (CDR3 Region) Expressed in the Solid Tumor from patient OV26T

Transcript No.	Vδ	N	Dδ2	N	Jδ	Transcript Frequency	p-value 1/17	2/17
6	Y Y C A C D T V A T S G G V T TACTACTGTGCCTGTGACACCGTCGCTACTAGTGGGGGAGTTACC				D K L I Vδ2Dδ3Jδ1 GATAAACTCATC	3/17 18%	NS	NS
1	Y Y C A C D T V G T G G Y P N T TACTACTGTGCCTGTGACACCGTG GGTACTGGGGGATAC CCTAACACC				D K L I Vδ2Dδ3Jδ1 GATAAACTCATC	3/17 18%	NS	NS
2	Y Y C A C D S V L G E R N P P T TACTACTGTGCCTGTGAC TCAGTACTGGGGGAACGCAACCCCCCTACC				D K L I Vδ2Dδ2Jδ1 GATAAGCTCATC	2/17 12%	NS	NS
3	Y Y C A C D T V S A G D T G S F T TACTACTGTGCCTGTGACACCGTGTCTGCGGGGGGATACGGGGAGTTTCACC				D K L I Vδ2Dδ2Jδ1 GATAAACTCATC	1/17 6%	NS	NS
5	Y Y C A C D T L R T G G Y V N TACTACTGTGCCTGTGACACCCTCCGTACTGGGGGATACGTGAAC				D K L I Vδ2Dδ3Jδ1 GATAAACTCATC	1/17 6%	NS	NS
10	Y Y C A C D R L G D K D TACTACTGTGCCTGTGACCGGCTGGGGGATAAGGAC				W D T R Vδ2Dδ3Jδ1 TGGGACACCCGA	1/17 6%	NS	NS
11	Y Y C A C S L V G S Q R V A TACTACTGTGCCTGTTCCCTGGTGGGATCCCAGAGGGTGGCC				D K L I Vδ2Dδ3Jδ1 GATAAACTCATC	1/17 6%	NS	NS
12	Y Y C A C D T V V L G D T R W T TACTACTGTGCCTGTGACACCGTAGTACTGGGGGATACGCGATGGACC				D K L I Vδ2Dδ3Jδ1 GATAAACTCATC	1/17 6%	NS	NS
9	Y Y C A C D T V V L G D T R R N T TACTACTGTGCCTGTGACACAGTCGTACTGGGGGATACGAGGAGAAACACC				D K L I Vδ2Dδ3Jδ1 GATAAACTCATC	1/17 6%	NS	NS
14	Y Y C A C D D V R G L G G TACTACTGTGCCTGTGACGACGTGAGGGGACTGGGTGGT				K L I Vδ2Dδ3Jδ1 AAACTCATC	1/17 6%	NS	NS
13	Y Y C A C D T I G G T TACTACTGTGCCTGTGACACCATCGGGGGCACC				D K L I Vδ2Dδ3Jδ1 GATAAACTCATC	1/17 6%	NS	NS

Table 28. Vδ2-chain TCR+ T-cell Transcripts (CDR3 Region) Expressed in the Solid Tumor from patient OV31T

Transcript No.	Vδ	N	Dδ2	N	Jδ	Transcript Frequency	p-value 1/31	2/31
16	Y Y C A C D T V		G G G G S		D K Vδ2Dδ3Jδ1			
	TACTACTGTGCCTGTGACACCGTG		GGGGGGGGAGGGTCC		GATAAA	14/31 45%	<0.0001	<0.0001
24	Y Y C A C D		S L L G D T		D K Vδ2Dδ2Jδ1			
	TACTACTGTGCCTGTGAC		TCCTTACTGGGGGATACC		GACAAA	5/31 16%	NS	NS
20	Y Y C A	W S	G G Y F P F P L W		D K Vδ2Dδ3Jδ1			
	TACTACTGTGCC	TGGTCG	GGGGGATACTTCCCCTTCCCCTTGTGG		GATAAA	2/31 6%	NS	NS
5	Y Y C A C D T V A	G G D H G Q D Y A		D K Vδ2Dδ2Jδ1			
	TACTACTGTGCCTGTGACACCGTGGCCGGAGGGGACCACGGACAGGACTACGCC				GATAAA	2/31 6%	NS	NS
18	Y Y C A C D T V		A S G D T S		D K Vδ2Dδ2Jδ1			
	TACTACTGTGCCTGTGACACCGTG		GCTTCGGGGGATACGTCC		GATAAA	2/31 6%	NS	NS
9	Y Y C A C D T V		G G Y V		T D Vδ2Dδ2Jδ1			
	TACTACTGTGCCTGTGACACCGTG		GGGGGATACGTC		ACCGA	1/31 3%	NS	NS
19	Y Y C A C D T V		L G D T R A R T		D K Vδ2Dδ2Jδ1			
	TACTACTGTGCCTGTGACACCGTA		CTGGGGGATACGCGGGCGAGGACC		GATAAA	1/31 3%	NS	NS
10	Y Y C A C D T V		S R G P Y T		D K Vδ2Dδ2Jδ1			
	TACTACTGTGCCTGTGACACCGTG		AGTCGGGGACCTTACACC		GATAAA	1/31 3%	NS	NS
3	Y Y C A C D T V		G L G T L S		D K Vδ2Dδ2Jδ1			
	TACTACTGTGCCTGTGACACCGTG		GGACTGGGGACACTCTCA		GATAAA	1/31 3%	NS	NS
14	Y Y C A C D T V		T D R G		D K Vδ2Dδ2Jδ1			
	TACTACTGTGCCTGTGACACCGTG		ACGGATAGGGGC		GATAAA	1/31 3%	NS	NS
18	Y Y C A C D T V		G R I T		D K Vδ2Dδ2Jδ1			
	TACTACTGTGCCTGTGACACCGTG		GGGAGAATAACC		GATAAA	1/31 3%	NS	NS

Table 29. Summary of clonal expansion of Vδ2-chain TCR+ T -cell transcripts in the solid tumor of patients with EOC

OV1T: 10/25:#4:40%:CDR3:YYCACDTAGDTRDKLI
OV42T: 18/24:#11:75%:CDR3:YYCACDTVGTGGGTDKLI
OV27T: 11/30:#13:36%:CDR3:YYCACDTVTLGINTDKLI
OV27T: 8/30:#22:27%:CDR3:YYCACDTVLGDRDKLI
OV31T: 14/31:#16:45%:CDR3:YYCACDTVGGGGGSDKLI

Table 30. Percent clonal expansion of Vδ2-chain TCR+ T-cell transcripts in the solid tumor of patients with EOC

EOC Patient Sample	% Clonal Expansion
OV1T	40%
OV42T	75%
OV27T	36%
OV27T	27%
OV31T	45%

In patient OV1T, sequence analysis of Vδ2-chain TCR+ T cell transcripts revealed that 10 out of 25 (40%) TCR+ T-cell transcripts each had a CDR3 region identical to that of OV1T number 4 with its CDR3 region as: VδDδ2Dδ3Jδ1 YYCACDTAGDTRDKLI $p < 0.05$ (a statistically significant oligoclonal expansion) (see Table 24). 7 out of 25 (28%) TCR+ T-cell transcripts each had a CDR3 region identical to that of OV1T number 8 with its CDR3 region as: VδDδ2Dδ3Jδ1 YYCACDTVLGDPRSTDKLI $p < 0.05$ (a statistically significant oligoclonal expansion). There were six non-clonally expanded TCR+ T-cell transcripts each had a CDR3 region as: VδDδ2Dδ3Jδ1 YYCACDFVLGDTGYTDKLI (4%) $p > 0.05$, VδDδ2Dδ3Jδ1 YYCACDSLGDTSDKLI (4%) $p > 0.05$, VδDδ2Dδ3Jδ1 YYCACDKLGVTDKLI (4%) $p > 0.05$, VδDδ2Dδ3Jδ1 YYCACDVLGDTPGT DKLI (4%) $p > 0.05$, VδDδ2Dδ3Jδ1 YYCACDMVGDTNAGYTDKLI (4%) $p > 0.05$,

VδDδ2Dδ3Jδ1 YYCACDTVNGGPYTDKLI (4%) p>0.05 which were transcripts 12, 20, 22, 17, 11, and 2, respectively.

In patient OV42T, sequence analysis of Vδ2-chain TCR+ T cell transcripts revealed that 18 out of 24 (75%) TCR+ T-cell transcripts each had a CDR3 region identical to that of OV42T number 11 with its CDR3 region as: VδDδ2Dδ3Jδ1 YYCACDTVGTGGGTDKLI p<0.05 (a statistically significant oligoclonal expansion) (see Table 25). There were three additional transcripts that did not reveal oligoclonal expansion with a CDR3 region as: VδDδ2Dδ3Jδ1 YYCACDILGDTDKLI (12.5%) p>0.05, VδDδ2Dδ3Jδ1 YYCACDVLGDNTDKLI (8%) p>0.05, VδDδ2Dδ3Jδ1 YYCACDGVASGDTSDKLI (4%) p>0.05 which were transcripts number 17, 2 and 24, respectively.

In patient OV27T, sequence analysis revealed that 11 out of 30 (36%) TCR+ T-cell transcripts each had a CDR3 region identical to that of OV27T number 13 with its CDR3 region as: VδDδ2Jδ1 YYCACDTVTLGINTDKLI p>0.05 (a statistically significant oligoclonal expansion) (Table 26). 8 out of 30 TCR+ T-cell transcripts each had a CDR3 region identical to that of OV27T number 22 with its CDR3 region as: VδDδ2Jδ1 YYCACDTVLGDRDKLI p>0.05 (a statistically significant oligoclonal expansion) (Table 26). There were nine non-clonally expanded transcripts number 3, 4, 1, 6, 7, 8, 5, 10 and 11 (see Table 26).

In patient OV26T, sequence analysis revealed that 3 out of 17 (18%) TCR+ T-cell transcripts each had a CDR3 region identical to that of OV26T number 6 with its CDR3 region as: VδDδ3Jδ1 YYCACDTVATSGGVTDKLI p >0.05 (a statistically insignificant oligoclonal expansion) (Table 27). There were
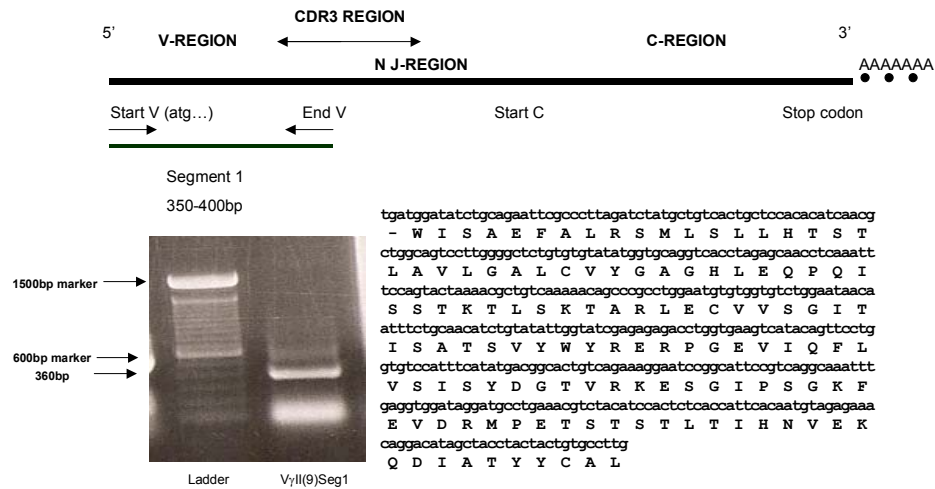
8 non-clonally expanded transcripts number 3, 5, 10, 11, 12, 9, 14 and 13 (see Table 27).

In patient OV31T, sequence analysis revealed that 14 out of 31 (45%) TCR+ T-cell transcripts each had a CDR3 region identical to that of OV45T number 16 with its CDR3 region as: VδDδ3Jδ1 YYCACDTVGGGGSDKLI $p < 0.05$ (a statistically significant oligoclonal expansion) (see Table 28). 5 out of 31 TCR+ T-cell transcripts each had a CDR3 region identical to that of OV45T number 24 with its CDR3 region as: VδDδ3Jδ1 YYCACDSLLGDTDKLI $p > 0.05$ (a statistically insignificant oligoclonal expansion). 2 out of 31 TCR+ T-cell transcripts each had a CDR3 region identical to that of OV45T number 20 with its CDR3 region as: VδDδ3Jδ1 YYCACWSGGYFPFPLWDKLI $p > 0.05$ (a statistically insignificant oligoclonal expansion). 2 out of 31 TCR+ T-cell transcripts each had a CDR3 region identical to that of OV45T number 5 with its CDR3 region as: VδDδ3Jδ1 YYCACDTVAGGDHGQDYADKLI $p > 0.05$ (a statistically insignificant oligoclonal expansion). 2 out of 31 TCR+ T-cell transcripts each had a CDR3 region identical to that of OV45T number 18 with its CDR3 region as: VδDδ3Jδ1 YYCACDTVASGDTSDKLI $p > 0.05$ (a statistically insignificant oligoclonal expansion). There were six non-clonally expanded TCR+ T-cell transcripts number 9, 19, 10, 3, 14 and 18 (Table 27).
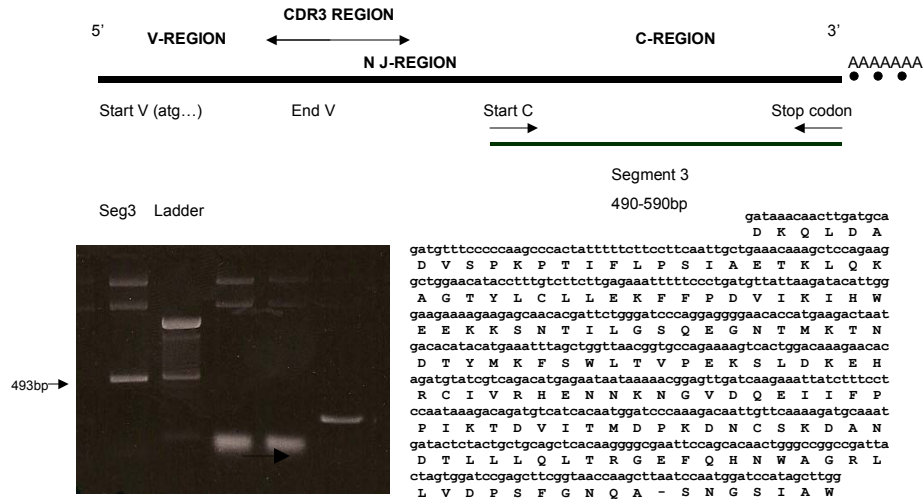
E) Full-length construction results

Once we determined the presence of clonally expanded γδ TCR+ T-cells infiltrating the solid tumor of patients with EOC the γI-, γII(9)-, δ1-, δ2-chain TCR+ T-cell transcripts containing the clonally expanded CDR3 were used for full-length construct. These full lengths were constructed using the primers mentioned previously to amplify each third of the full-length transcript followed by a PCR-mediated ligation of the transcripts.
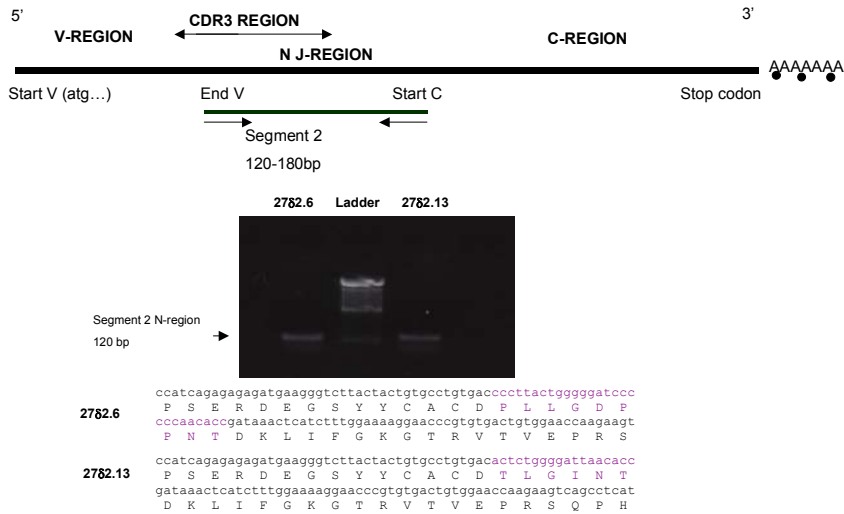
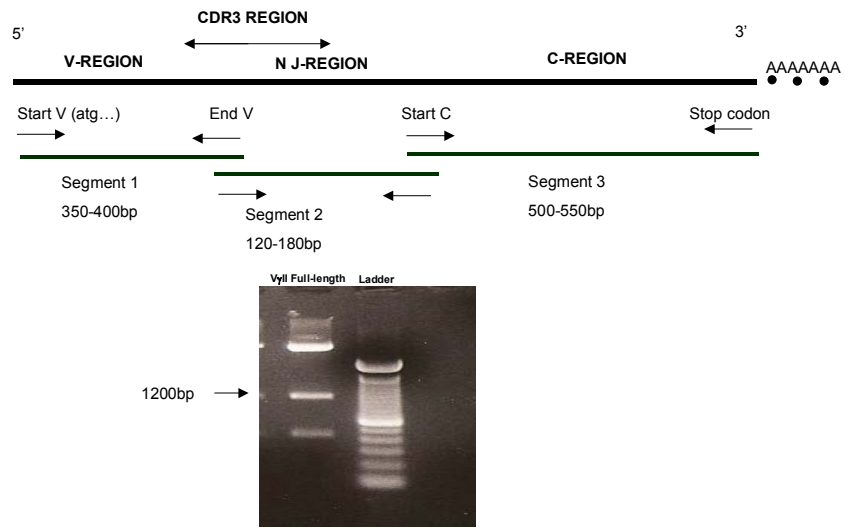**Figure 6 - VγII(9)-chain TCR+ T-cell transcript (Segment 1) used for full-length construction**


```
tgatggatatctgcagaattcgcccttagatctatgctgtcactgctccacacatcaacg
-  W  I  S  A  E  F  A  L  R  S  M  L  S  L  L  H  T  S  T
ctggcagtccttggggctctgtgtgtatatggtgcaggtcacctagagcaacctcaaatt
L  A  V  L  G  A  L  C  V  Y  G  A  G  H  L  E  Q  P  Q  I
tccagtactaaaacgctgtcaaaaacagcccgcctggaatgtgtggtgtctggaataaca
S  S  T  K  T  L  S  K  T  A  R  L  E  C  V  V  S  G  I  T
atttctgcaacatctgtatattggtatcgagagagacctggtgaagtcatacagttcctg
I  S  A  T  S  V  Y  W  Y  R  E  R  P  G  E  V  I  Q  F  L
gtgtccatttcatatgacggcactgtcagaaaggaatccggcattccgtcaggcaaattt
V  S  I  S  Y  D  G  T  V  R  K  E  S  G  I  P  S  G  K  F
gaggtggataggatgcctgaaacgtctacatccactctcaccattcacaatgtagagaaa
E  V  D  R  M  P  E  T  S  T  S  T  L  T  I  H  N  V  E  K
caggacatagctacctactactgtgccttg
Q  D  I  A  T  Y  Y  C  A  L
```

80

Figure 7 - Cγ-chain TCR+ T-cell transcript (Segment 3) used for full-length construction


```
                                                    gataaacaacttgatgca
                                                        D  K  Q  L  D  A
gatgtttccccaagcccactatttttcttccttcaattgctgaaacaaagctccagaag
 D  V  S  P  K  P  T  I  F  L  P  S  I  A  E  T  K  L  Q  K
gctggaacatacctttgtcttcttgagaaattttccctgatgttattaagatacattgg
 A  G  T  Y  L  C  L  L  E  K  F  F  P  D  V  I  K  I  H  W
gaagaaagaagagcaacacgattctgggatcccaggaggggaacaccatgaagactaat
 E  E  K  K  S  N  T  I  L  G  S  Q  E  G  N  T  M  K  T  N
gacacatacatgaaatttagctggttaacggtgccagaaagtcactggacaaagaacac
 D  T  Y  M  K  F  S  W  L  T  V  P  E  K  S  L  D  K  E  H
agatgtatcgtcagacatgagaataataaaaacggagttgatcaagaaattatctttcct
 R  C  I  V  R  H  E  N  N  K  N  G  V  D  Q  E  I  I  F  P
ccaataaagacagatgtcatcacaatggatcccaaagacaattgttcaaaagatgcaaat
 P  I  K  T  D  V  I  T  M  D  P  K  D  N  C  S  K  D  A  N
gatactctactgctgcagctcacaaggggcgaattccagcacaactgggccggccgatta
 D  T  L  L  L  Q  L  T  R  G  E  F  Q  H  N  W  A  G  R  L
ctagtggatccgagcttcggtaaccaagcttaatccaatggatccatagcttgg
 L  V  D  P  S  F  G  N  Q  A  -  S  N  G  S  I  A  W
```
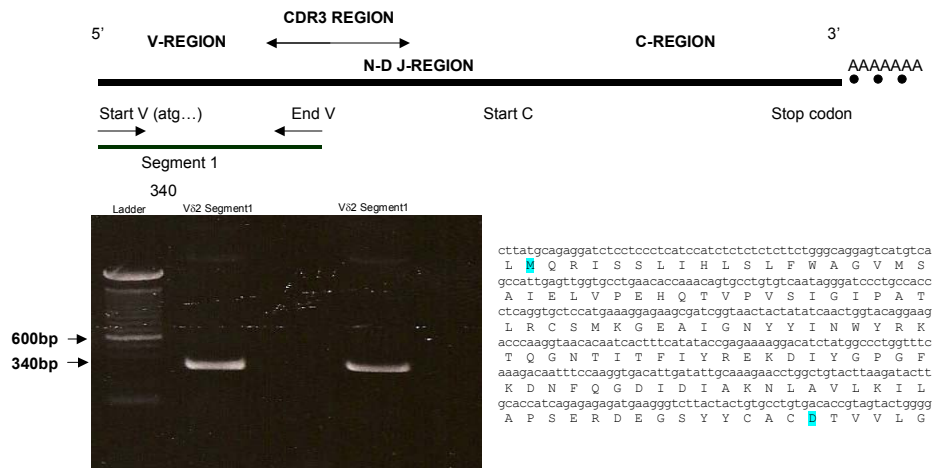
Figure 8 - VγII(9)-chain TCR+ T-cell transcript (Segment 2) used for full-length construction of OV27T transcript 6 and 13


```
2782.6
ccatcagagagagatgaagggtcttactactgtgcctgtgaccccttactgggggatccc
 P  S  E  R  D  E  G  S  Y  Y  C  A  C  D  P  L  L  G  D  P
cccaacaccgataaactcatctttggaaaaggaacccgtgactgtggaaccaagaagt
 P  N  T  D  K  L  I  F  G  K  G  T  R  V  T  V  E  P  R  S

2782.13
ccatcagagagagatgaagggtcttactactgtgcctgtgacactctgggattaacacc
 P  S  E  R  D  E  G  S  Y  Y  C  A  C  D  T  L  G  I  N  T
gataaactcatctttggaaaaggaacccgtgtgactgtggaaccaagaagtcagcctcat
 D  K  L  I  F  G  K  G  T  R  V  T  V  E  P  R  S  Q  P  H
```
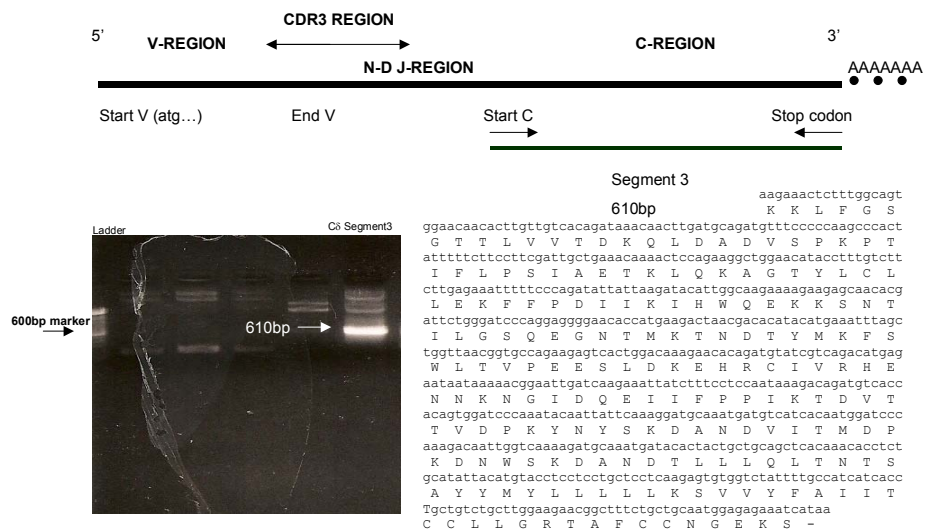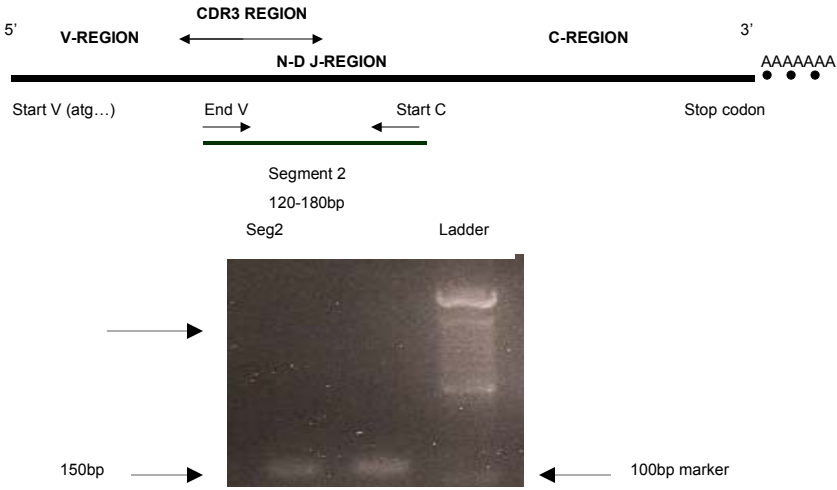
Figure 9 - Vγ9-chain TCR+ T-cell transcript (Segment 1+2+3) full-length construction of OV27T

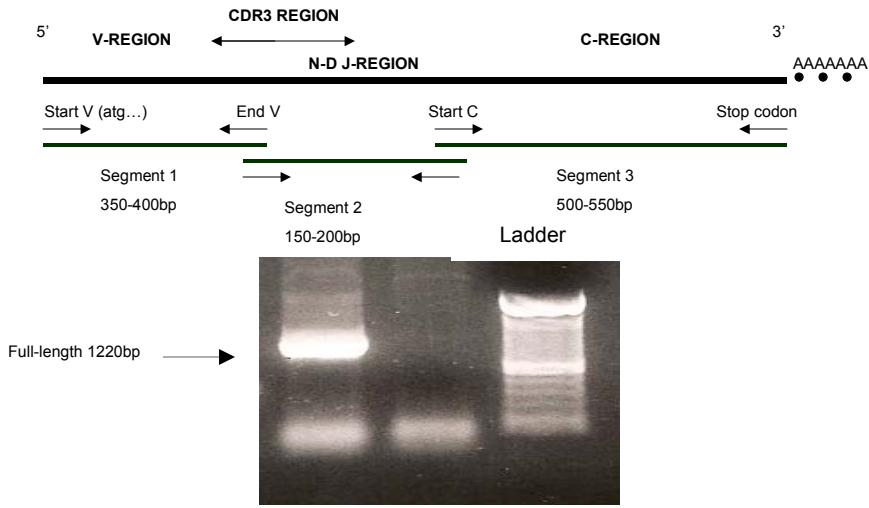## Figure 10 - Vδ2-chain TCR+ T-cell transcript (Segment 1) used for full-length construction of OV27T


```
cttatgcagaggatctcctccctcatccatctctctctcttctgggcaggagtcatgtca
 L  M  Q  R  I  S  S  L  I  H  L  S  L  F  W  A  G  V  M  S
gccattgagttggtgcctgaacaccaaacagtgcctgtgtcaatagggatccctgccacc
 A  I  E  L  V  P  E  H  Q  T  V  P  V  S  I  G  I  P  A  T
ctcaggtgctccatgaaaggagaagcgatcggtaactactatatcaactggtacaggaag
 L  R  C  S  M  K  G  E  A  I  G  N  Y  Y  I  N  W  Y  R  K
acccaaggtaacacaatcactttcatataccgagaaaaggacatctatggccctggtttc
 T  Q  G  N  T  I  T  F  I  Y  R  E  K  D  I  Y  G  P  G  F
aaagacaatttccaaggtgacattgatattgcaaagaacctggctgtacttaagatactt
 K  D  N  F  Q  G  D  I  D  I  A  K  N  L  A  V  L  K  I  L
gcaccatcagagagagatgaagggtcttactactgtgcctgtgacaccgtagtactgggg
 A  P  S  E  R  D  E  G  S  Y  Y  C  A  C  D  T  V  V  L  G
```

Figure 11 - Vδ2-chain TCR+ T-cell transcript (Segment 3) used for full-length construction of OV27T


```
                                         aagaaactctttggcagt
                                          K  K  L  F  G  S
ggaacaacacttgttgtcacagataaacaacttgatgcagatgtttcccccaagcccact
 G  T  T  L  V  V  T  D  K  Q  L  D  A  D  V  S  P  K  P  T
atttttcttccttcgattgctgaaacaaaactcccagaaggctggaacataccttgtctt
 I  F  L  P  S  I  A  E  T  K  L  Q  K  A  G  T  Y  L  C  L
cttgagaaatttttcccagatattattaagatacattggcaagaaaagaagagcaacacg
 L  E  K  F  F  P  D  I  I  K  I  H  W  Q  E  K  K  S  N  T
attctgggatcccaggaggggaacaccatgaagactaacgacacatacatgaaatttagc
 I  L  G  S  Q  E  G  N  T  M  K  T  N  D  T  Y  M  K  F  S
tggttaacggtgccagaagagtcactggacaaagaacacagatgtatcgtcagacatgag
 W  L  T  V  P  E  E  S  L  D  K  E  H  R  C  I  V  R  H  E
aataataaaaacggaattgatcaagaaattatctttcctccaataaagacagatgtcacc
 N  N  K  N  G  I  D  Q  E  I  I  F  P  P  I  K  T  D  V  T
acagtggatcccaaatacaattattcaaaggatgcaaatgatgtcatcacaatggatccc
 T  V  D  P  K  Y  N  Y  S  K  D  A  N  D  V  I  T  M  D  P
aaagacaattggtcaaaagatgcaaatgatacactgctgctgcaacttacaaacacctct
 K  D  N  W  S  K  D  A  N  D  T  L  L  L  Q  L  T  N  T  S
gcatattacatgtacctcctcctgctcctcaagagtgtggtctattttgccatcatcacc
 A  Y  Y  M  Y  L  L  L  L  L  K  S  V  V  Y  F  A  I  I  T
Tgctgtctgcttggaagaacggctttctgctgcaatggagagaaatcataa
 C  C  L  L  G  R  T  A  F  C  C  N  G  E  K  S  -
```

Figure 12 - Vδ2-chain TCR+ T-cell transcript (Segment 2) used for full-length construction of OV27T

Figure 13 - Vδ2-chain TCR+ T-cell transcript (Segment 1+2+3) full-length construction of OV27T

Table 32: CDR3 region of Transduced T cell lines

```
OV27Tδ2.22γ(9)II.13
Solid Tumor Patient OVT27 Delta 2
Clone  Vδ                              N        Dδ2      N        Jδ1                      Freq
22     Y Y C A C D T V                 L G D R           D K L I                          Vδ2NDδ2NJδ1
       TACTACTGTGCCTGTGACACCGTA   CTGGGGGATCGG           GATAAACTCATC                     8/30  27%
Solid Tumor OV27T Gamma (9)II
Clone  Vγ                          N                     Jγ1.3/2.3                        Freq
13     Y Y C A L W E V G E                                L G K K I                       Vγ9Jγ1.3/2.3
       TACTACTGTGCCTTGTGGGAGGTGGGGGAG                     TTGGGCAAAAAAATC                 15/18 84%


OV27Tδ2.22γ(9)II.3
Solid Tumor Patient OVT27 Delta 2
Clone  Vδ                              N        Dδ2      N        Jδ1                      Freq
22     Y Y C A C D T V                 L G D R           D K L I                          Vδ2NDδ2NJδ1
       TACTACTGTGCCTGTGACACCGTA   CTGGGGGATCGG           GATAAACTCATC                     8/30  27%
Solid Tumor OV27T Gamma (9)II
Clone  Vγ                          N                     Jγ1.3/2.3                        Freq
3      Y Y C A L W E V G                                  L G K K I                       Vγ9Jγ1.3/2.3
       TACTACTGTGCCTTGTGGGAGGTGGGG                        TTGGGCAAAAAAATC                 3/18  26%


OV27Tδ2.13γ(9)II.3
Solid Tumor Patient OVT27 Delta 2
Clone  Vδ                              N        Dδ2      N        Jδ1                      Freq
13     Y Y C A C D T V                 T L G I N T        D K L I                          Vδ2NDδ2NJδ1
       TACTACTGTGCCTGTGACACCGTA   ACTCTGGGGATTAACACC      GATAAACTCATC                    11/30 36%
Solid Tumor OV27T Gamma (9)II
Clone  Vγ                          N                     Jγ1.3/2.3                        Freq
3      Y Y C A L W E V G                                  L G K K I                       Vγ9Jγ1.3/2.3
       TACTACTGTGCCTTGTGGGAGGTGGGG                        TTGGGCAAAAAAATC                 3/18  26%
```

Table 33: CDR3 region of Transduced T cell lines (Contd.)

```
OV27Tδ2.13γ(9)II.13
SOLID TUMOR PATIENT OVT27 DELTA 2
CLONE Vδ                               N        Dδ2      N        Jδ1                      FREQ
13     Y Y C A C D T V                 T L G I N T        D K L I                          Vδ2NDδ2NJδ1
       TACTACTGTGCCTGTGACACCGTA   ACTCTGGGGATTAACACC      GATAAACTCATC                    11/30 36%
SOLID TUMOR OV27T GAMMA (9)IICLONE
CLONE      Vγ                      N                     Jγ1.3/2.3                        FREQ
13     Y Y C A L W E V G E                                L G K K I                       Vγ9Jγ1.3/2.3
       TACTACTGTGCCTTGTGGGAGGTGGGGGAG                     TTGGGCAAAAAAATC                 15/18 84%


OV27Tδ2.6γ(9)II.3
SOLID TUMOR PATIENT OVT27 DELTA 2
CLONE Vδ                               N        Dδ2      N        Jδ1                      FREQ
6      Y Y C A C D P            L L G D P P N T            D K L I                          Vδ2NDδ2NJδ1
       TACTACTGTGCCTGTGAC       CCC   TTACTGGGGGATCCCCCCAACACC   GATAAACTCATC              1/30  3%
SOLID TUMOR OV27T GAMMA (9)II
CLONE Vγ                           N                     Jγ1.3/2.3                        FREQ
3      Y Y C A L W E V G                                  L G K K I                       Vγ9Jγ1.3/2.3
       TACTACTGTGCCTTGTGGGAGGTGGGG                        TTGGGCAAAAAAATC                 3/18  26%


OV42Tδ2.11γ(9)II.7
SOLID TUMOR PATIENT OVT42 DELTA2
CLONE Vδ                               N        Dδ2      N        Jδ1                      FREQ
11     Y Y C A C D T V G T             G G G T           D K L I                          Vδ2NDδ2NJδ1
       TACTACTGTGCCTGTGACACCGTG        GGAACTGGGGGGGGCACC   GATAAACTCATC                  18/24 75%
SOLID TUMOR OV42T GAMMA (9)II
CLONE Vγ                           N                     Jγ                              FREQ
7      Y Y C A L W E V P C                                Y Y K K L F G                   Vγ9Jγ1.3/2.3
       TACTACTGTGCCTTGTGGGAGGTGCCGTGT                     TATTATAAGAAACTCTTTGGC           7/16  44%


OV1Tδ1.4γI.11
CELLS ISOLATED FROM SOLID TUMOR PATIENT OVT1 DELTA 1
CLONE Vδ                               N        Dδ2      N        Jδ1                      FREQ
4      Y F C A L G E L                 P W S T G G Y A P  D K L I                          Vδ1NDδ2NJδ1
       TACTTTTGTGCTCTTGGGGAACTC   CCATGGAGTACTGGGGGATACGCACCC   GATAAACTCATC              1/26  3.8%

CELLS ISOLATED FROM SOLID TUMOR PATIENT OV1T GAMMA I
CLONE Vγ                           N                     Jγ                              FREQ
11     Y Y C A T W D   G                                  Y Y K K L F                     Vγ5Jγ1.3/2.3
       TATTACTGTGCCACCTGGGATGGG                           TATTATAAGAAACTCTTT              3/17  18%
```

Retroviral vector construction and transduction of target cell line J.RT3-T3.5

Three retroviral vectors, pMSCVneo, pMSCVpuro and pMSCVhygro (Clontech) were used, harboring the γ-chain or δ-chain cDNAs. Both constructs used the retroviral MSCV LTR to drive the expression of either γ- chain gene or δ- chain gene governed by an IRES or an internal promoter (Figure 4). These plasmid constructs were transfected into the NIH 3T3 packaging cell lines using the calcium precipitation method. 24h following transfection media with transfection reagents was removed and replaced with fresh media and the cells were incubated 48-72h prior to selection. The cell lines were selected for stable transfectants using G418, puromycin, or hygromycin antibiotics. Retroviral supernants were collected 10-14 days following selection and used to transduce the human T cell line J.RT3-T3.5. Following transduction and antibiotic selection CD3 and γδ TCR expression was analyzed by FACS analysis. Clones exhibited both high physical titer and high transduction efficiency, and those with detectable expression levels were used for additional study.

F) Expression

To determine whether the J.RT3-T3.5 T cell lines expressed on the cell surface the γδ TCR transduced FACs analysis using Flow Cytometry was performed.

OV27Tδ2.22γ(9)II.13 γδ TCR+ transduced T-cell line
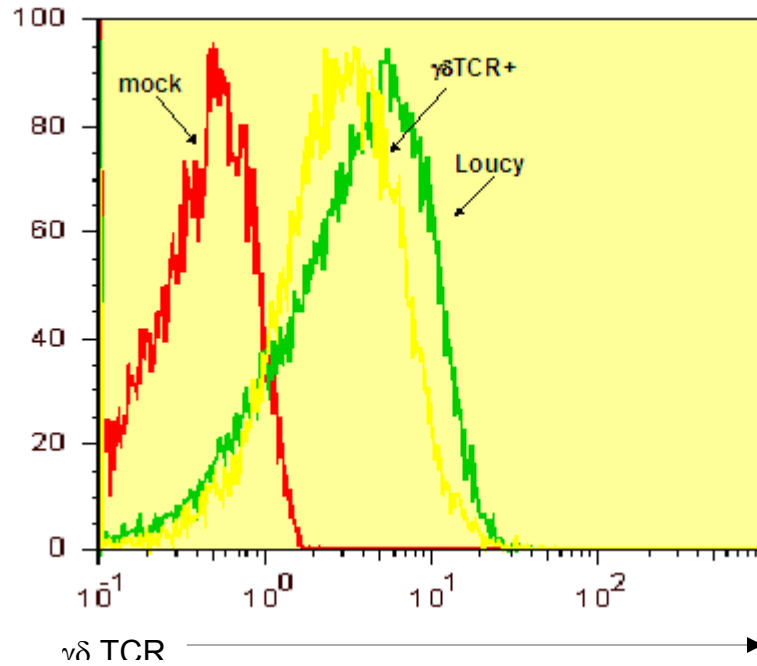
Figure 14: MSCV based retroviral expression in J.RT3-T3.5 Jurkat Mutant T cell line. Mock (red) cells infected with vector only, Loucy (green) γδ TCR+ T cell line and OV27Tδ2.22γ(9)II.13 (yellow) γδ TCR+ transduced T-cell line. The results are from one representative experiment of three performed.

OV27Tδ2.22γ(9)II.3 γδ TCR+ transduced T-cell line
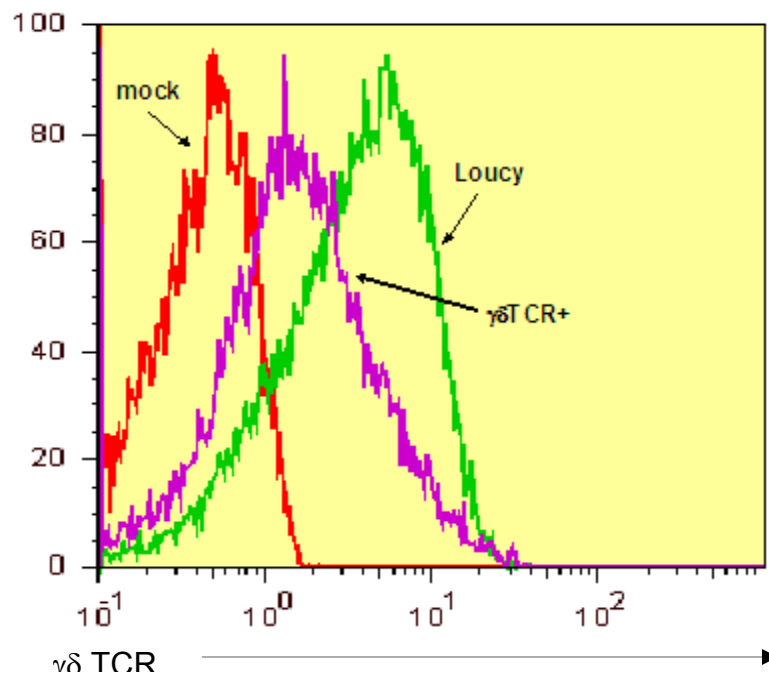
Figure 15: MSCV based retroviral expression in J.RT3-T3.5 Jurkat Mutant T cell line. Mock (red) cells infected with vector only, Loucy (green) γδ TCR+ T cell line and OV27Tδ2.22γ(9)II.3 (purple) γδ TCR+ transduced T-cell line. The results are from one representative experiment of three performed.

OV27Tδ2.13γ(9)II.13 γδ TCR+ transduced T-cell line
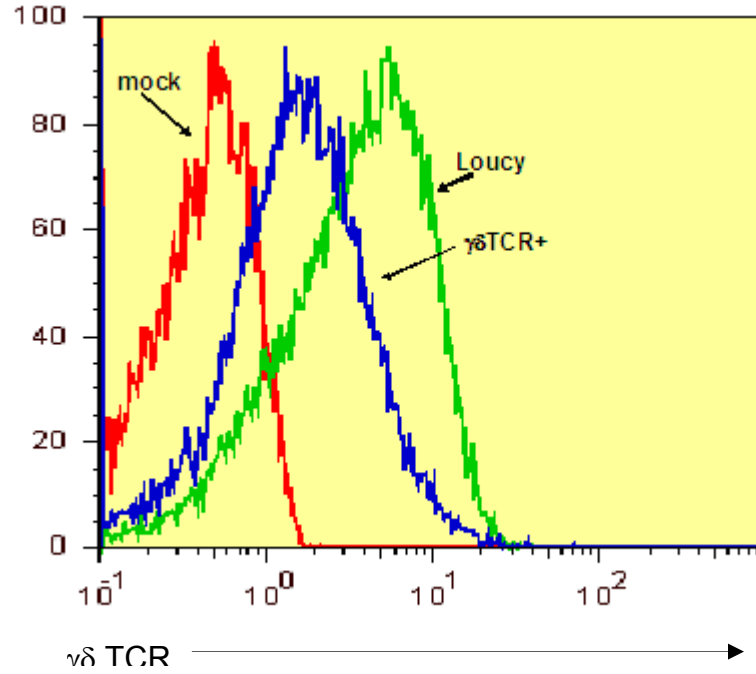
Figure 16: MSCV based retroviral expression in J.RT3-T3.5 Jurkat Mutant T cell line. Mock (red) cells infected with vector only, Loucy (green) γδ TCR+ T cell line and OV27Tδ2.13γ(9)II.13 (blue) γδ TCR+ transduced T-cell line. The results are from one representative experiment of three performed.

OV27Tδ2.13γ(9)II.3 γδ TCR+ transduced T-cell line
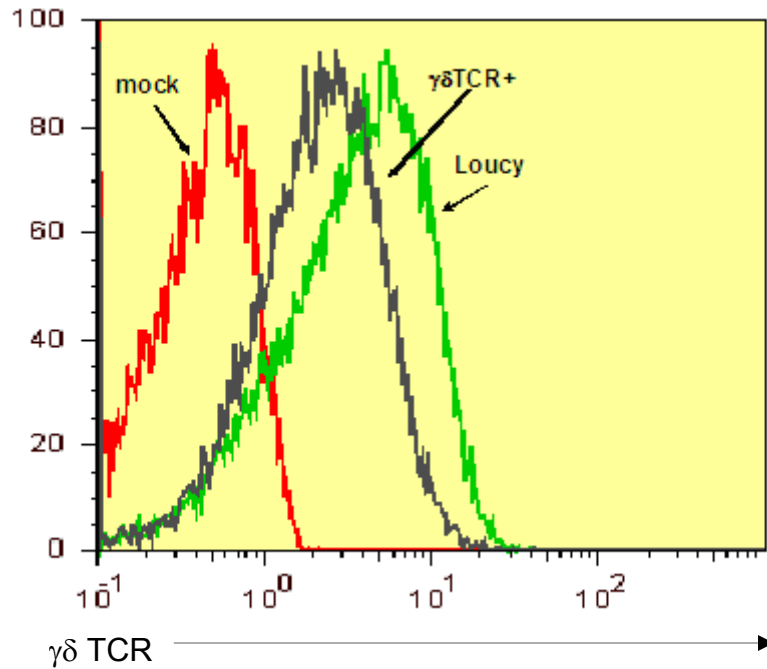
Figure 17: MSCV based retroviral expression in J.RT3-T3.5 Jurkat Mutant T cell line. Mock (red) cells infected with vector only, Loucy (green) γδ TCR+ T cell line and OV27Tδ2.13γ(9)II.3 (black) γδ TCR+ transduced T-cell line. The results are from one representative experiment of three performed.

OV27Tδ2.6γ(9)II.3 γδ TCR+ transduced T-cell line
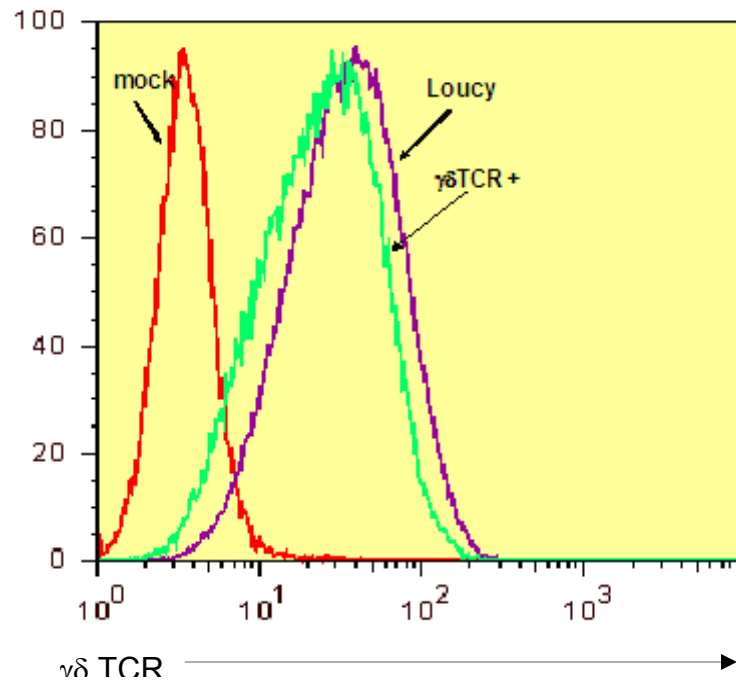
Figure 18: MSCV based retroviral expression in J.RT3-T3.5 Jurkat Mutant T cell line. Mock (red) cells infected with vector only, Loucy (purple) γδ TCR+ T cell line and OV27Tδ2.13γ(9)II.3 (green) γδ TCR+ transduced T-cell line. The results are from one representative experiment of three performed.

The yield of γδ TCR+ T-cells following transduction procedures varied.

Under the present transduction method the γδ TCR+ T-cells positive control,

Loucy cell line, expressed detectable levels of γδ TCR (81.4%; Figure 14, green).

The cells transduced with vector only expressed undetectable levels of γδ TCR

(0.05%; Figure 14, red). The cell lines transduced with full-length γδ TCR

and expressed detectable levels of γδ TCR following multiple transductions were

used for subsequent cytotoxicity and caspase assays. Those include

OV27Tδ2.22γ(9)II.13 (58.32%; Figure 14, yellow), OV27Tδ2.22γ(9)II.3 (64.3%;

Figure 15, purple), OV27Tδ2.13γ(9)II.13 (49.5%; Figure 16, blue),

OV27Tδ2.13γ(9)II.3 (53.7%; Figure 17, black), and OV27Tδ2.6γ(9)II.3 (72.3%;

Figure 18, green).

G) Caspase activation in ovarian cells following incubation with γδ TCR+ transduced T cell lines

To establish whether transduced cell lines expressing γδ TCR+ T cells

would induce apoptosis via caspase activation ovarian cell lines were incubated

with transduced γδ TCR+ and caspase-8, -9, and 3 activities were measured.

Caspase 9 and Caspase 8 activities were observed following 30-45min co-

incubations. The luminescence was measured in relative light units (RLU), which

indicates the presence or absence of caspase activity.
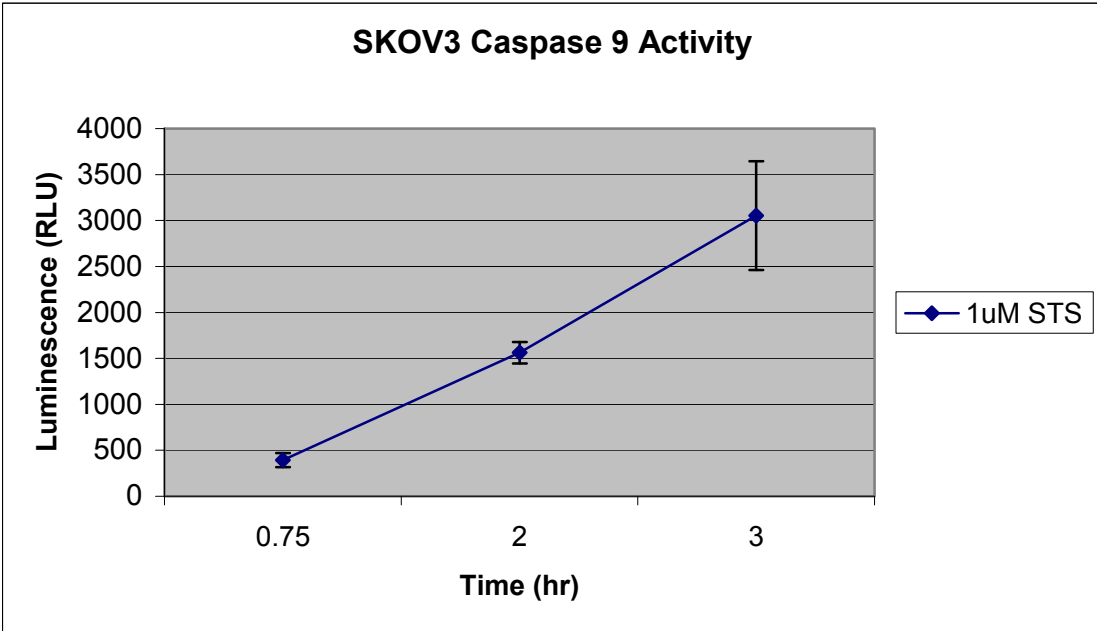
Figure 19: 1x10^4 SKOV3 cells were measured for caspase 9 activity following 1uM STS treatment at .75, 2 and 3hrs. Caspase 9 activity was measured by luminescence (RLU).
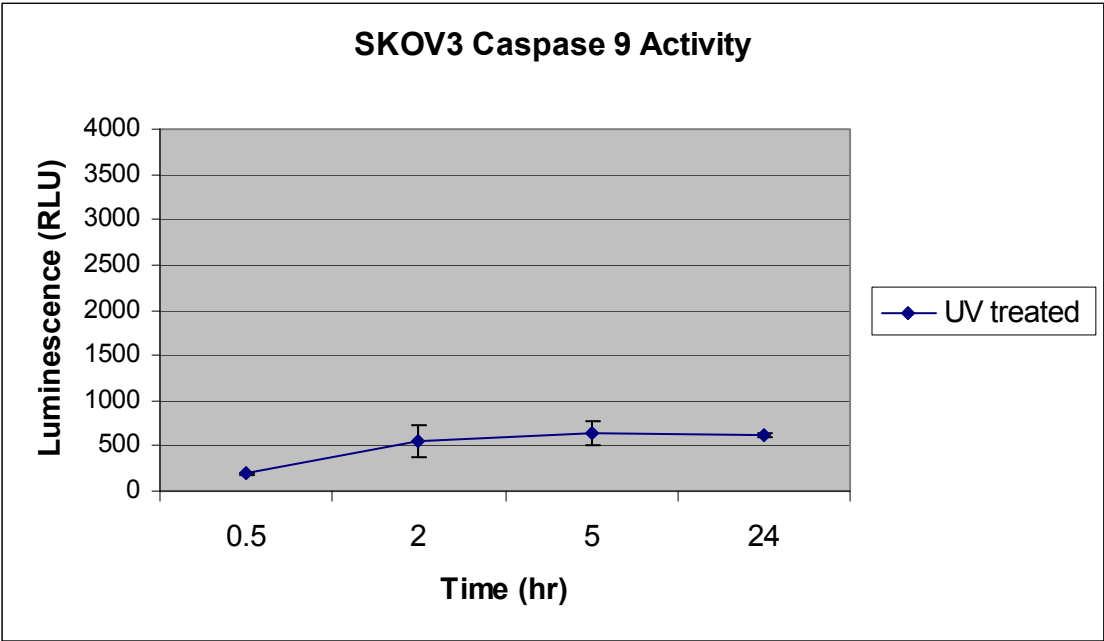
Figure 20: $1x10^4$ SKOV3 cells were measured for caspase 9 activity following following UV treatment at .5, 2, 5 and 24hrs. Caspase 9 activity was measured by luminescence (RLU).
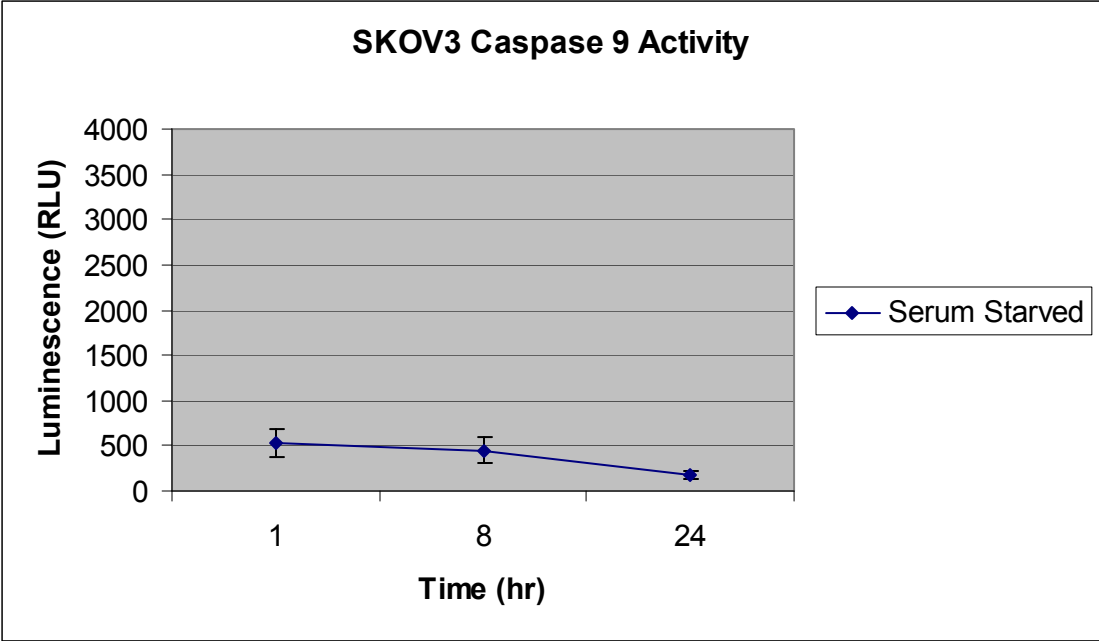
Figure 21. 1x10^4 SKOV3 cells were measured for caspase 9 activity following following serum starvation at 1, 8 and 24hrs. Caspase 9 activity was measured by luminescence (RLU).
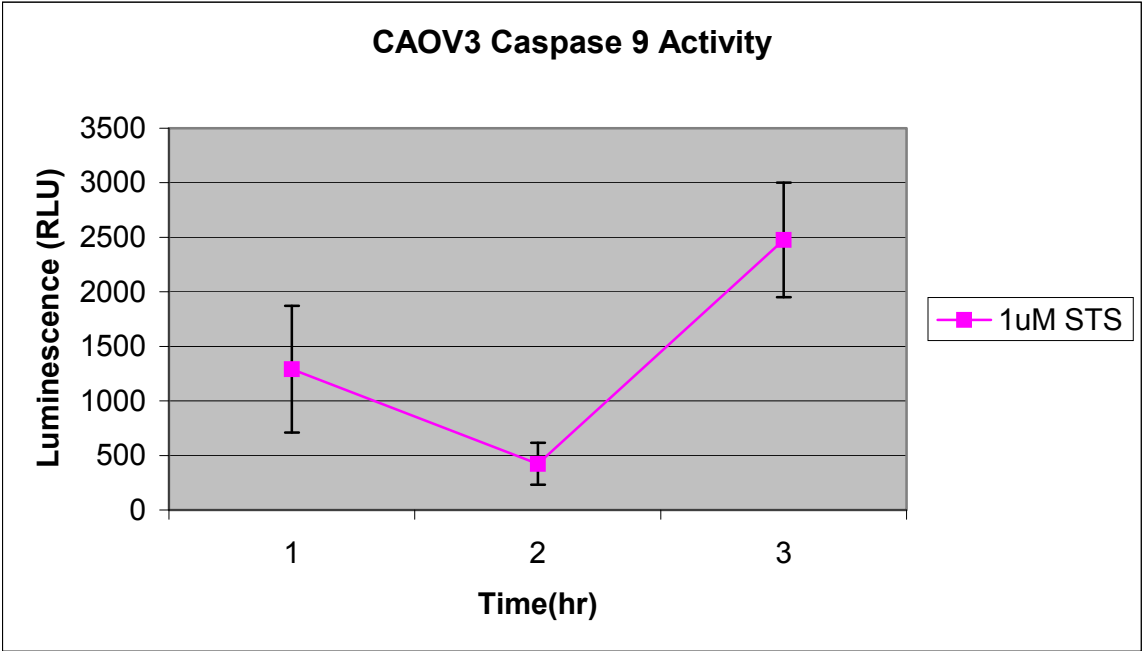
Figure 22. 1x 10^5 CAOV3 cells were measured for caspase 9 activity following incubation following 1uM STS with $\gamma\delta$ TCR+ transduced T-cell line.
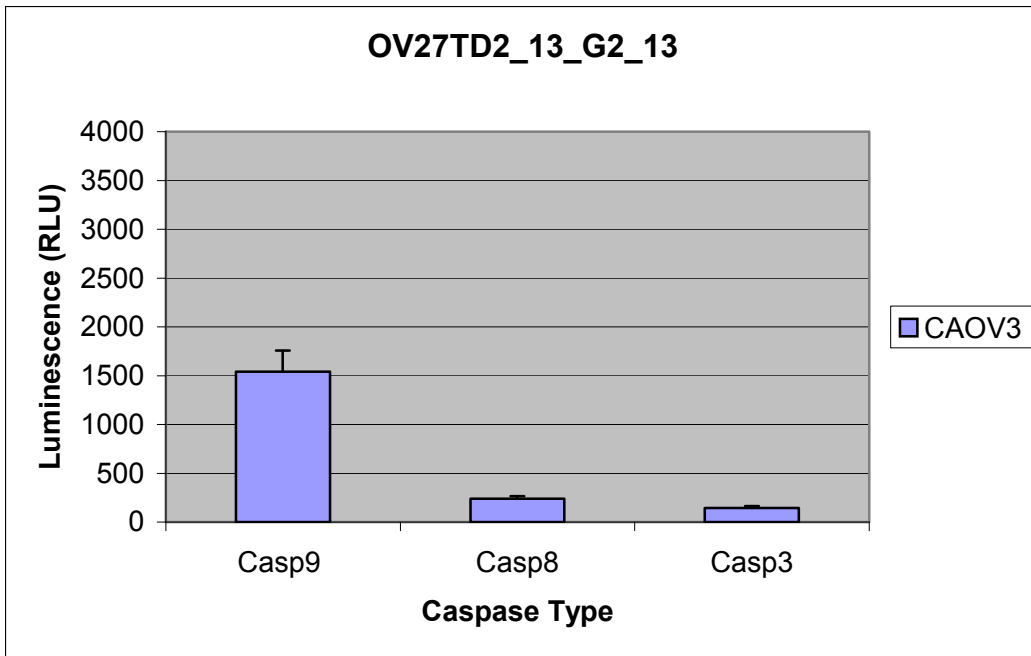
Figure 23. 1x 10^5 CAOV3 cells were measured for caspase 9, 8 and 3 activity following 5 hours of incubation with $\gamma\delta$ TCR+ transduced T-cell line.
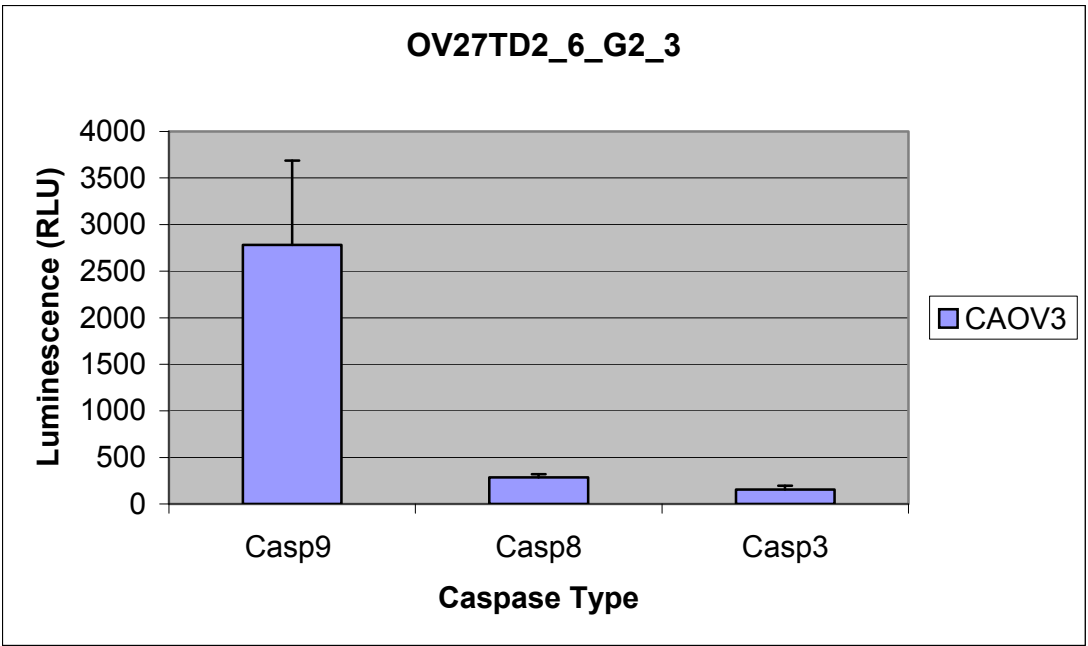
Figure 24. 1x 10^5 CAOV3 cells were measured for caspase 9, 8 and 3 activity following 5 hours of incubation with $\gamma\delta$ TCR+ transduced T-cell line.
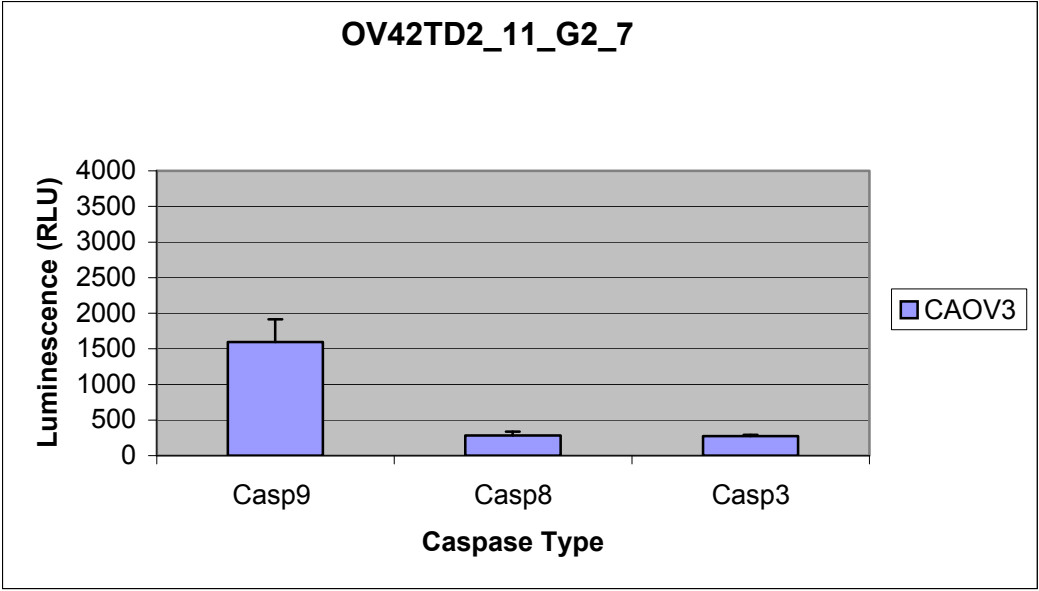
Figure 25. 1x 10^5 CAOV3 cells were measured for caspase 9, 8 and 3 activity following 5 hours of incubation with $\gamma\delta$ TCR+ transduced T-cell line.
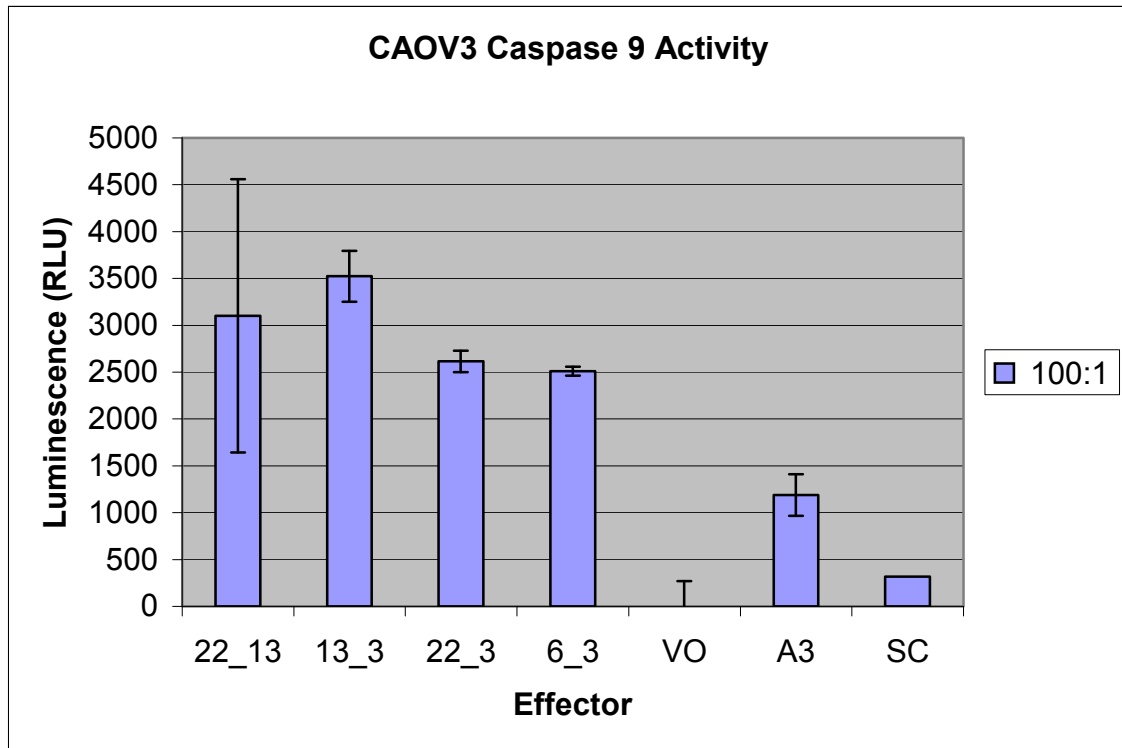
Figure 26. Summary of Caspase 9 activity in CAOV3 cells following 5hrs incubation with $\gamma\delta$ TCR+ transduced T-cell line, vector only (VO), control (A3) and single chain (SC) cells.
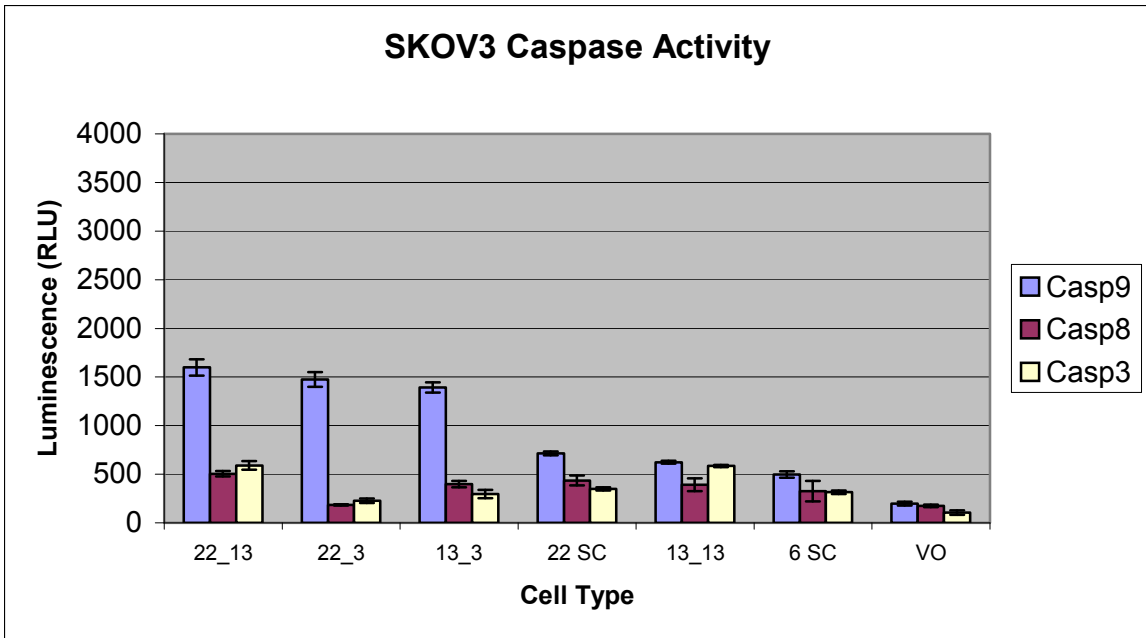
Figure 27. Summary of Caspase 9, 8 and 3 activity in SKOV3 cells following 5hrs incubation with $\gamma\delta$ TCR+ transduced T-cell line, vector only (VO) and single chain (SC) cells.
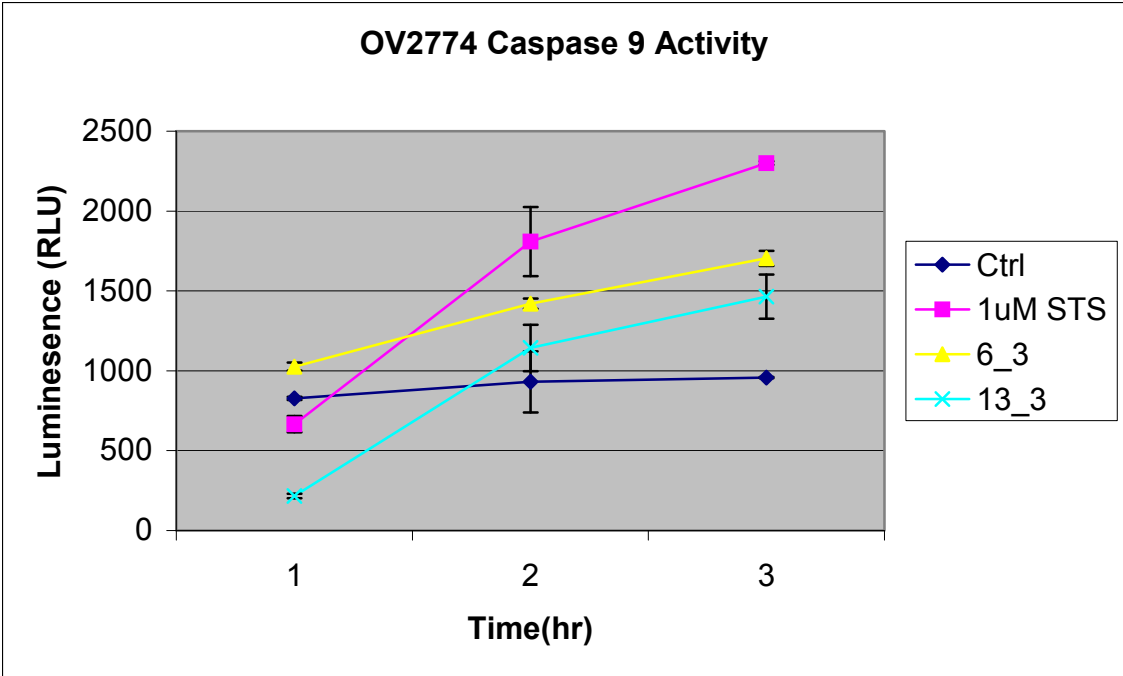
Figure 28. Caspase 9 activity in 1×10^5 OV2774 cells following incubation with 1uM STS or $\gamma\delta$ TCR+ T-cell lines.
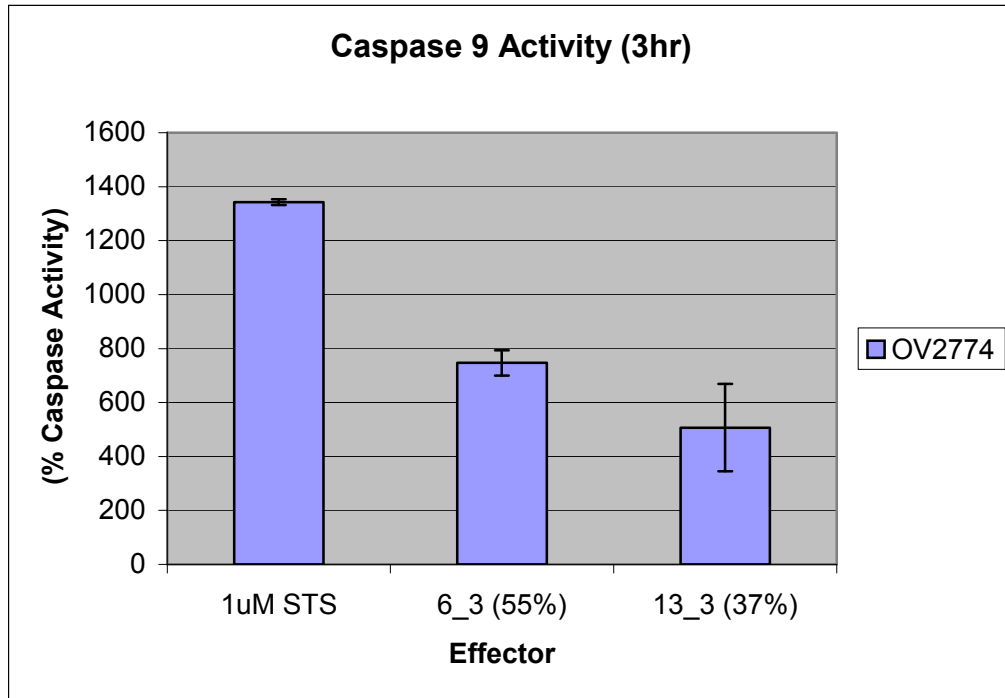
Figure 29. Caspase 9 activity following incubation with 1uM STS or $\gamma\delta$ TCR+ T-cell lines measured in percent (%) of maximum.

The ability of γδ TCR+ T-cells to induce caspase activity on ovarian tumor cell lines was observed using the Jurkat transduced cells and the ovarian tumor cell lines during co-incubation experiments. However, the caspase activity induced on SKOV3 cells following staurosporine treatment, UV irradiation, and serum starvation was performed. Once we identified the amount of caspase activity generated from a known apoptotic inducing agent we compare this to the amount of caspase activation induced (Figure 19, Figure 20 and Figure 21) by our genetically engineered γδ TCR+ T-cell lines). Using CAOV3 cells following 1uM STS the level of caspase activation measured in 2475.3 RLUs (Figure 22). Using TCR transduced cell lines as effectors and CAOV3 as target tumor cells OV27TD2_13_G2_13 induced caspase activity on tumor cells in the amount of 1540.5 RLUs (Figure 22), OV27TD2_6_G2_3 induced caspase activity on tumor cells in the amount of 2781.1 RLUs (Figure 24), OV42TD2_11_G2_7 induced caspase activity on tumor cells in the amount of 1594.6 RLUs (Figure 25), OV27TD2_22_G2_3 induced caspase activity on tumor cells in the amount of 2615.3 RLUs (Figure 26), and OV27TD2_22_G2_13 induced caspase activity on tumor cells in the amount of 3100.6 RLUs (Figure 26).

Using SKOV3 cells following 1uM STS treatment the level of caspase activation measured in luminescence (RLU) was 3053. Using TCR transduced cell lines as effectors and SKOV3 as target tumor cells OV27TD2_22_G2_13 induced caspase activity on tumor cells measured in luminescence (RLU) in the amount of 1599 (Figure 27), OV27TD2_22_G2_3 induced caspase activity on tumor cells measured in luminescence (RLU) in the amount of 1474 (Figure 27),

OV27TD2_13_G2_3 induced caspase activity on tumor cells measured in luminescence (RLU) in the amount of 1393 (Figure 27), and OV27TD2_13_G2_13 induced caspase activity on tumor cells measured in luminescence (RLU) in the amount of 623 (Figure 27).

Using OV2774 cells following 1uM STS treatment the level of caspase activation measured in luminescence (RLU) was 1343. Using TCR transduced cell lines as effectors and OV2774 as target tumor cells OV27TD2_6_G2_ 3 induced caspase activity on tumor cells measured in luminescence (RLU) in the amount of 747 (Figure 29), and OV27TD2_13_G2_3 induced caspase activity on tumor cells measured in luminescence (RLU) in the amount of 507 (Figure 29).

H) Recognition and cytotoxicity

Ovarian carcinoma cell lines (SKOV3, CAOV3 and OV2774) were observed for cytotoxicity as a result of incubation with $\gamma\delta$ TCR+ transduced T cell lines at ratios of effector to target cells (100:1, 50:1, 40:1, 25:1, and/or 10:1).

Previous studies have demonstrated that activated $\gamma\delta$ TCR+ T cells exhibit a lytic activity against a variety of tumor cells (Groh et. al., 1999 and Zocchi et. al., 1990). Furthermore Vδ1+ T cells were shown to recognize ovarian cancer cells by production of IFNγ and cytotoxicity (Maeurer et. al., 1996 and Chen et. al., 2001). To investigate this question, genetically engineered $\gamma\delta$ TCR+ T cell lines were incubated with SKOV3, CAOV3 or OV2774 ovarian tumor cell lines as well as control cell lines and cytotoxicity was measured.
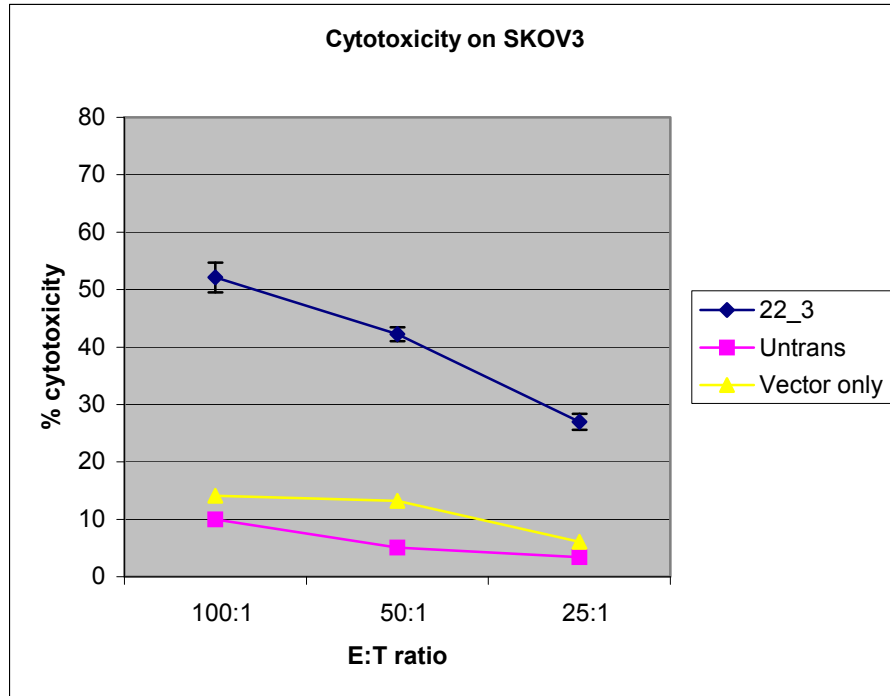
Figure 30. Cytotoxicity on 1×10^4 SKOV3 cells was measured following 5.5 hours incubation with vector only, untransduced T-cell line and genetically engineered $\gamma\delta$ TCR+ T-cell line 22_3.
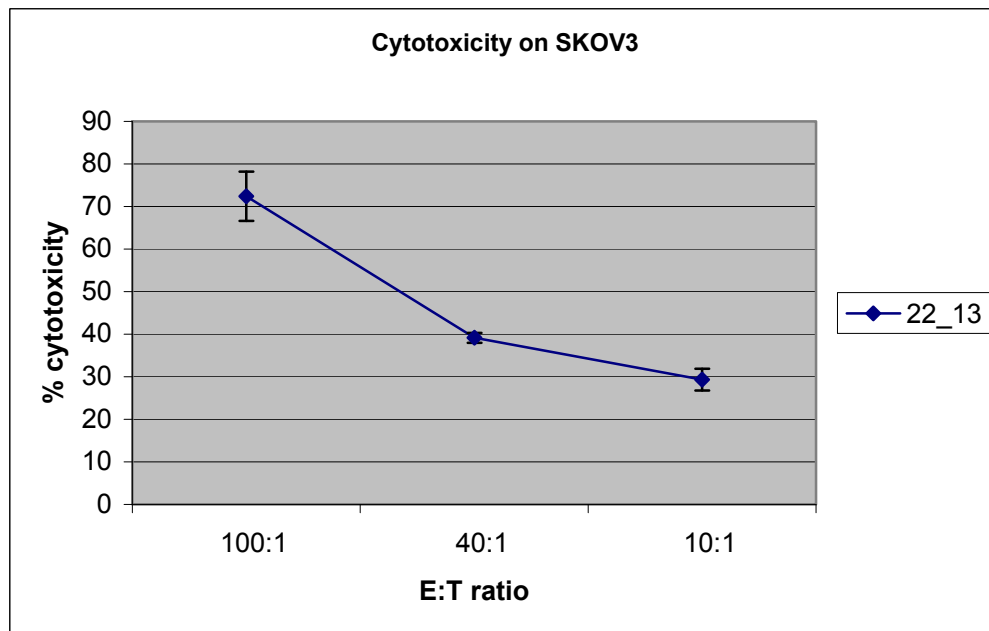
Figure 31. Cytotoxicity on 1×10^4 SKOV3 cells was measured following 5.5 hours incubation with genetically engineered $\gamma\delta$ TCR+ T-cell line 22_13.
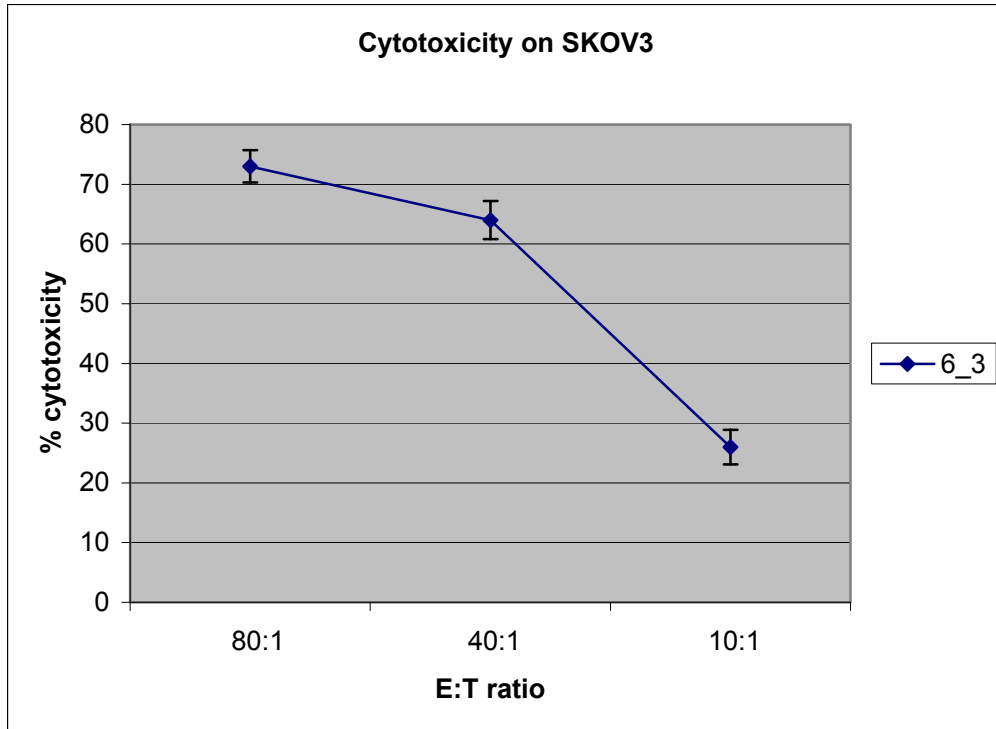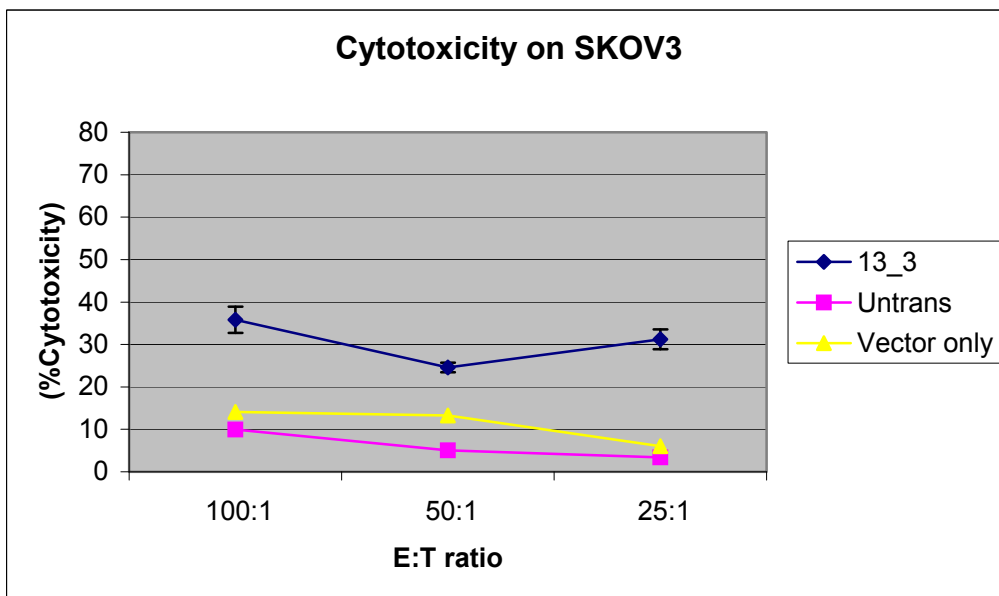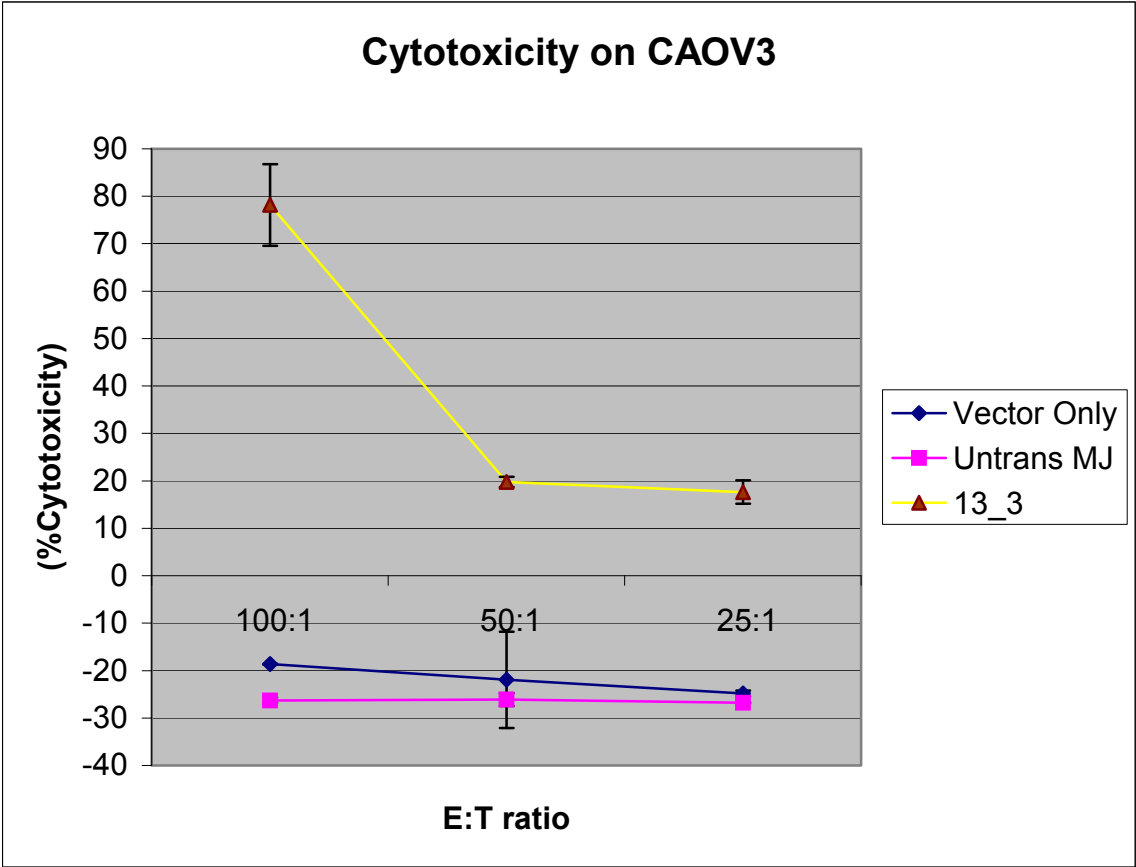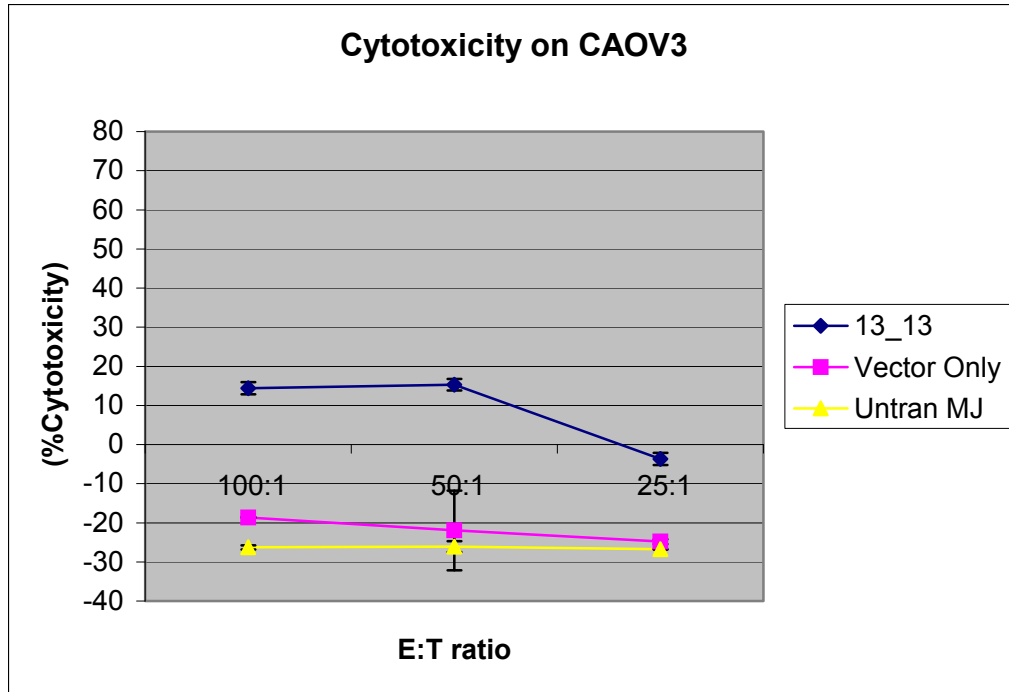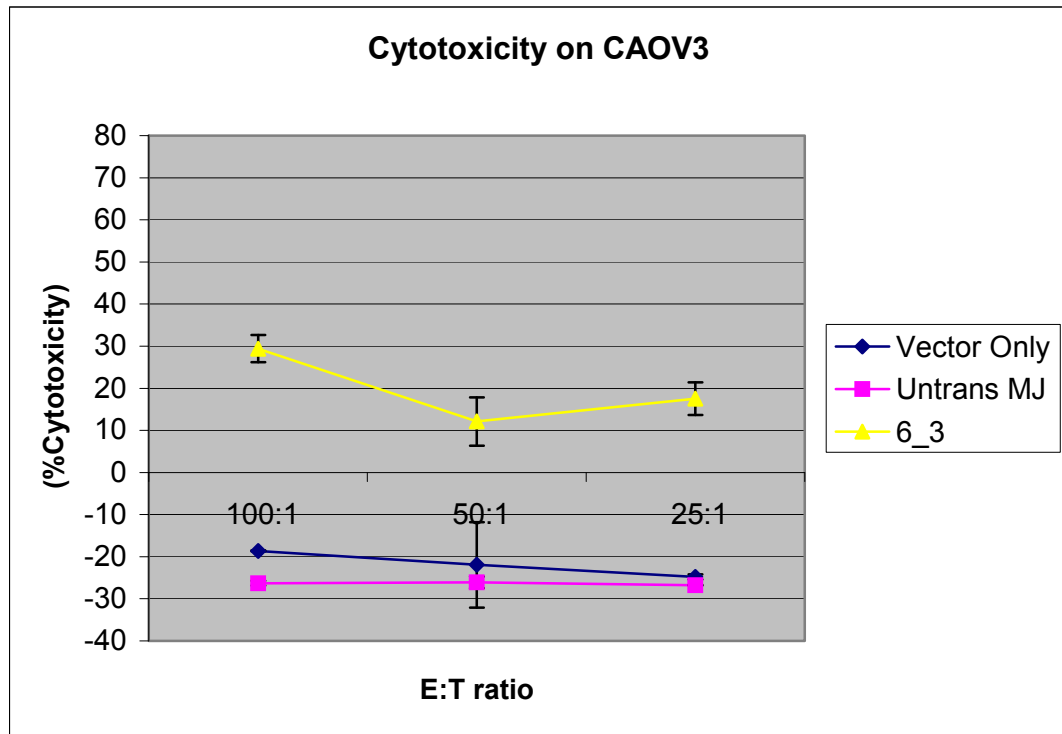
:
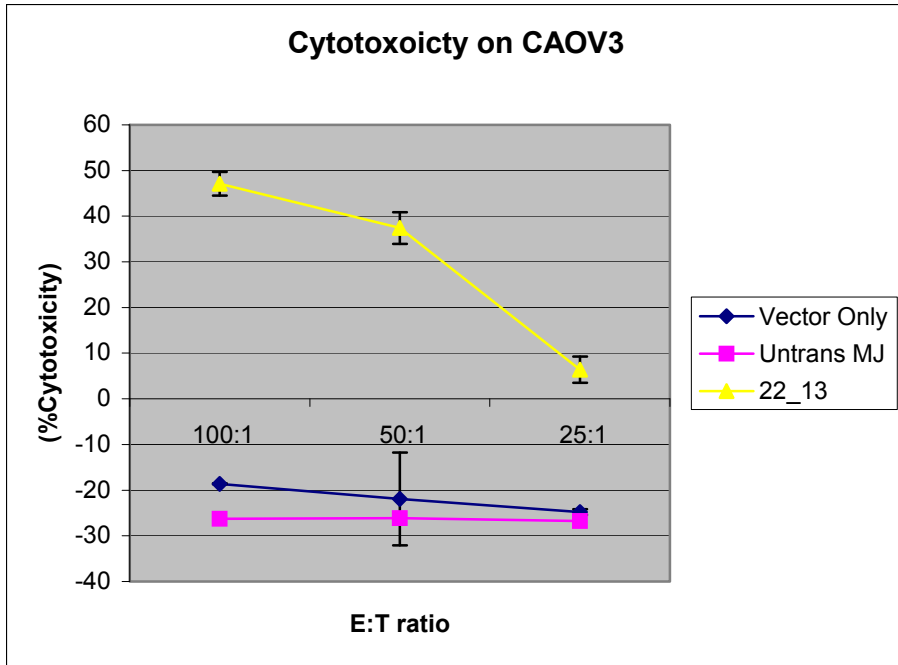**Figure 32.** Cytotoxicity on $1x10^4$ SKOV3 cells was measured following 5.5 hrs incubation with genetically engineered $\gamma\delta$ TCR+ T-cell line 6_3.

Figure 33. Cytotoxicity on $1x10^4$ SKOV3 cells was measured following 5.5 hrs incubation with genetically engineered $\gamma\delta$TCR+ T-cell lines.

Figure 34. Cytotoxicity on $1\text{x}10^4$ CAOV3 cells was measured following 5.5 hr incubation with genetically engineered $\gamma\delta$TCR+ T-cell line 13_3.

Figure 35. Cytotoxicity on 1×10^4 CAOV3 cells was measured following 5.5 hrs incubation with genetically engineered $\gamma\delta$TCR+ T-cell line 13_13.
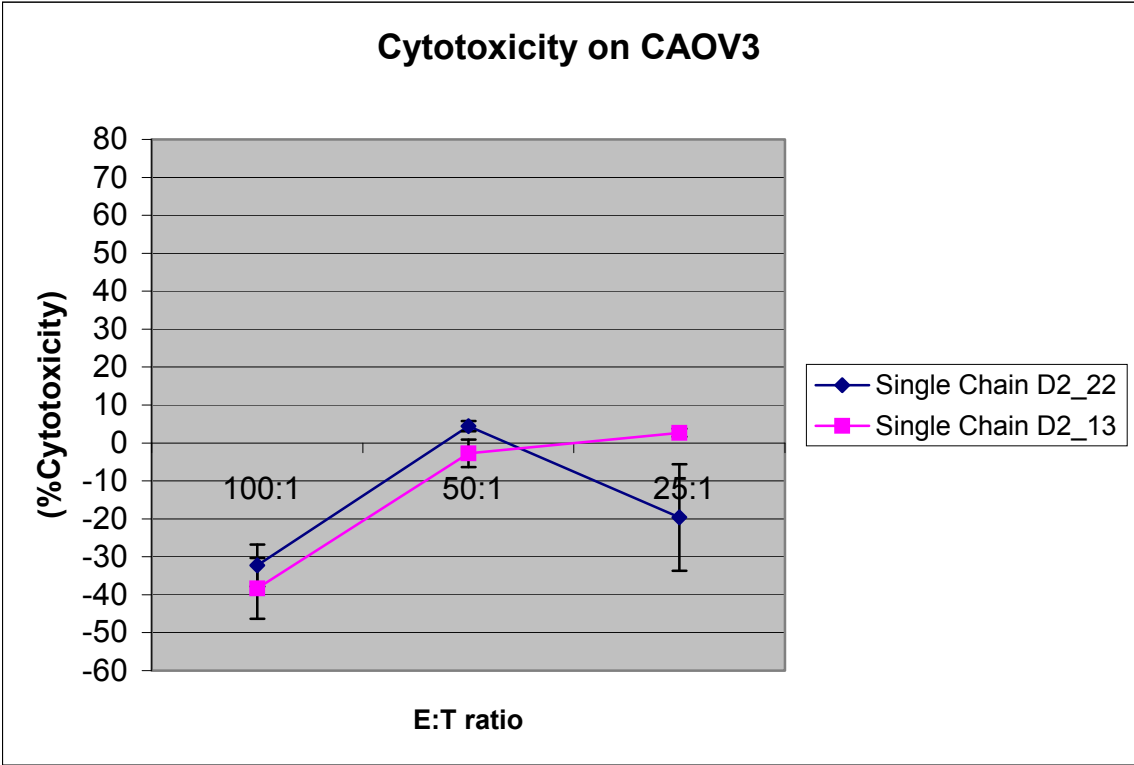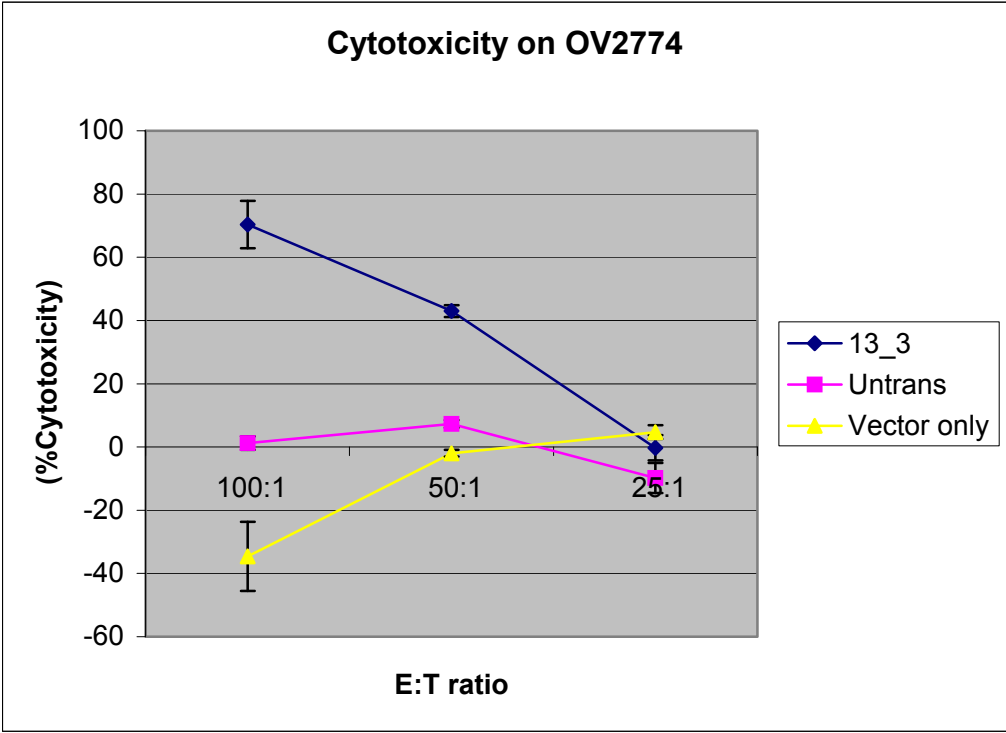
Figure 36. Cytotoxicity on 1×10^4 CAOV3 cells was measured following 5.5 hrs incubation with genetically engineered $\gamma\delta$TCR+ T-cell line 6_3.
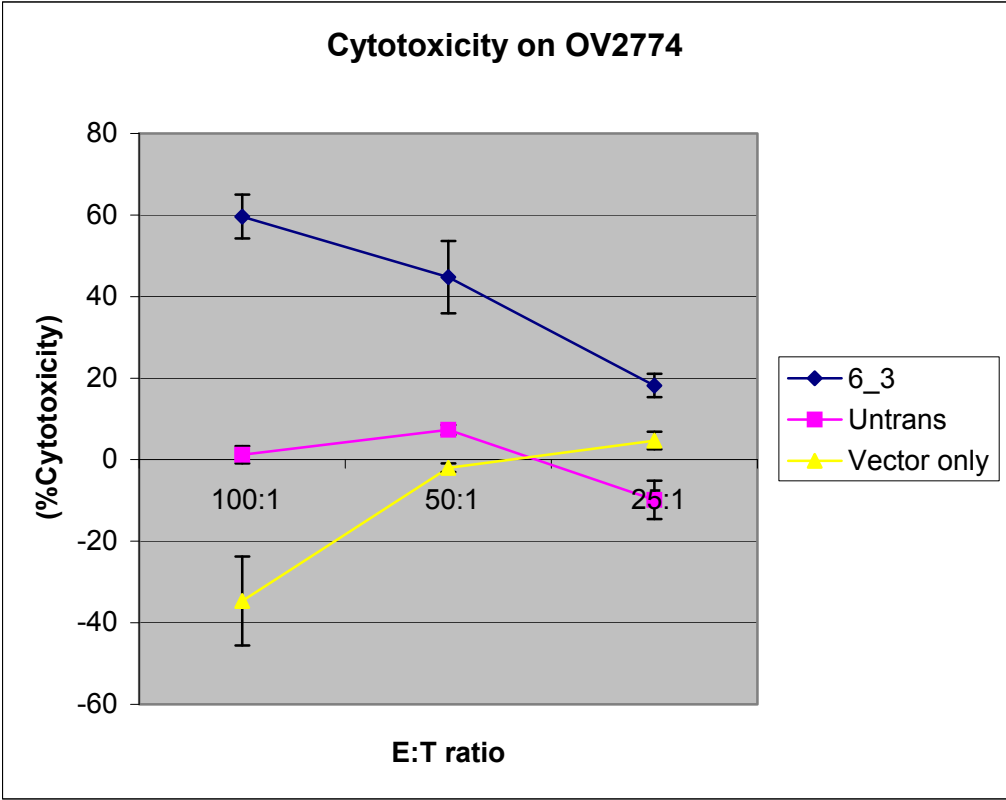
Figure 37. Cytotoxicity on 1x10^{4}CAOV3 cells was measured following 5.5 hrs incubation with genetically engineered γδTCR+ T-cell line 22_13.
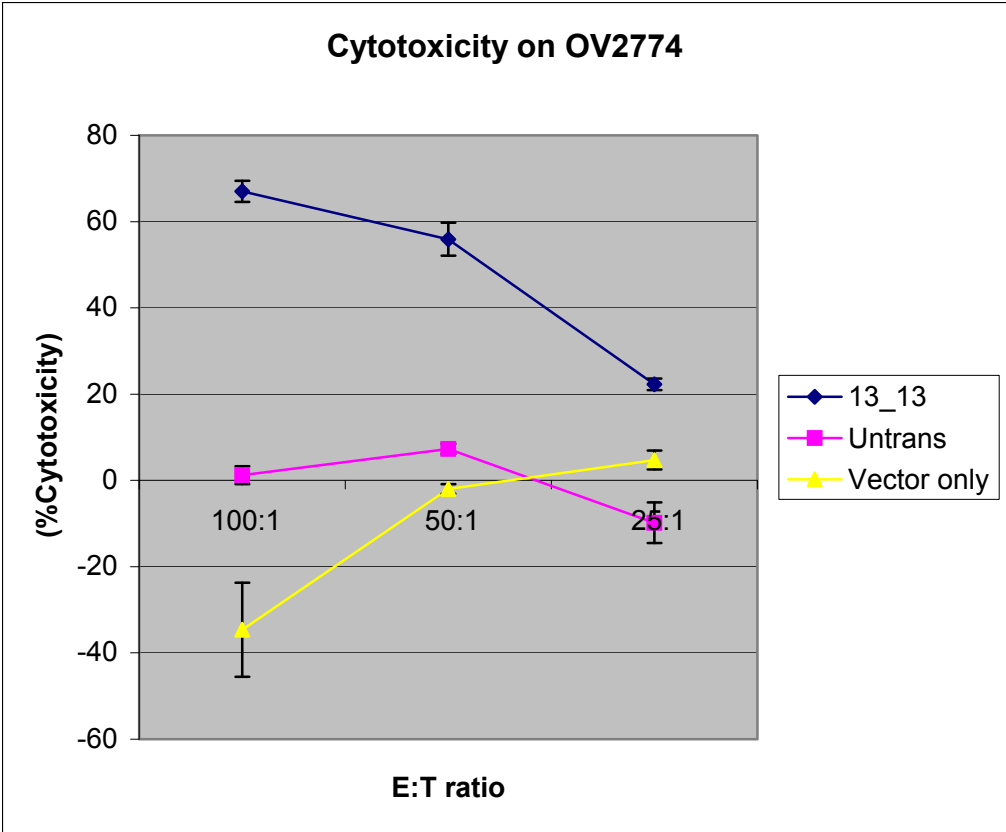
Figure 38. Cytotoxicity on 1×10^4 CAOV3 cells was measured following 5.5 hrs incubation with genetically engineered single chain δTCR+ T-cell lines.
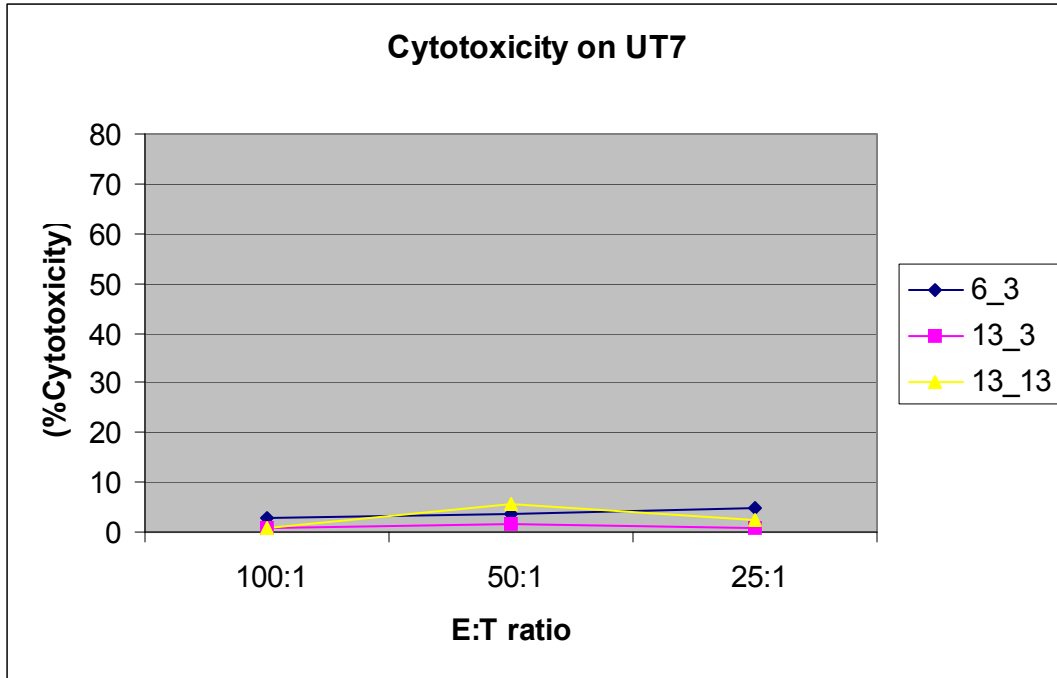
Figure 39. Cytotoxicity on 1×10^4 OV2774 cells was measured following 5.5 hrs incubation with genetically engineered $\gamma\delta$TCR+ T-cell line 13_3.

Figure 40. Cytotoxicity on 1×10^4 OV2774 cells was measured following 5.5 hr incubation with genetically engineered $\gamma\delta$TCR+ T-cell line 6_3.

Figure 41. Cytotoxicity on 1×10^4 OV2774 cells were measured following 5.5 hr incubation with genetically engineered $\gamma\delta$TCR+ T-cell line 13_13.

Figure 42. Cytotoxicity on 1×10^4 UT7 cells were measured following 5.5 hr incubation with genetically engineered $\gamma\delta$ TCR+ T-cell lines 6_3, 13_3 and 13_13.

Table 33. γδ TCR+ T-cell lines recognition of SKOV3 cell line

%Clonal Expansion	Cell Line	%Cytotoxicity	Casp 9
24/84	22_13	39.2	3200
27/26	22_3	42.9	2949
36/26	13_3	24.6	2787
3/26	6_3	64	nd

Table 34. γδ TCR+ T-cell lines recognition of CAOV3 cell line

%Clonal Expansion	Cell Line	%Cytotoxicity	Casp 9
36/26	13_3	19.8	3500
36/84	13_13	15	1499
3/26	6_3	12	2700

Table 35. γδ TCR+ T-cell lines recognition of OV2774 cell line

%Clonal Expansion	Cell Line	%Cytotoxicity	Casp 9
36/26	13_3	43	1123
36/84	13_13	56	nd
3/26	6_3	42	1420

We measured lysis of SKOV3, CAOV3 and OV2774 tumor cells by genetically engineered γδ TCR+ transduced T cell lines. Following analysis using an Effector:Target ratio of 100:1, 50:1 and 25:1 the genetically engineered transduced cell line OV27Tδ2_22_γII(9)3 induced 51, 42 and 27% cytotoxicity on SKOV3 cells. Genetically engineered TCR+ T-cell transduced cell line OV27Tδ2_22_γII(9)13 induced 72.4, 39.2 and 29.3% cytotoxicity on SKOV3 cells. Genetically engineered TCR+ T-cell transduced cell line OV27Tδ2_6_γII(9)3 induced 73, 64, and 26% cytotoxicity on SKOV3 cells. Genetically engineered TCR+ T-cell transduced cell line OV27Tδ2_13_γII(9)3

induced 35.8, 24.6 and 31% cytotoxicity on SKOV3 cells. The TCR- T-cell line (untransduced control) induced 10, 5 and 3% cytotoxicity (see Figure 28).

Using CAOV3 ovarian cancer cell targets the genetically engineered TCR+ T-cell transduced cell line OV27Tδ2_13_γII(9)3 induced 78.2, 19.8 and 17.6% cytotoxicity on CAOV3 cells. Genetically engineered TCR+ T-cell transduced cell line OV27Tδ2_13_γII(9)13 induced 14, 15 and <0% cytotoxicity on CAOV3 cells. Genetically engineered TCR+ transduced T cell line OV27Tδ2_6_γII(9)3 induced 29.4, 12 and 17.5% cytotoxicity on CAOV3 cells. Genetically engineered TCR+ transduced T cell line OV27Tδ2_22_γII(9)13 induced 47, 37 and 4.7% cytotoxicity on CAOV3 cells. The single chain TCR-transduced T-cell line showed minimal induction of cytotoxicity on CAOV3 cells.

Using OV2774 ovarian cancer cell line targets the genetically engineered TCR+ transduced T-cell line OV27Tδ2_13_γII(9)3 induced 70, 43 and .2% cytotoxicity on OV2774 cells. TCR+ T-cell line OV27Tδ2_6_γII(9)3 induced 59, 42 and 18% cytotoxicity on OV2774 cells. TCR+ T cell line OV27Tδ2_13_γII(9)13 induced 67, 56 and 23% cytotoxicity on OV2774 cells. The untransduced TCR- T-cell line induced minimal cytotoxicity on OV2774 cells.

Using UT7 leukemia cell line targets the genetically engineered TCR+ T-cell line OV27Tδ2_3_γII(9)3, OV27Tδ2_13_γII(9)3 and OV27Tδ2_13_γII(9)13 induced less than 5% cytotoxicity on UT7 cells.

CHAPTER 5
DISCUSSION

In this present study we examined the presence of oligoclonal populations of $\gamma\delta$ TCR+ T cells transcripts in the solid tumors specimens from patients with EOC. $\gamma\delta$ TCR+ T cells have been identified in TILs derived from patients with a variety of solid tumors and their increased presence is associated with increased survivial (Kobayashi et. al., 2001 and Maeurer et. al., 1996). To determine whether $\gamma\delta$ TCR+ T cells are clonally expanded in vivo we amplified using Vγ- and Vδ-specific PCR γ- and δ-chain TCR transcripts from EOC tumors. The amplified transcripts were cloned, sequenced and analyzed. Analysis revealed the presence of substantial proportions of identical γ- and δ-chain TCR transcripts that were statistically significant in tumor specimens. Sequence analysis revealed the presence of statistically significant identical oligoclonal/monoclonal γI-chain TCR transcripts in five out of seven patients. Five out of five patients revealed statistically significant identical oligoclonal γII(9)-chain TCR transcripts. Four out of six patients revealed statistically significant identical oligoclonal δ1-chain TCR transcripts. Four out of five patients revealed statistically significant identical oligoclonal δ2-chain TCR transcripts. Multiple identical copies of TCR transcripts can be derived only by specific antigen-driven activation, proliferation and clonal expansion of the T-cell clones, which recognize these antigens. Two possibilities could explain the clonal expansion of $\gamma\delta$ TCR+ T cells in patients with EOC. First, the expansion may result from circulating $\gamma\delta$ TCR+ T cells, which encountered a tumor antigen leading to activation, proliferation and expansion of

a particular $\gamma\delta$ TCR+ T cell utilizing an antigen reactive CDR3 region. On the other hand, in situ $\gamma\delta$ TCR+ T cells that reside in the normal reproductive tract specifically the ovary underwent a TCR-mediated antigen driven clonal expansion within the solid tumor of patients with EOC.   These results demonstrate that T cells infiltrating solid tumor specimens of patients with EOC contain oligoclonal populations of T cells, which confirm and extend previous work within our laboratory.

T cells recognize through their $\gamma\delta$ TCR mainly whole proteins, in general, unrestricted to MHC class I or II (Rock et. al., 1994). In contrast, $\alpha\beta$ TCR recognize small peptides derived from endogenous or exogenous antigens in association, in general, with MHC class I or II restriction. Furthermore, $\gamma\delta$ TCR+ T cells recognize in an MHC-independent manner, lipids, carbohydrates, glycolipics, and other ligands. T-cells each express a different TCR molecule, which serves as a unique fingerprint of the T-cell clone. Therefore, the probability of finding by chance mulitiple identical copies (two or more) of a particular γ- or δ-chain TCR transcript within an independent sample of T cells is negligible. Researchers have observed that in the host a specific antigen-driven proliferation and clonal expansion of the T-cell clones that recognize tumor antigen(s) takes place but in some patients this specific anti-tumor response appears to be suppressed by regulatory T cells, T(reg)s. Evidence indicates that these T(reg)s inhibit in vitro proliferative responses, cytokine production, and the cytolytic activity of autologous T cells. Therefore, the tumor has evolved to evade the host immune response.

Once we determined the presence of oligoclonal/monoclonal expansion of $\gamma\delta$ TCR+ T-cells in patients with EOC the next step was to determine their reactivity to tumor cells. Therefore, we carried out in vitro experiments to assess the ability of T-cells transduced with the oligoclonal $\gamma\delta$ TCR transcript expressed on the cell surface to recognize and kill tumor cells.

We first constructed full-length transcripts of both γ-chain and δ-chain TCR transcripts using the CDR3 regions of the clonally expanded $\gamma\delta$ TCR+ T cell transcripts amplified from the tumors of patients with EOC. Then using a MSCV retroviral expression system we expressed these transcripts in the mutant jurkat cell line. Knowing many human tumors are immunogenic and elicit an antigen-specific T-cell immune responses our goal was to generate cytotoxic T-cells that are able to recognize tumor cells. We wanted to identify the existence of an antitumor immune response in humans in which $\gamma\delta$ TCR+ T-cells play a role.

We then analyzed the induction of cell death protease activity by measuring caspase 9, 8 and 3 activity and then determined whether genetically engineered $\gamma\delta$ TCR+ T-cells that expressed the clonally expanded TCR transcripts on the cell surface induce lysis of tumor cells. For each set of $\gamma\delta$ TCR we constructed two retroviral vectors that contain either a γ-chain or δ-chain TCR full-length transcript. These retroviral vectors were used to mediate genetic transfer of the $\gamma\delta$ TCR transcripts. This procedure required multiple-vector transduction as well as antibiotic selection. The results of this investigation show that genetically engineered TCR+ T-cell lines induced caspase activity as well as cytotoxicity towards the ovarian cancer cell lines SKOV3, CAOV3 and OV2774.

Further investigations will involve the identification of the putative self or non-self antigen(s) recognized by the genetically engineered $\gamma\delta$ TCR+ T-cells. This will assist in understanding the role of antigen-driven oligoclonal expansion of $\gamma\delta$ TCR+ T-cells in EOC.

The identification of cytotoxic T cells that express natural or by genetically engineering T-cell transcripts that recognize tumor cells will serve as a novel immunotherapy. Patients with ovarian cancer are often diagnosed at an advance stage and the cancer cells are often resistant to normal doses of chemotherapeutic agents. These patients have a survival rate of one-year. The effectiveness of adoptive immunotherapy in cancer patients has been identified in recent studies where high-dose therapy followed by autologous stem cell transplantation was shown to be effective resulting in a minimal disease state and improved survival in patients with myeloma (Rapoport et. al., 2005). Many cancer patients experience a dysfunctional tumor immune response and need an alternate to traditional adoptive cellular transfer (ACT) therapy. Primarily the lack of cytotoxic T cells that recognize tumor cells needed for in vitro expansion limits the ability to utilize tradition ACT.

The novel approach of using $\gamma\delta$ TCR+ T-cell transcripts for the retroviral transduction of patient cytotoxic T-cells may be useful as an alternate therapeutic method or in support of high-dose therapy. By using the $\gamma\delta$ TCR+ T-cell transcripts for expression in cytotoxic peripheral T cells we can generate and/or enhance the patients immune response. Cytotoxic T lymphocytes express either $\alpha\beta$ TCR or $\gamma\delta$ TCR+ CD3+ T-cells and exhibit cytotoxicity following antigen driven

123

TCR receptor stimulation/activation. As stated previously the mechanisms involved in cell-mediated cytotoxicity include specific-antigen recognition and cell-to-cell contact. The secretory pathway involving receptor-triggered exocytosis of preformed secretory granules that contain granzymes or the use of receptor-induced surface membrane Fas ligand (FasL), which cross-links Fas on target cells both have the ability to result in effector cell induced cytotoxicity on tumor target cells. Since $\alpha\beta$ TCR and $\gamma\delta$ TCR+ CD3+ T-cells are capable of being cytotoxic against cancer cells an antitumor immune response involving both subsets of cytotoxic T lymphocytes may enhance and/or support one another.

Both experimental and clinical studies suggest that $\gamma\delta$ TCR+ T-cells play a role in the antitumor cell immune response (Rospollini et. al., 2005, Choudhary et. al., 1995, and Kabelitz et. al., 2004). $\gamma\delta$ TCR+ T-cells recognize tumor cell antigens and are activated and exert the aforementioned cytotoxicity and release cytokines toward the target tumor cell. The significant component of this recognition is the ability of $\gamma\delta$ TCR+ T cell to recognize whole protein in an HLA-unrestricted manner. Unfortunately there are few definitive ovarian cancer tumor cell antigens identified that are recognized by $\gamma\delta$ TCR+ T cells. Therefore, identifying clonally expanded $\gamma\delta$ TCR+ T cells in patients with EOC and the antigens they recognize will aid in the treatment of patients with EOC.

As part of identifying the antitumor immune response researchers are continuing to understand the pathogenesis of EOC (Garson et. al., 2005 and Liu et. al., 2004) but believe many factors are involved and include the following:

A) Genetic factors

As previously described, several genetic factors have been indicated to be involved in the initiation and progression of EOC. BRAC1 and BRAC2 account for 5-10% of inherited EOC. Many of these genes 1) induce cellular proliferation, 2) inhibit cellular proliferation or 3) regulate programmed cell death. Furthermore, genetic factors that regulate the coagulation pathway and inflammation have been shown to be involved in tumor cell proliferation, angiogenesis, invasion and metastasis (Wang et. al., 2005).

B) Inflammation

There is increasing evidence that infiltrating immune cells are present in EOC and the peritoneal environment. Previous studies showed that 70% of the cells within the EOC tumors were mononuclear infiltrates (Freedman et. al., 1994). The tumor rejection process includes cytotoxic T lymphocytes (CTLs) killing the tumor cells and producing cytokines and/or chemokines. Cancer research has shown that tumor immunity and the subsequent tumor elimination process is highly complex and involves various components of the host immune system. For example, the tumor stroma is a mixture of various cell types and stromal agents. The stroma provides growth factors, blood supply, and the extracellular matrix that sustains the tissue. Furthermore, the microenvironment of the peritoneium in EOC includes cytokines/chemokines involved in inflammation (Roskelley et. al., 2002). The antiproliferative effect of cytokines such as IFNγ is important for tumor regression and the release IL-12 (Broderick

et. al., 2006) is necessary for memory T cells to proliferate, secrete IFN-γ, and kill tumor cells.

Chemokines also play an important role in the antitumor response (Schutyser et. al., 2002). Interleukin-8 (IL-8) is considered an important chemokine associated with tumor progression and appears to be the point of linkage for coagulation and inflammation in malignancy. The inflammation process may include cross talk between tumor cells and the surrounding cellular stroma. The inflammatory infiltrates are comprised of different leukocyte populations and interact with the cancer cells and their surroundings, which may influence the phenotypic changes in the tumor (Freedman et. al., 2004). More specifically $\gamma\delta$ TCR+ T-cells may function at the site of the tumor by producing soluble mediators to further recruit and activate other inflammatory cells as well as directly recognize tumor surface antigens leading to tumor cell death.

C) Autoimmunity

Research indicates that immuno-suppression may contribute to the progession of ovarian cancer. The presence of regulatory T-cells (Treg) and the secretion of soluble molecules in cancer patients could be important in inducing T-cell suppression, therefore allowing tumor growth. Suppressor cells have been thought to play a part in the progression of cancer. CD4+CD25+ regulatory T cells present in EOC tumors have been shown to be associated with poor patient survival. Evidence indicates Tregs preferentially move to and accumulate in tumors and ascites in later cancer stages (Curiel et. al., 2004). Furthermore, dysregulation of the immune response may also include a loss of signal-

transducing proteins leading to decreased T-cell activation (Choi et. al., 1998). In addition, HSP-10 appears to be expressed and released from many proliferating cell types including ovarian cancer cells. This circulating HSP-10 exhibit suppression of T-cell signaling leading to decreased T-cell activation (Akyol et. al., 2006). These factors contribute to the down-regulation of the tumor immune response, therefore allowing the tumor to grow and escape the host immune surveillance.

Over the past twenty years there has been substantial evidence demonstrating an antitumor response takes place in humans. Immunogenic tumor antigens that elicit an immune response can be used for the purpose of vaccine development to aid in the treatment of patients with various malignancies. In the microenvironment of EOC, mononuclear cells infiltrate into the pelvic peritoneum and stroma, where they may become activated, clonally expand and are targeted towards tumor cells in response to a self or non-self antigen(s). This cellular immune response is often down-regulated by cytokines such as IL-10, IL-6 and TGF-β, as well as growth factors and chemokines that may promote the progression of EOC by suppressing the antitumor response. Therefore, while discovering and developing novel immunotherapy such as $\gamma\delta$ TCR+ T-cells we must consider the significance of decreasing the number of regulatory T lymphocytes in the microenvironment of the solid tumor.